

VTT Technical Research Centre of Finland

A review of aeronautical fatigue investigations in Finland April 2011 - February 2013

Siljander, Aslak

Published: 01/01/2013

Document Version
Publisher's final version

[Link to publication](#)

Please cite the original version:

Siljander, A. (Ed.) (2013). *A review of aeronautical fatigue investigations in Finland April 2011 - February 2013*. VTT Technical Research Centre of Finland. ICAF National Review - Finland No. 2428VTT Research Report No. VTT-R-0215-13

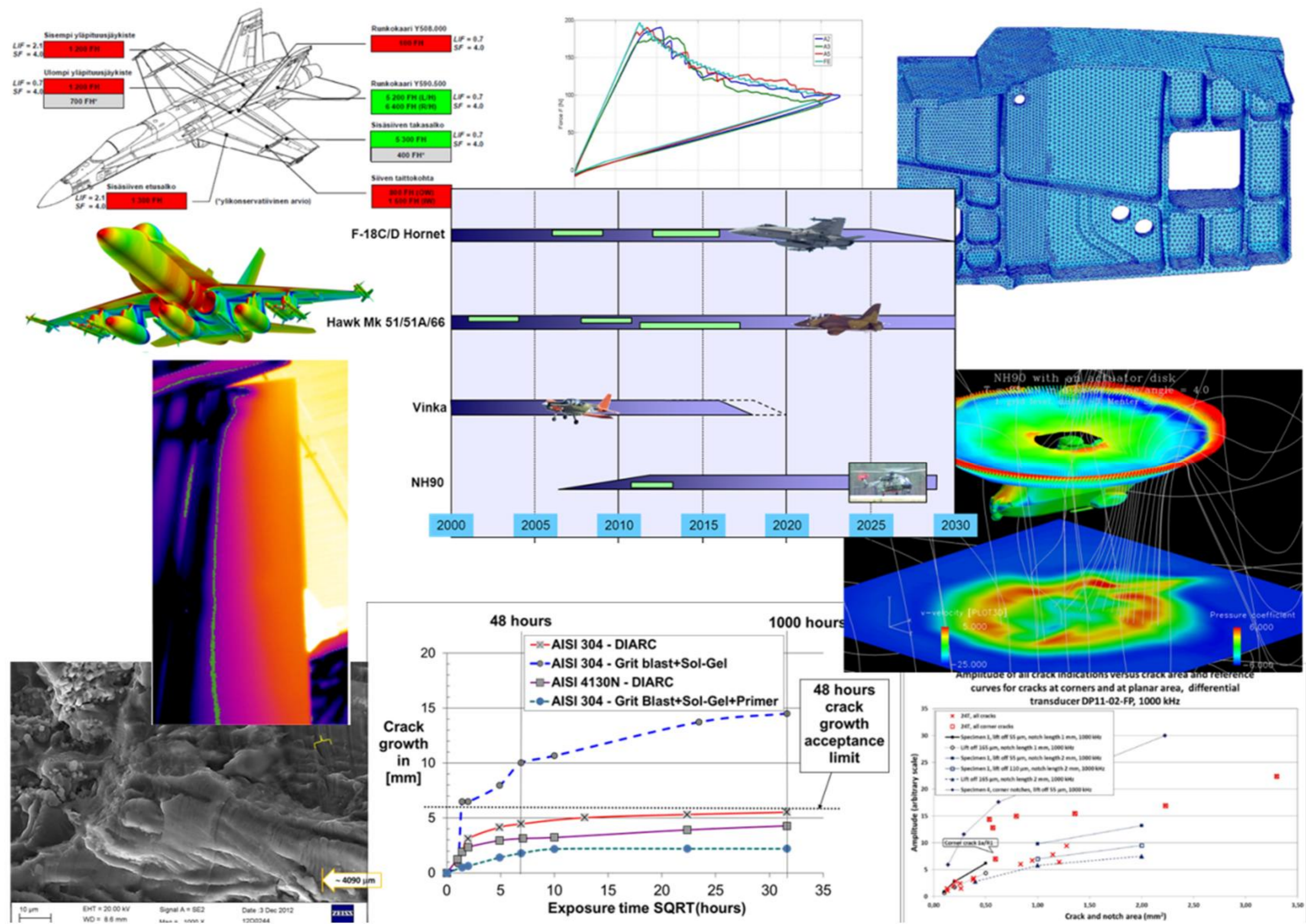


VTT
<http://www.vtt.fi>
P.O. box 1000FI-02044 VTT
Finland

By using VTT's Research Information Portal you are bound by the following Terms & Conditions.

I have read and I understand the following statement:

This document is protected by copyright and other intellectual property rights, and duplication or sale of all or part of any of this document is not permitted, except duplication for research use or educational purposes in electronic or print form. You must obtain permission for any other use. Electronic or print copies may not be offered for sale.



A REVIEW OF AERONAUTICAL FATIGUE INVESTIGATIONS IN FINLAND APRIL 2011 – FEBRUARY 2013

Presented at the 33rd Conference of the International Committee on Aeronautical Fatigue and Structural Integrity (ICAF), Jerusalem, Israel, 3-4 June 2013

Compiled by Aslak Siljander

Confidentiality Public

Preface

The Finnish Air Force Materiel Command (FINAFMC), Programmes Division, initiated and supported this work. The editor is indebted to the following individuals who helped in the preparation of the review (organizations and individuals in alphabetical order – the reference list refers to paragraph-specific contributions):

Aalto	<i>Aalto University, School of Engineering, Department of Applied Mechanics, Aeronautical Engineering:</i> Jarkko Aakkula, Olli Saarela, Markus Wallin;
Emmecon	<i>Emmecon Ltd:</i> Risto Hedman;
FINAFMC	<i>Finnish Air Force Materiel Command, Programmes Division:</i> Mikko Järvinen, Ari Kivistö, Kari Renko, Kalle Vaaraniemi, Ari Välikangas; <i>Finnish Air Force Materiel Command, Plans Division:</i> Henry Paajanen; <i>Finnish Air Force Materiel Command, Aircraft Division:</i> Jukka Taattola;
FINAFFTC	<i>Finnish Air Force, Flight Test Center:</i> Raimo Enberg, Hannu Heinele, John Öström;
FINAFLAC	<i>Finnish Air Force, Lapland Air Command:</i> Teemu Tuovila;
FINAFKAC	<i>Finnish Air Force, Karelian Air Command:</i> Kari Kilkki;
FINAFSAC	<i>Finnish Air Force, Satakunta Air Command:</i> Peter Ylinen;
Finflo	<i>Finflo Ltd:</i> Juho Ilkko, Esa Salminen, Timo Siikonen;
Millidyne	<i>Millidyne Ltd:</i> Mika Kolari, Petri Sorsa;
Patria	<i>Patria Aviation Oy, RTD & Aeronautical Engineering:</i> Toivo Hukkanen, Mika Keinonen, Mirve Liius, Janne Linna, Simo Malmi, Antero Miettinen, Mikko Orpana, Jouni Pirtola, Jukka Raunio, Tuomo Salonen, Jaakko Sotkasiira, Maria Stenberg, Piia Stenhäll, Jarkko Tikka; <i>Patria Aviation Oy, Systems / Avionics:</i> Juha Alanko, Jari Koivu, Maunu Mäntylä, Marika Vuori, Lauri Walden; <i>Patria Aviation Oy, Aircraft, Engines Unit:</i> Jani Simelius;
TUT/DSP	<i>Tampere University of Technology, Department of Signal Processing:</i> Juha Jylhä, Marja Ruotsalainen, Ari Visa;
TUT/DMS	<i>Tampere University of Technology, Department of Materials Science:</i> Elina Huttunen-Saarivirta, Turi Salomaa, Veli-Tapani Kuokkala, Viivi Pirttiniemi;
TUT/IHA	<i>Tampere University of Technology, Department of Intelligent Hydraulics and Automation:</i> Jussi Aaltonen, Vänni Ala-Rotu, Kari T. Koskinen;
VTT	<i>VTT Technical Research Centre of Finland:</i> Pertti Auerkari, Harri Janhunen, Petra Jauhiainen, Juha Juntunen, Keijo Koski, Arto Kukkonen, Risto Laakso, Kari Lahdenperä, Esa Leskelä, Sauli Liukkonen, Johanna Lukin, Juha Mannila, Sakari Merinen, Juha Nikkola, Arto Nyholm, Tauno Ovaska, Enna Peltoniemi, Juhani Rantala, Eetta Saarimäki, Jorma Salonen, Matti Sarkimo, Jarmo Siivinen, Aslak Siljander, Laura Sirkiä, Tuomas Teittinen, Piritta Varis, Päivi Varis, Esa Varis, Juha Veivo, Tomi Viitanen, Sanni Yli-Olli.

Espoo 3rd April 2013

Editor

Contents

13.1	Introduction	4
13.1.1	Valmet Vinka	5
13.1.2	Hawk Mk51/51A and Mk66	6
13.1.3	F-18C/D Hornet.....	7
13.1.4	Scope of the review	9
13.2	Current activities: ASIMP 2010-2012 and ASIMP 2013-2016.....	10
13.2.1	Loads and stresses	10
13.2.1.1	Computational fluid dynamics (CFD) – update.....	10
13.2.1.1.1	Flow simulations for NH90 helicopter fuselage with an actuator disc	10
13.2.1.1.2	Computational Fluid Dynamics activities at Finflo Ltd.....	12
13.2.1.1.3	Initial value provisions for the F-18 CFD analyses	13
13.2.1.2	Flight simulations	14
13.2.1.3	Hornet FE modeling – update.....	15
13.2.2	Fatigue tracking systems.....	16
13.2.2.1	FINAF F-18 HOLM jets in routine squadron service	16
13.2.2.1.1	Vertical tail measurements of International Mini-HOLM flights.....	17
13.2.2.1.2	HOLM modification.....	17
13.2.2.2	Flight maneuver identification (FMI) – update.....	18
13.2.2.2.1	Fatigue damage of nominally similar flight maneuvers.....	19
13.2.2.2.2	Reasoning flight parameter based rules that explain the degree of damage.....	20
13.2.2.3	Parameter based fatigue life analysis - update	21
13.2.2.3.1	Updated results (CFD – FEA – transfer functions)	21
13.2.2.3.2	In-service maintenance.....	23
13.2.2.3.3	Add in new structural locations and future plans	24
13.2.2.4	Research efforts towards an OLM replacement system (Hawk Upgrade 2).....	24
13.2.2.4.1	Structural health monitoring (SHM).....	24
13.2.2.4.2	Integrated eddy current inspection system for FINAF Hawks	24
13.2.3	Structural integrity of composite materials	25
13.2.3.1	Thermographic studies – update	25
13.2.3.2	Fracture mechanics based analysis and tests of delaminations	27
13.2.4	Structural integrity of metallic materials.....	29
13.2.4.1	FISIF Hole Salvage project	29
13.2.4.2	Non-destructive inspection (NDI) activities (metallic materials).....	30
13.2.4.2.1	Experimental study of the sensitivity of the crack detection techniques applicable in the periodic in-service inspections using painted test specimen with real fatigue cracks.	30
13.2.5	Repair technologies	33
13.2.5.1	Repair technologies for composite structures	33
13.2.5.1.1	Aircraft battle damage repair of composite structures	33
13.2.5.2	Repair technologies for the FINAF F-18 metallic primary structures	34
13.2.5.2.1	DIARC plasma coating for reliable and durable structural bonding of metals.....	34
13.2.5.2.2	Computational fatigue life assessment of a metallic structure with a bonded composite repair	36
13.2.6	Mechanical systems integrity	38
13.2.6.1	Simulation and modeling.....	38
13.2.6.2	Laboratory testing	38
13.2.6.3	Condition control and monitoring.....	38
13.2.7	Engine integrity.....	39
13.2.7.1	Microstructural degradation of a single-crystal gas turbine blade.....	39
13.2.7.2	Guideline - turbine blade failures.....	40
13.2.7.3	The effect of volcanic ash on gas turbine blades and vanes.....	42
13.2.7.4	The effect of volcanic ash on gas turbine vanes.....	43
13.3	Related activities	44
13.3.1	Environmentally friendly corrosion protection studies	44
13.4	References	46

13.1 Introduction

The year 2013 marks the 95th anniversary of the Finnish Air Force (FINAF) – one of the oldest independent air forces in the world. It was founded as an independent service on the 6th March 1918 [1]. The fixed wing aircraft inventory of the FINAF at the time of writing this review is summarized in *Fig. 1*. The third C295M was received in 2011. The PC-12NG aircraft have replaced the six (6) twin-engine Piper Chieftains, which were 25 years in the FINAF operation. The Chieftains were retired in 2011. Ten (10) Valmet Redigos will be retired, one by one, by the year of 2013.

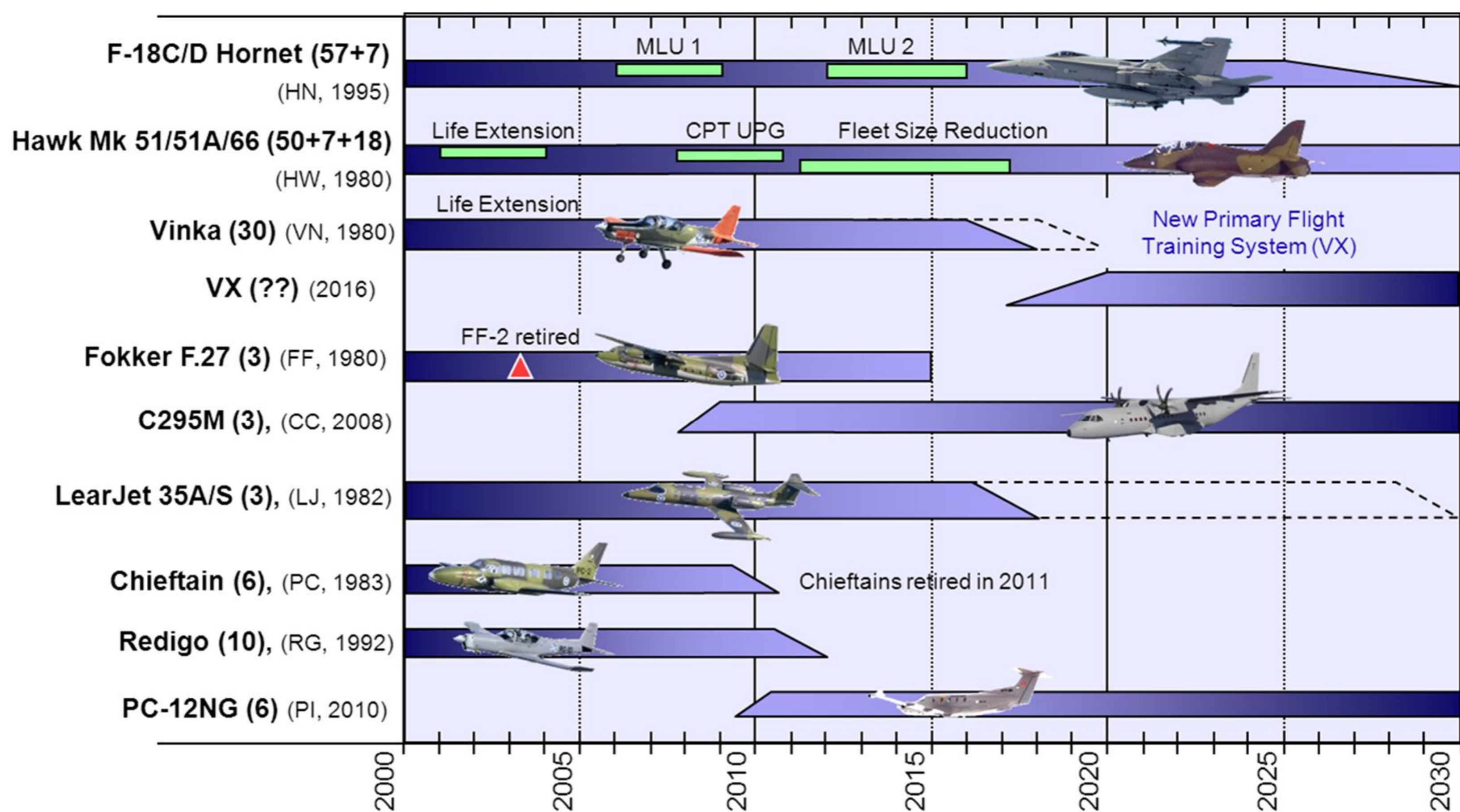


Figure 1: An overview of the fixed wing aircraft inventory of the Finnish Air Force (FINAF). Picture by courtesy of the FINAF.

By the end of year 2012, of the 20 TTH/SAR NH90 helicopters purchased by the Finnish Defence Forces (FDF), a total of 15 helicopters have been assembled by Patria. Five of the received NH90's are in the initial operational configuration (IOC) and ten in the IOC+ configuration. The last five NH90s will be delivered in future and those helicopters correspond to the full operational configuration (FOC), while those NH90s delivered earlier will be upgraded to the FOC. The helicopters of the FDF at the time of writing this review are summarized in *Fig. 2*.

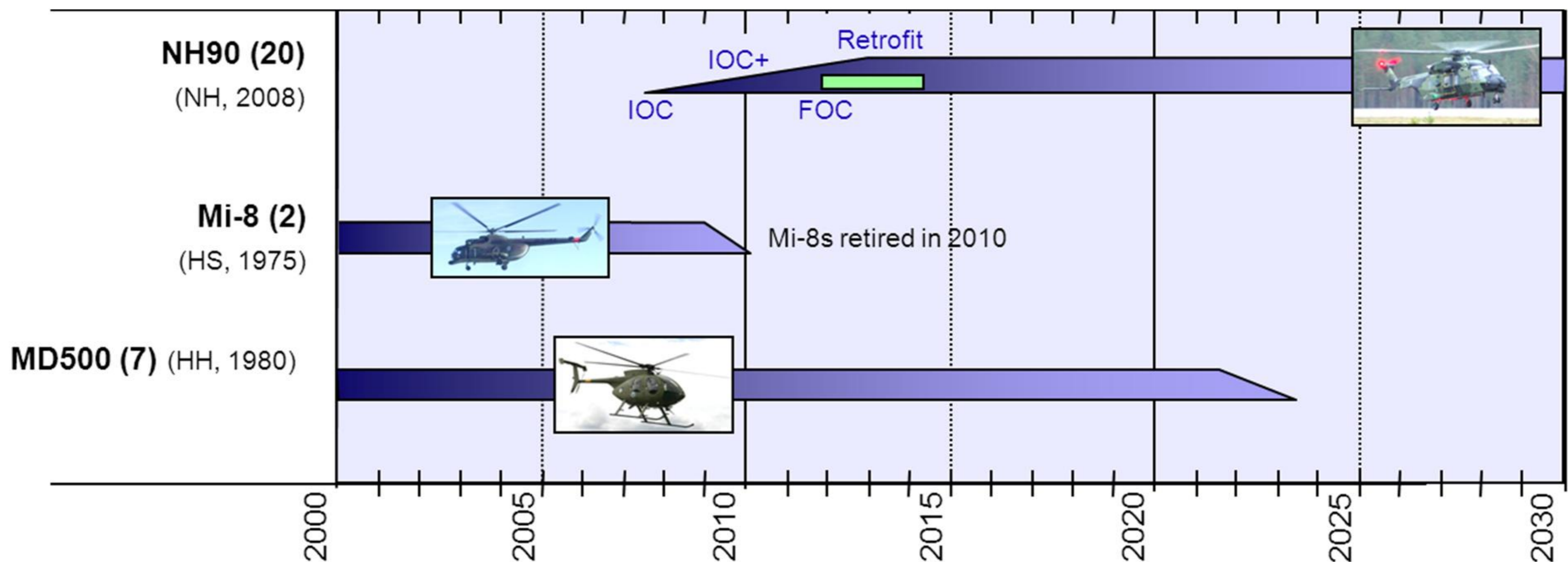


Figure 2: An overview of the rotary wing aircraft inventory of the Finnish Defence Forces (FDF). Picture by courtesy of the FINAF.

Before going into highlights of the structural integrity management activities, a brief update of the FINAF's fighter aircraft and associated pilot training aircraft is provided below.

13.1.1 Valmet Vinka

Previous activities related to the Valmet Vinka primary trainer of the FINAF were outlined in e.g. [2 Chapter 13.1.1]. During the life extension program (LEP) of the Vinka primary trainers, the entire fleet was equipped with a g counter. The structural life consumption and severity of the usage is monitored by Patria Aviation by using the tail number-specific g counter. Patria also issues recommendations on yearly basis regarding the rotation of the Vinka fleet as well as its fleet leaders. This is to obtain a more even rate of structural life expended and to keep the fleet leaders reasonably ahead of the rest of fleet in flight hours.

Based on the g counter information, the primary trainers are in good structural condition with regard to the flight hours. The severity of usage in view of the g counter status is more benign than that on the basis of LEP assumptions, see *Fig. 3*. It is possible to operate with Vinka until 2020 under its current type certificate. If there is a need to operate beyond 2020, the Vinka fleet will require another LEP.

All options are being held open when it comes to how the Vinka fleet is going to be replaced in the future. A new type of aircraft is one possibility. In addition to that, collaboration with another country and buying the training from a company are other possibilities. Currently the FINAF procures the primary training from Patria, while the aircraft used in training are owned by the FINAF.

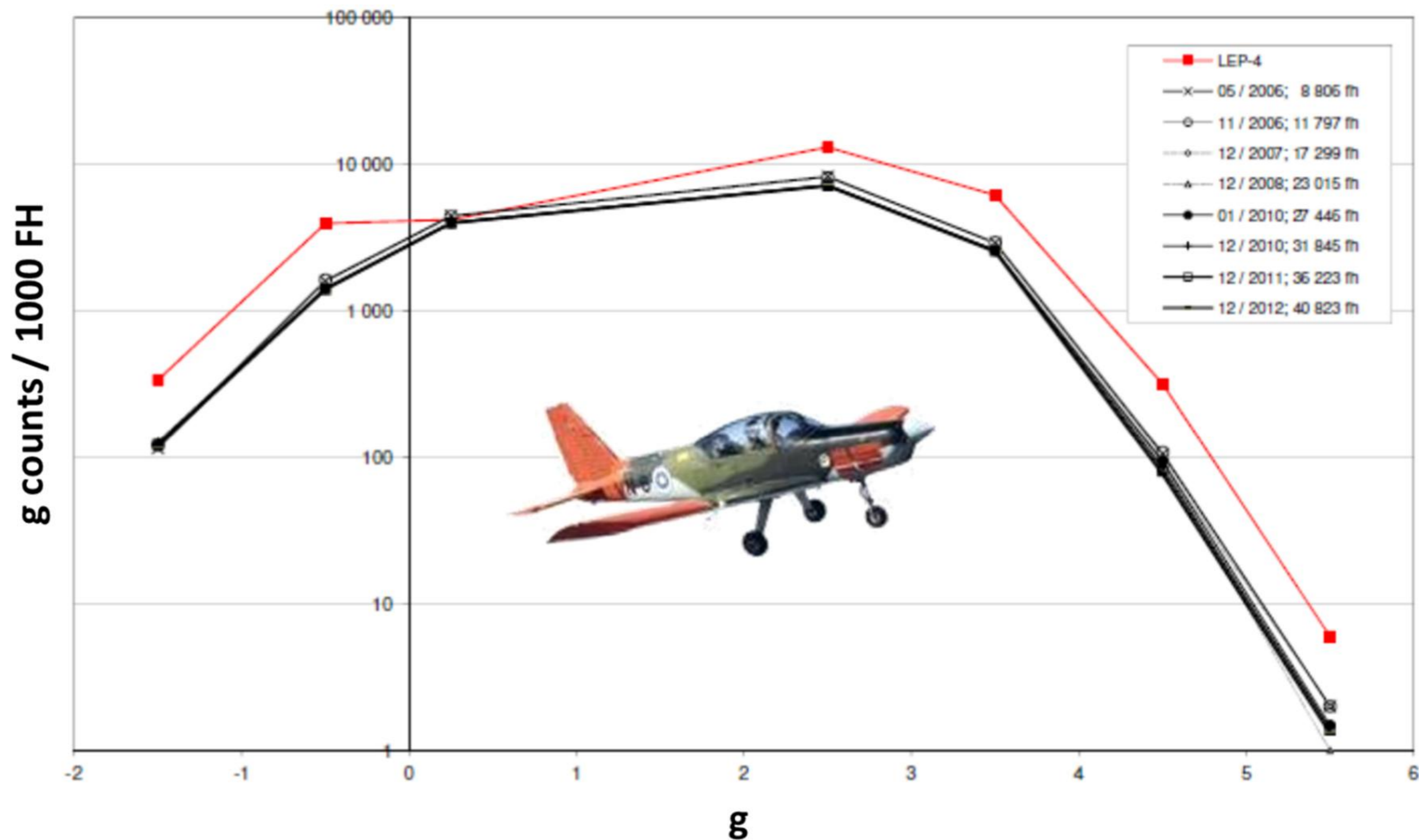


Figure 3: The g counts (x-axis) per 1000 FH (y-axis) of the Valmet Vinka. The spectrum representing the LEP design assumptions (LEP-4). The post LEP g counter spectrum as of May 2006 (- x -), as of November 2006 (- o -), as of December 2007 (- \diamond -), as of December 2008 (- Δ -), as of January 2010 (-•-), as of December 2010 (- -), and the updates from the previous review: as of December 2011 (- · -) and as of December 2012 (- \square -). All curves (excluding the red LEP-4) represent the fleet average from all Vinkas, as ranked according to the a/c center of gravity normal acceleration. Picture by courtesy of Patria Aviation.

13.1.2 Hawk Mk51/51A and Mk66

In 2007, the Finnish Air Force purchased 18 pre-owned Hawk Mk.66s from Switzerland. These supplemented the Hawk Mk.51/51A fleet purchased earlier. In 2009, this was followed up by an order placed with Patria, for an extensive cockpit and avionics upgrade of the aircraft. The upgrade includes the replacement of all important avionics devices and cockpit display systems by new digital IT systems. The design is based on the upgrade already implemented on Mk.51/51A aircraft. Under the current programme, Patria is also responsible for developing software for the aircraft's mainframe, the Mission Computer. During 2011 Patria delivered six (6) and during 2012 eight (8) modified aircraft to the FINAF. All 18 aircraft will be modernized and delivered during 2013 [3]. The aircraft which are not modernized will be retired in the coming years. In 2015 all the FINAF Hawks will be modernized and the fleet will consist of one (1) Mk.51, seven (7) Mk.51As, and 18 Mk.66s.

The structural fatigue consumption of the FINAF Mk.51/51A Hawks is summarized in *Fig. 4*. Further Hawk-related research efforts are provided in Chapter 13.2.2.4.

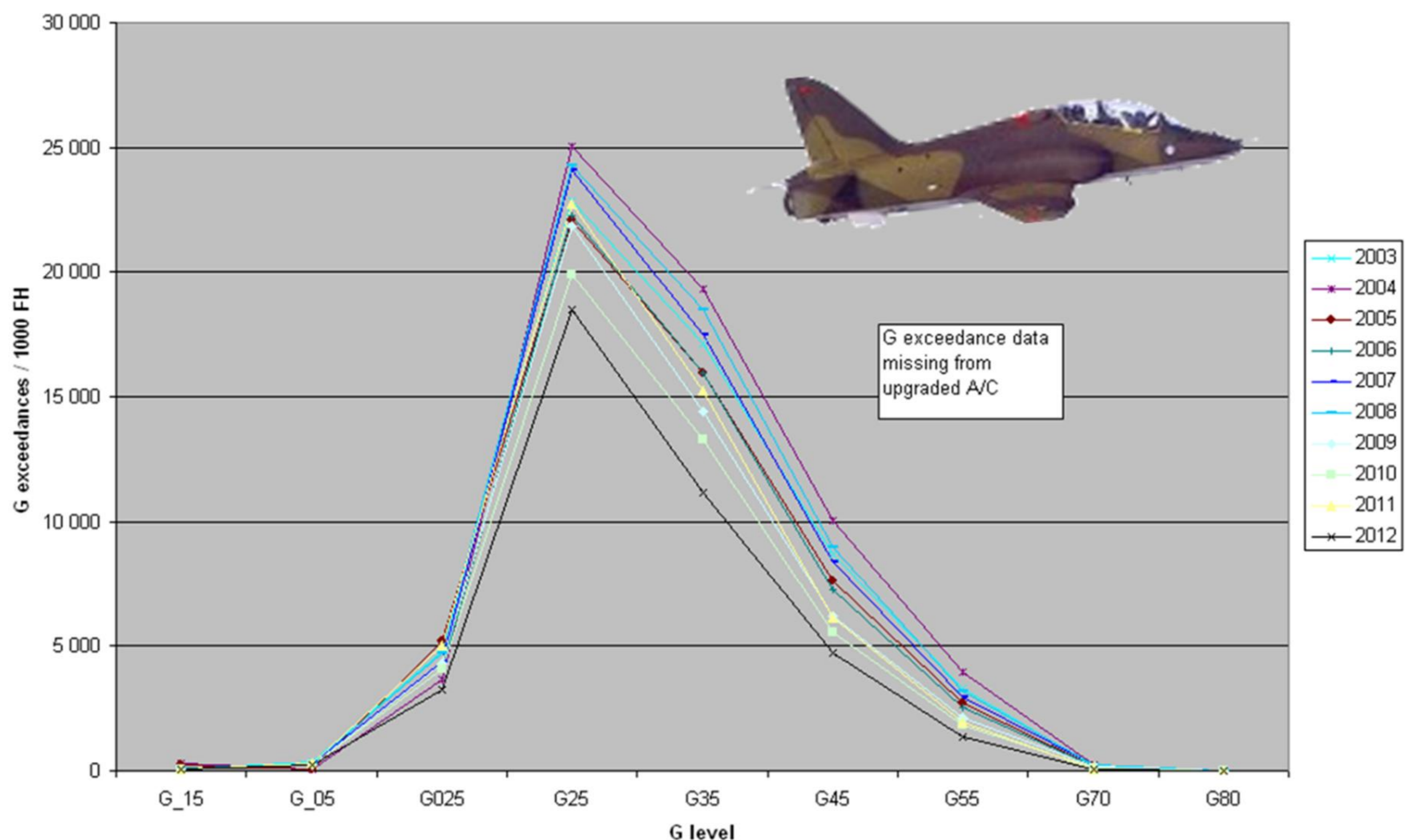


Figure 4: *G exceedance development of the FINAF Hawks (Mk.51 & Mk.51A) at the end of year 2012 (fleet average; data from all 57 aircraft included (excluding the modified Mk.66 aircraft), as ranked according to the a/c center of gravity normal acceleration. Note that all of the FINAF Hawks have been operating from the Kauhava air base since the end of 2005. Picture by courtesy of the FINAF.*

13.1.3 F-18C/D Hornet

Between 2012-2015, Patria will conduct the Mid-Life Upgrade 2 (MLU2) systems upgrade's series installations for the first 35 FINAF Hornet fighters and related manufacturing of components and harnesses. The work will take place in conjunction with scheduled maintenance and structural updates of the aircraft. The goal of the FINAF is to upgrade all of its 62 fighters by the end of 2016. Patria has earlier implemented the first systems upgrade (MLU1) between 2007-2010 and performed the final assembly and testing of 57 single-seat F-18 C models when the fighters were purchase [4].

After the MLU2 upgrade the FINAF Hornets will have the ability to perform air-to-ground operations. This will reflect on training programs and the use of the aircraft. Other significant upgrades are, for example, the cockpit upgrade with new displays and the BOL countermeasures dispensers. There are special arrangements to manage the C and D model differences between the USN and the FINAF in the MLU2-induced configurations: The software testing will be done in Finland by the FINAFFTC and Patria's STIC laboratory (Software Test and Integration Centre). For the first time in the history of the Hornet, there is a foreign (Finnish) organization approved as a part of the approval process of the US software. The MLU2 preparation work is done in co-operation with the Swiss Air Force.

The current structural life consumption of the FINAF F-18 fleet is shown in **Fig. 5**. As presented in the figure, the aircraft usage seems less severe than the design target. However, when compared to other F-18 operators the usage is more severe. The current target for the FINAF F-18 aircraft is 4500 FH and 0.75 FLE (simultaneously).

It is worth noting that the structural life consumption (Fig. 5) is mainly decided based on a single detail of structure. The data collected from the said detail is processed by a piece of software

provided by the aircraft manufacturer. As a result the structural life consumption for each aircraft in fleet is given. Recently a new version of the software was taken into use by the FINAF and on average the results were lower for structural life consumption than using the previous software version.

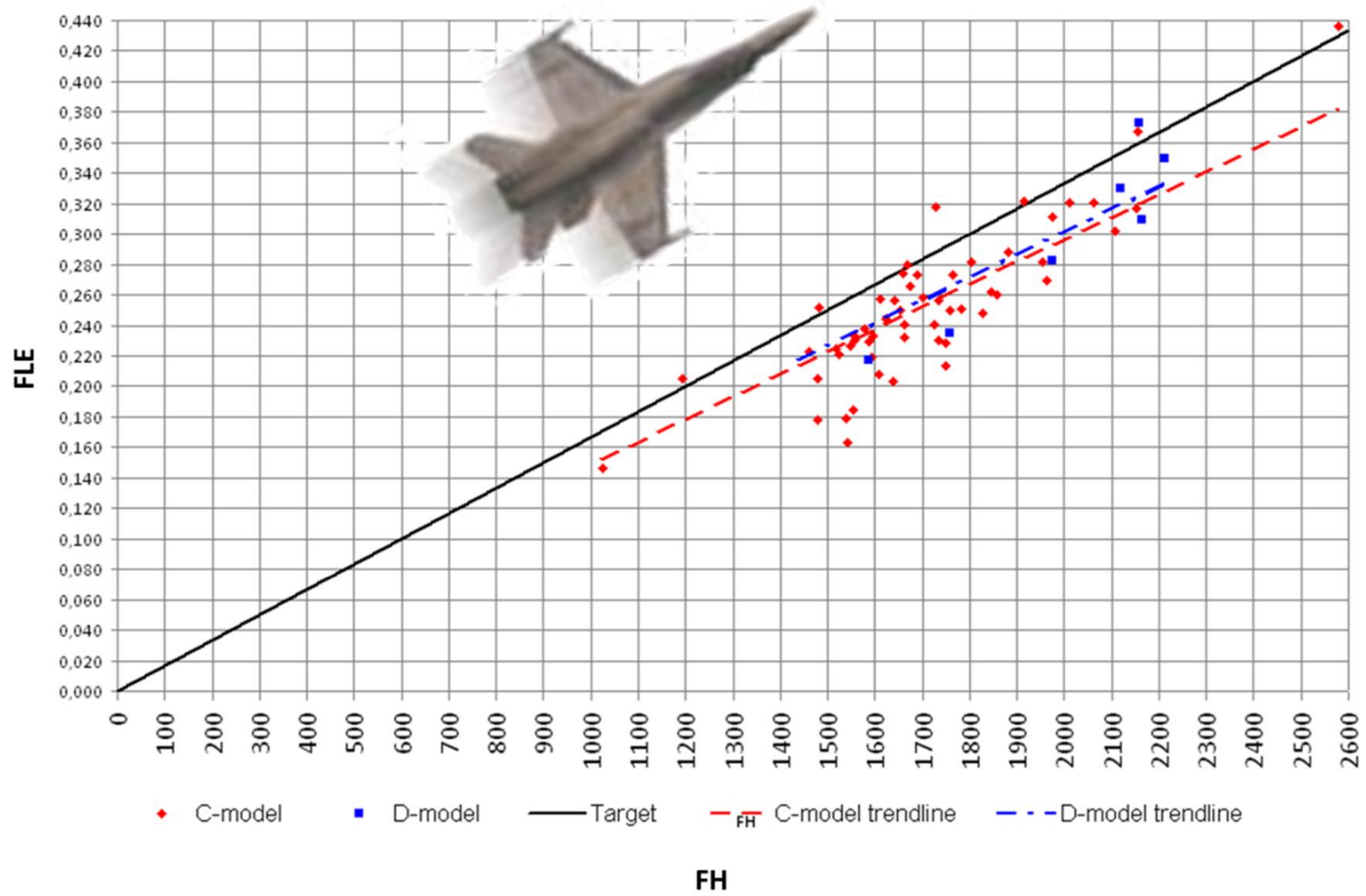


Figure 5: Summary of the wing root fatigue life expended (FLE) of the FINAF F-18C/D fleet at the end of year 2012. The data is from all 62 aircraft included. The target is 4500 FH and simultaneously 0.75 FLE. Picture by courtesy of the FINAF.

13.1.4 Scope of the review

This national review on aeronautical fatigue concentrates on the fixed wing aircraft inventory of the FINAF related to fighter jets and associated pilot training aircraft. The FINAF inventory today includes 62 F-18C/D Hornet fighters, 48 Mk.51 Hawk jet trainers (+18 Mk.66 aircraft from Switzerland) and 28 Valmet Vinka primary trainers. During the writing of this review, approximately 124 000 FH have been flown with the Hornets, 236 000 FH with the Mk.51 and Mk.51A Hawks (+20 000 FH Mk.66 Hawks) and 163 000 FH with the Vinkas.

No FINAF aircraft of these type designations have been lost due to structural issues.

The severity of the Finnish usage in view of structural fatigue with the two jets of noteworthy maneuvering capability can be seen in *Fig. 4* (Hawk) and *Fig. 5* (Hornet). Figs. 4 and 5 clearly demonstrate the need to maintain, further develop and apply concrete and systematic efforts to cope with the structural deterioration effects of these two aircraft types.

During 2005, the International Committee on Aeronautical Fatigue (ICAF) formally welcomed Finland as a full member of the ICAF, making Finland the 13th full member. This Finnish national review of current aeronautical fatigue investigations up to February 2013 – although the 7th review but the 4th review as a full member – was compiled by Aslak Siljander (VTT).

The review comprises inputs from the organizations listed below (in alphabetical order).

Emmecon	Emmecon Ltd, P. O. Box 35, FI-53851 Lappeenranta, Finland (http://www.emmecon.fi/)
FINAFMC	The Finnish Air Force Materiel Command, P. O. Box 210, FI-33101 Tampere, Finland. The Finnish Air Force Materiel Command, Programmes Division, Aircraft Section, P. O. Box 14, FI-41161 Tikkakoski; Finland. (http://www.ilmavoimat.fi/index_en.php)
Finflo	Finflo Ltd, Tekniikantie 12, FI-02150 Espoo, Finland (http://www.finflo.fi/)
Millidyne	Millidyne Ltd, Hermiankatu 6A, FI-33720 Tampere (www.millidyne.fi)
Patria	Patria Aviation Oy, RTD & Aeronautical Engineering, FI-35600 Halli, Finland (http://www.patria.fi/index2.htm)
Aalto	Aalto University, School of Engineering, Department of Applied Mechanics, Aeronautical Engineering, PO Box 14300, Puumiehenkuja 5 A , FI-00076 Aalto, Finland (http://appmech.tkk.fi/en/research/research_group1/)
TUT/DSP	Tampere University of Technology, Department of Signal Processing, Korkeakoulunkatu 1, FI-33720 Tampere, Finland (http://sp.cs.tut.fi)
TUT/DMS	Tampere University of Technology, Department of Materials Science, Korkeakoulunkatu 6, FI-33720 Tampere, Finland (http://www.tut.fi)
TUT/IHA	Tampere University of Technology, Department of Intelligent Hydraulics and Automation, P.O. Box 589, FI-33101 Tampere, Finland (http://www.iha.tut.fi/research/aircraft/)
VTT	VTT Machine and Vehicle Industries, P. O. Box 1000, FI-02044 VTT, Finland (http://www.vtt.fi/?lang=en)

13.2 Current activities: ASIMP 2010-2012 and ASIMP 2013-2016

The Aircraft Structural Integrity Management Program (ASIMP) 2010-2012, as briefly outlined in [4], has been completed. The follow-on program, the ASIMP 2013-2016 with its various sub-programs, is about to start. An attempt is provided below to provide highlights of the ASIMP 2010-2012 achievements, including those from the parallel research programs.

13.2.1 Loads and stresses

13.2.1.1 Computational fluid dynamics (CFD) – update

13.2.1.1.1 Flow simulations for NH90 helicopter fuselage with an actuator disc

Previous CFD activities (flow simulations) have been reported in e.g. [4 Chapter 13.2.1.1]. In the ICAF 2011 report, time-accurate CFD studies for a helicopter rotor in forward flight were described to demonstrate the capability for dynamic rotor studies. Since then, the helicopter CFD work has concentrated on modelling the flowfield around the NH90 fuselage to be able to study local modification effects and loads related to them. The work has been done in co-operation with Finflo Oy, Espoo. For this purpose, a structured multi-block grid [5] was generated around the fuselage based on a representative geometric model created earlier at Patria. The grid covers the whole asymmetric fuselage with its tail surfaces and contains some of the larger antennas and a simplified axisymmetric main rotor hub. Flows through the engine inlets and exhausts are specified via boundary conditions. The fuselage grid consists of 99 blocks and has around 17 million cells.

As the flow induced by the main rotor plays an important role in the fuselage flowfield, the rotor effects are taken into account in the simulations by an actuator disc model [6]. The main rotor is represented by an axisymmetric overset grid block that covers the aerodynamic parts of the blades. The rotor can be tilted as desired and have a cone angle. On the circular rotor disc plane itself, analytical time-averaged distributions of axial, tangential and radial flow forcing actions are calculated as functions of the prescribed thrust resultant and flight conditions based on a classic rotor theory. The effects are fed into the Navier-Stokes simulations via source terms of the momentum and energy equations. The grid block for the disc contains just about 0.33 million cells.

Test calculations for the NH90 [7] were performed with the domestic RANS-type FINFLO flow solver in two conditions representing level flight at 132 kt and hover. The computations aiming at steady states by pseudo-time integrations took long times to converge, and the solutions remained somewhat oscillatory. This was to be expected, since the helicopter with its rotor hub, exhaust stacks and some bulky antennas is not particularly streamlined. Especially the hover case with the fuselage perpendicular to the rotor outflow represents the boundaries of meaningful time-averaged simulations.

In cruise at zero angle of attack, the lift of the fuselage is negative and is caused by its shape with little rotor influence. The computed lift magnitude corresponds to about 7 per cent of the helicopter weight. The fuselage drag is about the same as the horizontal component of the thrust vector tilted 4 degrees forward. The results conform to expectations, but there are no real data available for validation. The computed flowfield is illustrated in *Fig. 6* by the pressure distribution on the fuselage, Mach number distribution on the nominal symmetry plane, vertical velocities on the rotor plane and by some streamlines.

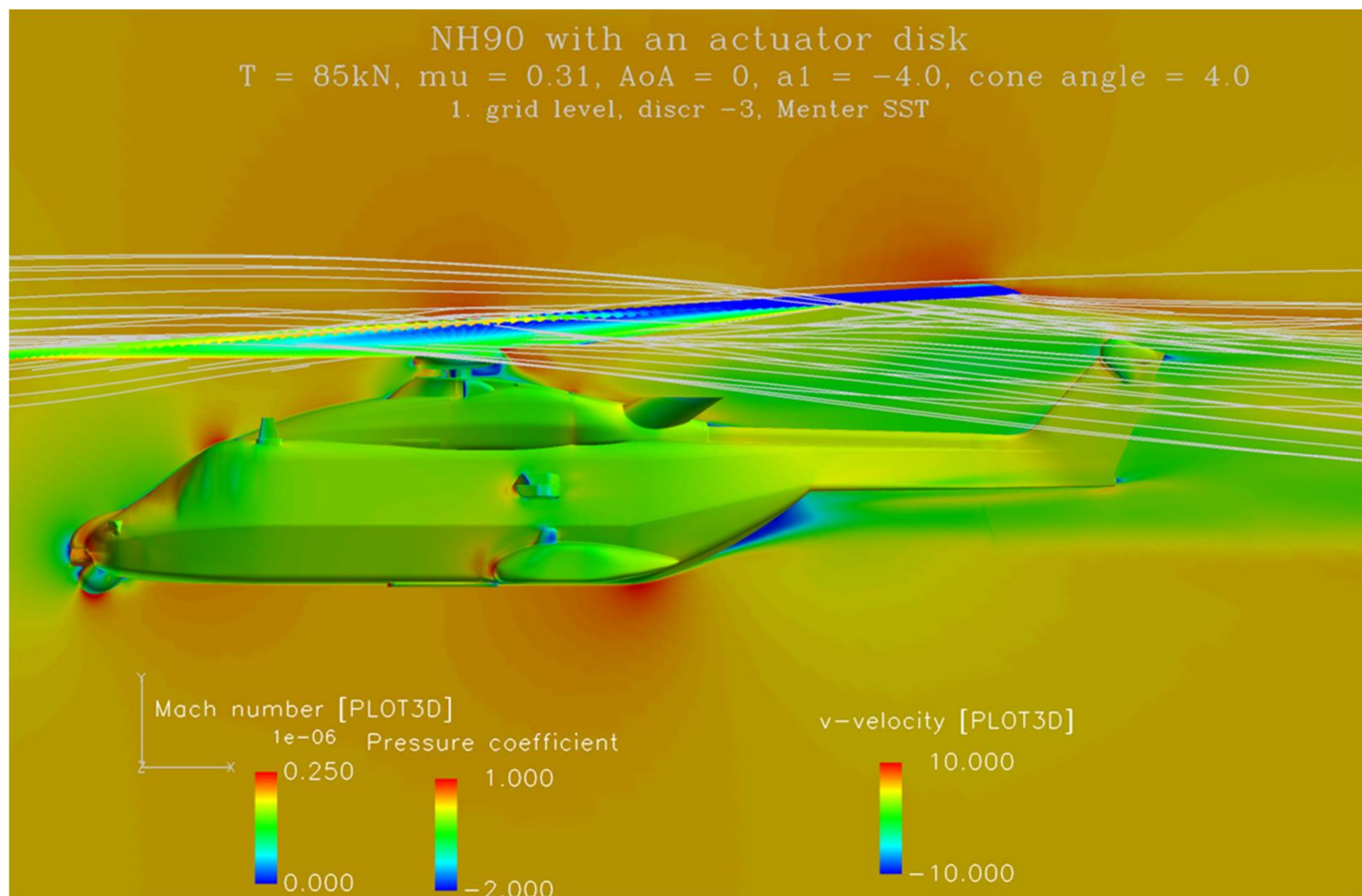


Figure 6: Computed flowfield around NH90 in cruise. Picture by courtesy of Patria Aviation.

In the hover case, the averaged down-force acting on the fuselage and entirely caused by the rotor blowing again represents about 7 per cent of the helicopter weight, and the horizontal forces are small. Also the moment balance is reasonably good. **Fig. 7** shows the fuselage pressure distribution and vertical velocity on the rotor plane and on a plane 6 meters below the fuselage. It is clearly seen that the fuselage disturbs the rotor outflow strongly and the pattern below the helicopter is far from axisymmetric. On the rotor disc plane, the distortion effects of the fuselage are also clearly visible

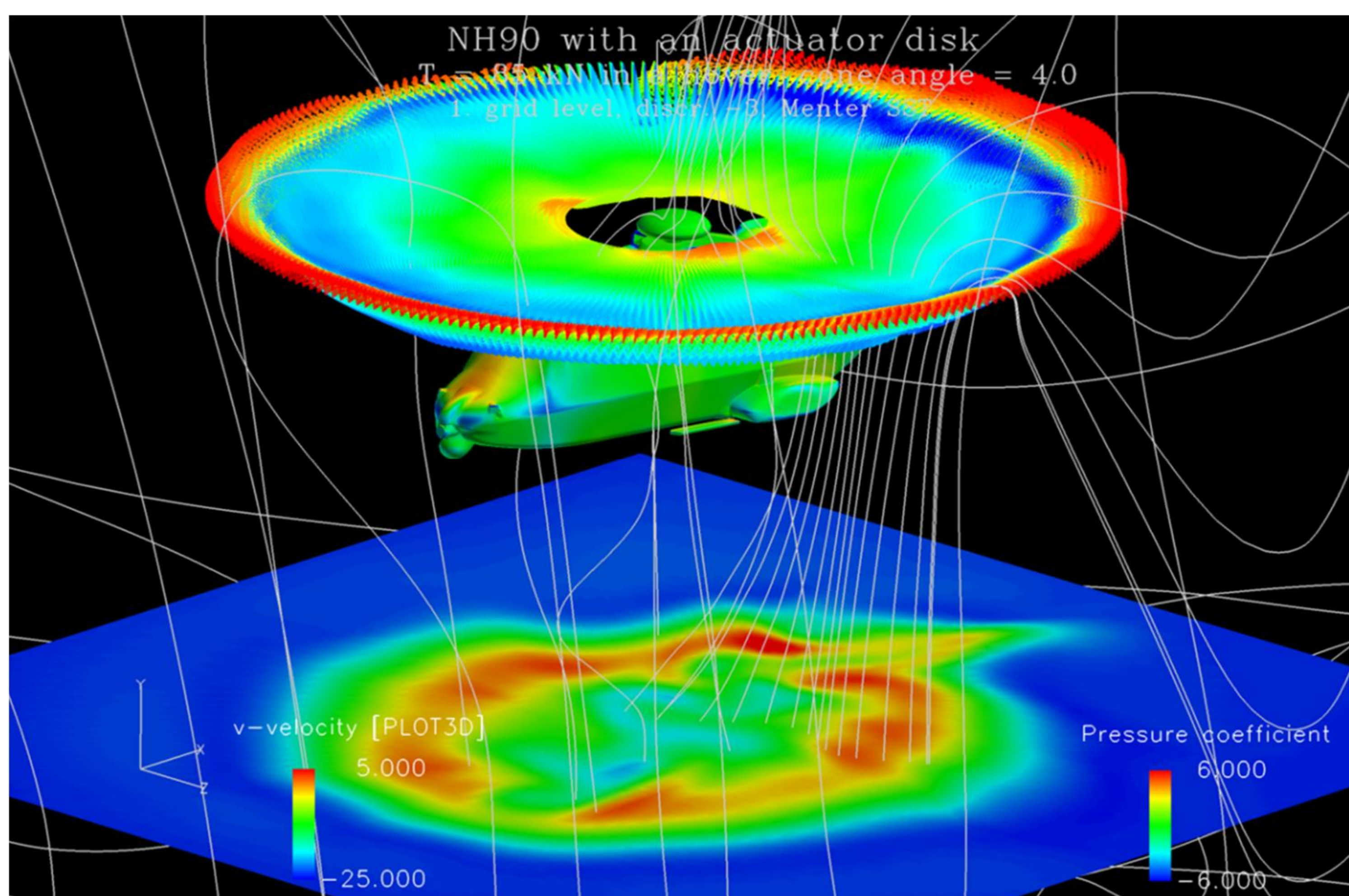


Figure 7: Computed flowfield around NH90 and on a horizontal plane below it in hover. Picture by courtesy of Patria Aviation.

13.2.1.1.2 Computational Fluid Dynamics activities at Finflo Ltd.

Computational fluid dynamics (CFD) research at Finflo Ltd. is based on the in-house flow solver FINFLO. An essential feature of the code is a Chimera method applied in simulating flow fields around the FINAF F-18C fighter. Basic features of the method are described in [8]. Since then, significant improvements have been made in the algorithm. The Chimera method currently utilizes accurate wall distances, a refined interpolation method and completely new dominating criteria for the overlapping grid blocks. The computation of the wall distances is time-consuming, but the procedure has been significantly enhanced during the recent years. In 2010 a new high-resolution grid for the F-18C was developed and considerable improvement has been obtained in the accuracy of the Chimera interpolation in the narrow gaps between the flaps and the wing. The repetition task of all previously simulated flight conditions using the new grid was completed in 2012.

As a part of the FINAF Hornet Mid Life Upgrade 2 (MLU2) Program, the FINAF is currently integrating the BOL countermeasures dispensing system (CMDS) from the Swedish defence and security company Saab on the F-18 Hornet fighter. The BOL CMDS protects the aircraft against heat-seeking and radar guided missiles. The BOL system uses wing-tip vortices to distribute the chaff- and IR payload, which improves dispersion and the rapid formation of a protective cloud. As a part of the integration program, CFD studies were used to estimate the effect of the BOL cassettes and BOL adapter covers on the shock waves and on the external loads, *Fig. 8*.

Co-operation with CFSE and RUAG of Switzerland has been continued. Meetings have been arranged to handle technical aspects and general CFD development. Recently the FINFLO and the NSMB codes were evaluated by calculating two flow cases at a high angle of attack for the F/A-18. The results were presented in ICAS 2012 Congress in Brisbane, Australia [9].

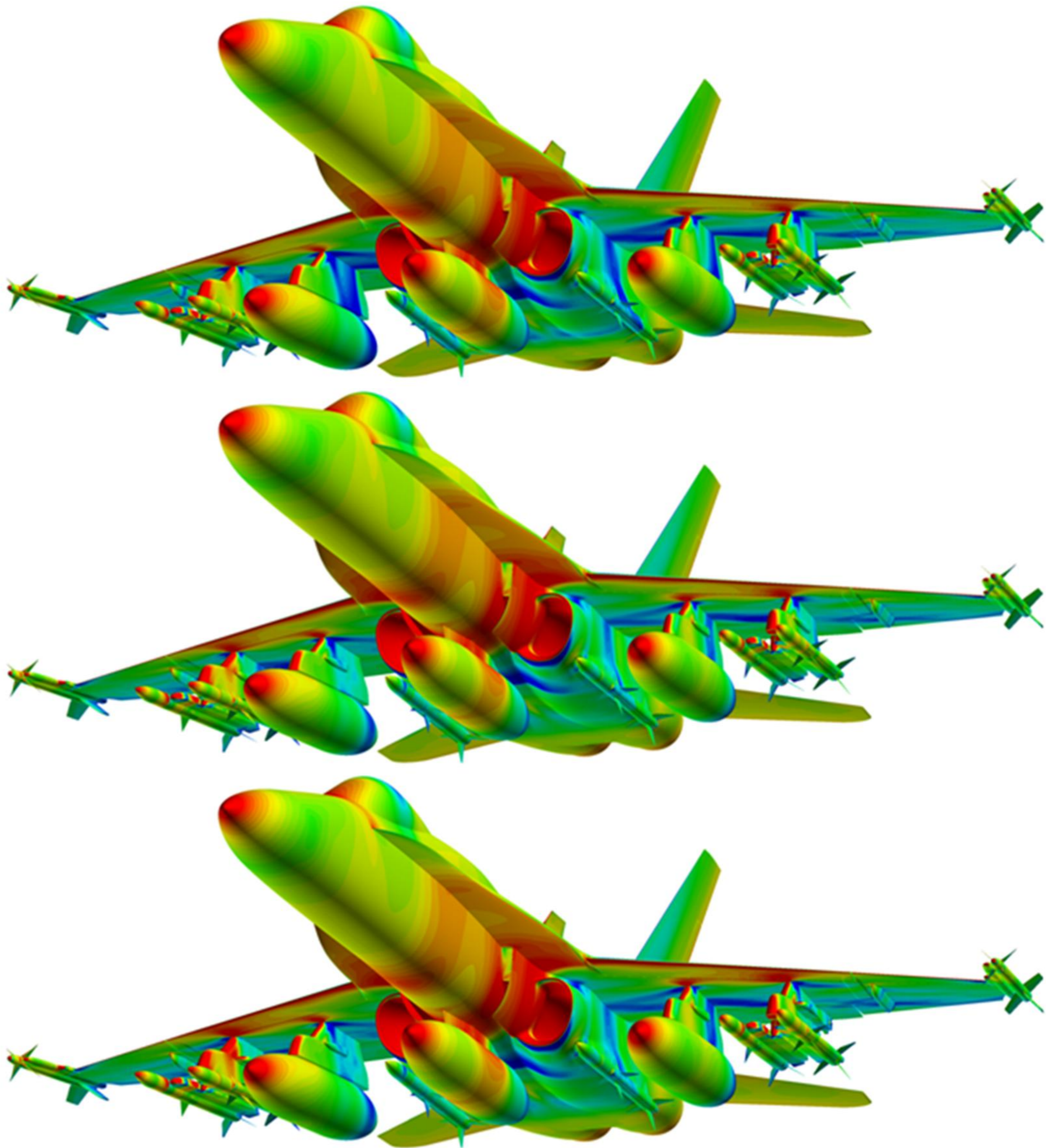


Figure 8: *A pressure distribution on a complex F-18C configuration. Clean wing pylon sides (top), modified wing pylons equipped with BOL adapter covers (middle), and BOL cassette pairs on sides of the outboard wing pylons and adapter cover pairs on sides of the inboard wing pylon (bottom). Level flight at $Ma=0.95$. Picture by courtesy of Finflo Ltd.*

13.2.1.1.3 Initial value provisions for the F-18 CFD analyses

One crucial step prior running computational fluid dynamics (CFD) analyses for the aircraft is to set the aircraft model in question into equilibrium. This can be executed by the recently developed trim routine [4 Chapter 13.2.1.2.3] or by the OEM's software. In the given flight condition, aircraft's state (flight parameters), control surface deflections and engine properties like net thrust and exhaust nozzle properties can be obtained as a result of the trimming.

During the last research period VTT supplied initial values to Finflo Ltd. for the CFD analyses of the Finnish F-18 Hornet. In 8 of 11 cases the aircraft was in so called Fighter Escort configuration and 3 cases include non-default configurations [10].

13.2.1.2 Flight simulations

As it has been outlined in e.g. [2 Chapter 13.2.1.2], the flight simulations have been utilized in various projects to support the structural life management of the Finnish F-18 Hornet aircraft. For this purpose, the FINAF has continued the funding of the development and maintenance of the low-cost Matlab/Simulink based flight simulation software called HUTFLY2. The program's modular design allows the implementing of different aircraft models into it. Currently the most important one is the F-18C aircraft model [11 - 14].

In order to maintain the flight simulation results as realistic as possible for the actual FINAF flying, some upgrades have been implemented into the HUTFLY2 software recently [15, 16]. Among the listed items in [2 Chapter 13.2.1.2] is the Flight Control System (FCS) model which has been upgraded along the real life counterpart during the last research period [17].

The F/A-18 Flight Control System (FCS) is a fly-by-wire Control Augmentation System (CAS) whose inner loop has been divided into longitudinal, lateral and directional control law computations. The control laws are reconfigured for the Auto Flap Up (AFU, up and away flight) and Power Approach (PA, takeoff and landing) flight phases.

The existing Simulink-model of the HUTFLY2 F-18 Flight Control System (FCS) was upgraded from the Flight Control Computer (FCC) Operation Flight Program (OFP) version V10.5.1 to version V10.7 according to the Original Equipment Manufacturer's (OEM) documentation [17, 18]. The digital inner loop control laws have been modeled as a continuous system instead of the initial multi-rate discrete version. The upgraded model consists of approx. 5200 blocks, including sensor models and hydraulic servo-actuator (high order) models. In addition to the Auto Flap Up flight mode, the Power Approach flight mode has been taken into account but automatic flight control modes (outer loop), out of control flight mode and degraded flight control modes (i.e. failure logics) have been excluded from the model because their impact on the structural research of the Finnish F-18 aircraft is considered to be of minor importance. As an output the FCS model provides command values for the control surface actuators from the pilot inputs.

The essential phase in the development of the system is verification and validation (ver/val). Validation is yet to be done. At the moment, verification of the upgraded FCS model includes the time history comparisons of the given pilot inputs. For example response of the directional control (i.e. rudder) doublet without aerodynamics can be seen from **Fig. 9**. From the figure it can be seen that for the same input, the commanded rudder deflections are smaller in the upgraded FCS version than in the reference version due to the increased full pedal input departure resistance. Rate limiters have been remained the same which is manifested by the identical slopes of the responses.

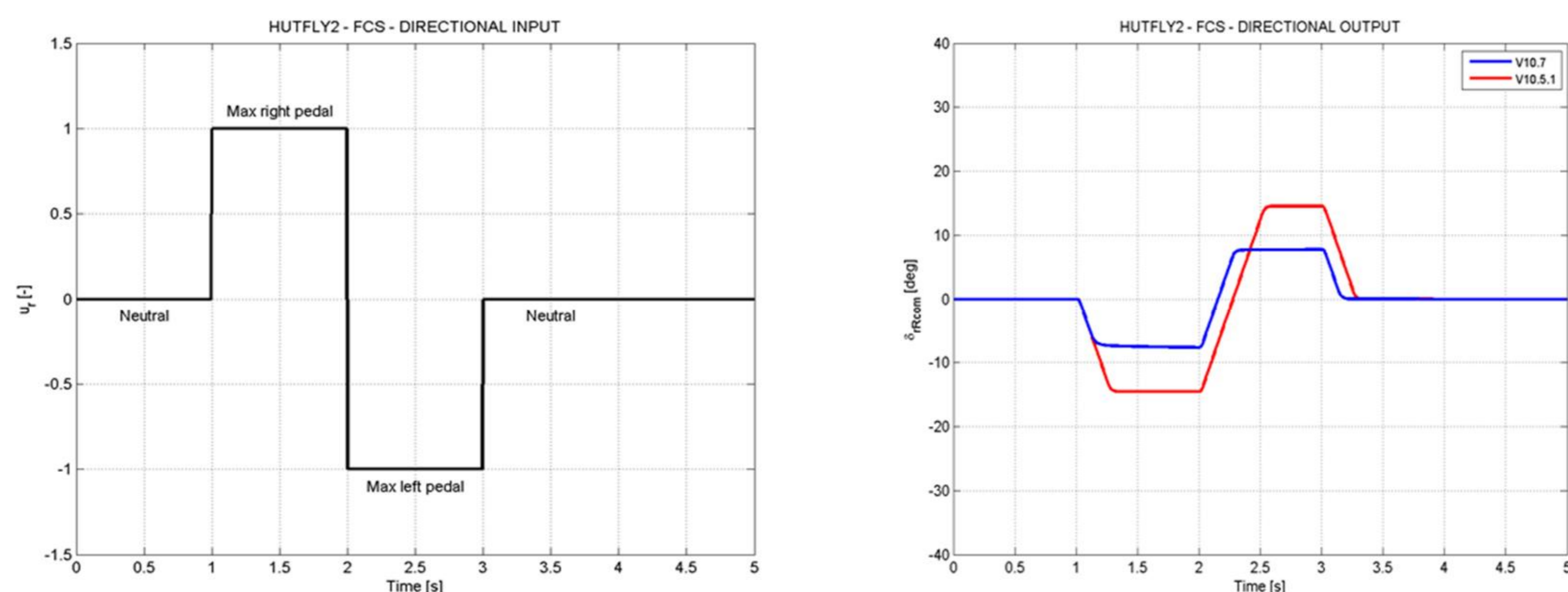


Figure 9: Right rudder actuator command as a response (output; shown right) for the normalized directional control doublet (input, shown left). In output, the red line represents the actuator command from the reference FCS V10.5.1 –model and the blue line represents the command from the upgraded FCS V10.7 –model. Picture by courtesy of VTT.

13.2.1.3 Hornet FE modeling – update

Previous development phases of the global and detailed finite element (FE) modeling of the FINAF F-18C Hornet have been outlined in [4 Chapter 13.2.1.3]. Since then some new detailed FE models have been prepared: former Y508 shear tie [19], inner wing aft closure rib [20] and outer wing missile rib [21], *Fig. 10*. Geometry modeling of the previously prepared horizontal tail spindle box detailed FE model was enhanced at the spindle root area and the new fatigue life estimates showed it to be clearly Full Life in FINAF usage [22].

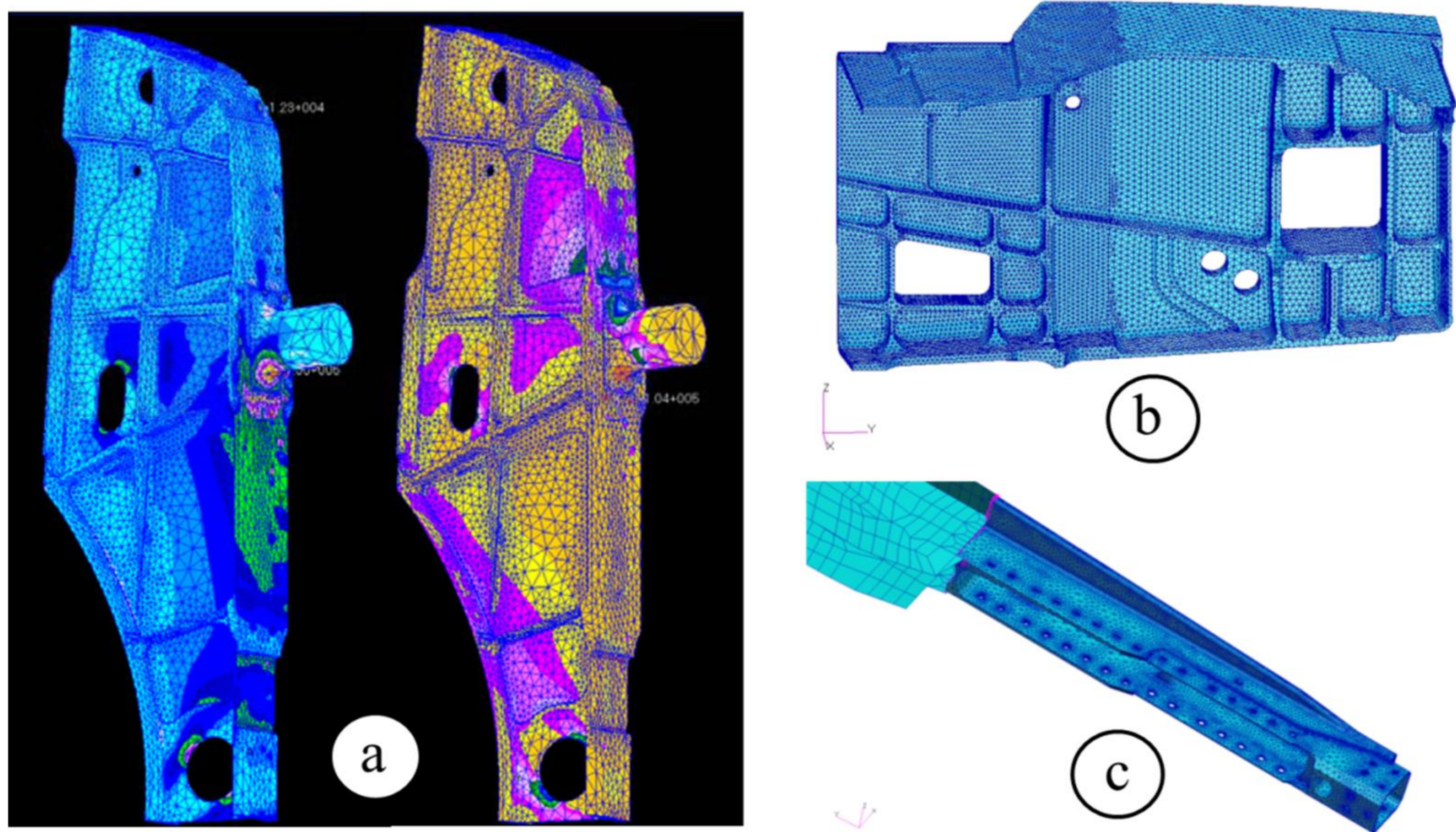


Figure 10: Detailed FE models: *a) former Y508 shear tie, b) inner wing aft closure rib, and c) outer wing missile rib. Picture by courtesy of Patria Aviation.*

The previously FE-modeled structural details of inner wing fold rib, inner wing shear tie, engine door former Y657, upper inboard longeron (dorsal longeron), upper outboard longeron, vertical tail stub Y590, horizontal tail spindle box, former Y488 main landing gear well area, outer wing fold rib and horizontal tail bootstrap were reanalyzed (FE-analyses, transfer functions and life estimates) using the new enhanced FINFLO-3g CFD-model (see Chapter 13.2.1.1.2) aerodynamic loads for 14 different flight conditions [23 - 25].

The fatigue life estimates for all structural locations above have been determined with applicable strain gauge data of 10 Mini-HOLM 1 test flights representing FINAF average usage [26 Chapter 13.5.1.3.1]. These locations have also been included under continuous monitoring in the HOLM (two special instrumented a/c, see [4 Chapter 13.2.2.1]) and the parameter based (whole fleet, see [4 Chapter 13.2.2.3]) fatigue tracking systems.

13.2.2 Fatigue tracking systems

13.2.2.1 FINAF F-18 HOLM jets in routine squadron service

Previous research activities of the two FINAF F-18 HOLM (Hornet Operational Loads Measurement program) jets can be found in [4 Chapter 13.2.2.1]. Like the other Hornets, the two HOLM jets, the tail numbers HN-432 and HN-416, are rotated in the Satakunta, Lapland and Karelian Air Commands.

The “production” version of the HOLM onboard system has collected statistically reliable flight data from routine fleet usage of the FINAF since 2006. The flights are analyzed continuously at VTT as the flight data is delivered from the FINAF squadrons to VTT:

- Up to 1054 flights (HN-416/425 flights + HN-432/632 flights) were analyzed and reported in [27].
- Up to 1325 flights (HN-416/495 flights + HN-432/830 flights) were analyzed and reported in [28].
- Up to 1554 flights (HN-416/620 flights + HN-432/934 flights) were analyzed and reported in [29].
- A new version for the “executive summary” of all in-country analysis results concerning FINAF F/A-18 fatigue management was proposed by VTT [30]. The “executive summary” provides a quick visualization of the key findings from the in-country fatigue tracking results (SAFE + parameter based fatigue life analysis + HOLM), see *Fig. 11*.

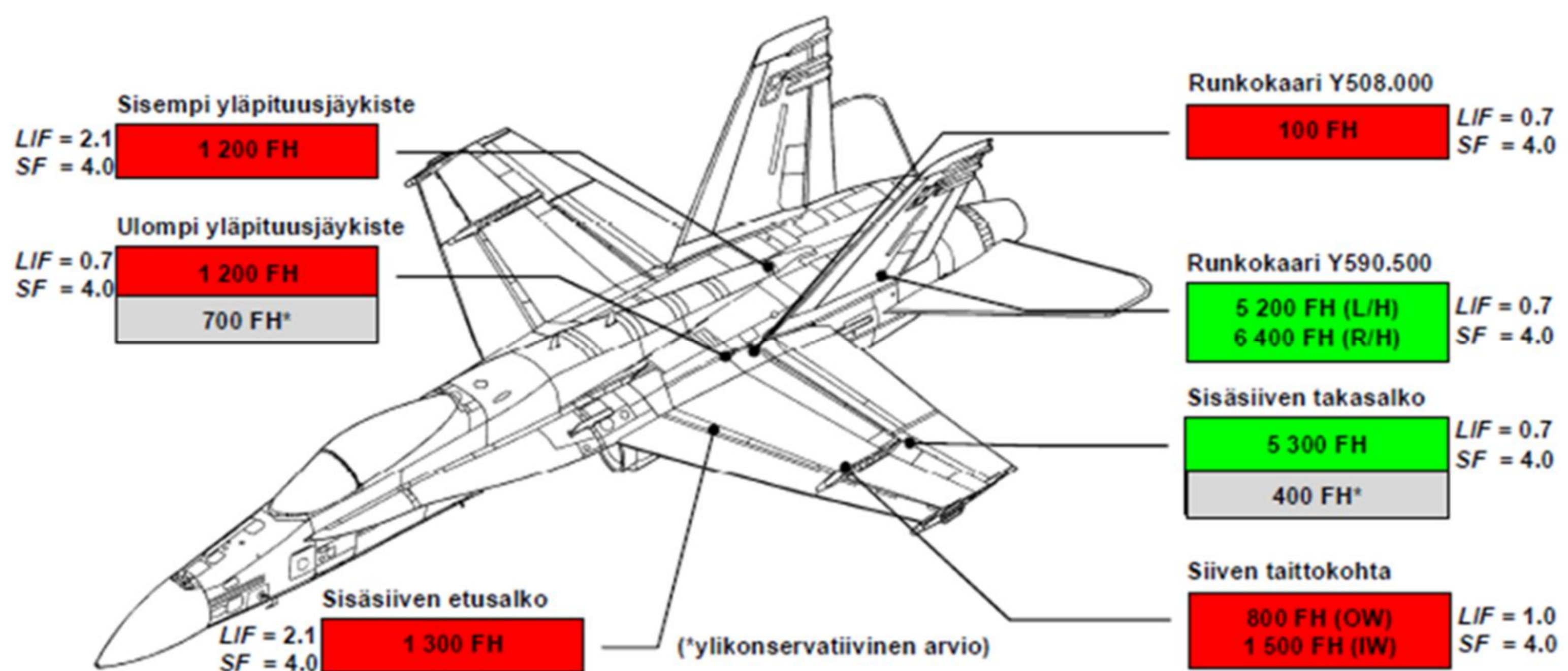


Figure 11: An overview of some of the shortest calculated life estimates (100 FH accuracy) of the two HOLM jets. SF = scatter factor, LIF = life improvement factor. Red = life below 3750 FH, green = life above 4275 FH, grey = overly conservative estimate [29]. Picture by courtesy of VTT.

- The onboard HOLM instrumentation is periodically calibrated by VTT. The annual electrical calibration of HN-416 and HN-432 reveals if any changes have occurred or the calibration coefficients need to be adjusted. Based on the calibration results from the recent years e.g. [31, 32], the quality of the system is outstanding: the quality of the strain signals is good (no spikes found) and all the recordable strain data has been captured (minimal missing data). This all forms a good base for all the analyses that are made based on the HOLM data.
- The HOLM fatigue analysis database has been updated [33]. The database works seamlessly with the data from the HOLM ground analysis environment. In addition to data from the

fatigue tracking system the database includes all the needed information from the data analysis process.

13.2.2.1.1 Vertical tail measurements of International Mini-HOLM flights

It has become evident that the Finnish Air Force (FINAF) long-time high-AOA usage decreases the fatigue life of the vertical tail. The time spent in the structurally challenging AOA-Q combinations is higher than that in most other F/A-18 countries. Current FINAF flying is reflected as ever-increasing external signs of emerging structural fatigue concerns, namely the loose "leaking" fasteners in the vertical tail (VT) area. These structural effects on the VTs need to be studied in more detail. One step prior to measurement modifications of the HOLM system was to get deeper understanding of dynamics of the F-18 ASPJ vertical tail and to compare the results with the OEM's SAFE software.

As a part of the FISIF cooperation, the FINAF conducted a special flight test program in December 2005, in which inputs from the other F/A-18 operators were included [26 Chapter 13.5.1.3.2]. The measured data (without any analysis results) from these International Mini-HOLM Flights was provided to the FISIF partners to be used as they see fit [34]. RUAG Aerospace analyzed the data against the SAFE software results and concluded that the analytical spectra obtained from the SAFE software is more severe than that obtained from the flight test data. Thus, unrealistically low life estimates of the VT would be obtained with the SAFE-derived spectra.

The data from the three International Mini-HOLM flights were analyzed [35]. The results showed that the dynamical behavior of the VT agrees with the OEM's analyses. Analytically generated dynamic spectra (SAFE results provided by Patria) of the VT typically matched well with that obtained from the measured accelerations. Also Peak-Valley exceedance curves based on the measured VT acceleration were well in line with RUAG's results (different SAFE version than that used by Patria). As a conclusion, three important points can be raised on the basis of the analyses of this study:

1. The analytical dynamic spectrum of the reference location in general is not more severe than that created from the measured acceleration signal.
2. The analytical spectrum contains values that did not occur in reality, as manifested by the flight measurements data used.
3. The use of the analytically derived dynamic spectrum provides conservative life estimation values.

On the basis of the results obtained using only a limited number of flights data, a decision was made within the FINAF that the HOLM system need to be upgraded, see Chapter 13.2.2.1.2.

13.2.2.1.2 HOLM modification

Two FINAF F18C Hornets (HN-416, HN-432) have been equipped with the Hornet Operational Loads Measurement (HOLM) system. The on-board HOLM system configuration consist of 36 strain channels with over 200 aircraft parameters (MIL-1553 bus) in each of the two jets with which in-flight data from normal FINAF squadron use have been collected since 2006. The main goal in the HOLM program was to get to a position in which there is the necessary in-country capability to analyze how Finnish flying consumes the structural life of the Hornets. The goal was planned to be achieved by combining the information from only two HOLM aircraft equipped with the onboard fatigue tracking system, and by combining these data with those obtained from other projects/sources e.g. the parameter based fatigue life analysis (NN – neural network) [4 Chapter 13.2.2.3], the structural life consumption of the whole FINAF F18 fleet could be evaluated with adequate reliability, *Fig. 12*. Further details, background including the feasibility phases of the prototype design have been reported earlier e.g. [4 Chapter 13.2.2, 26 Chapter 13.5.1.3.3].

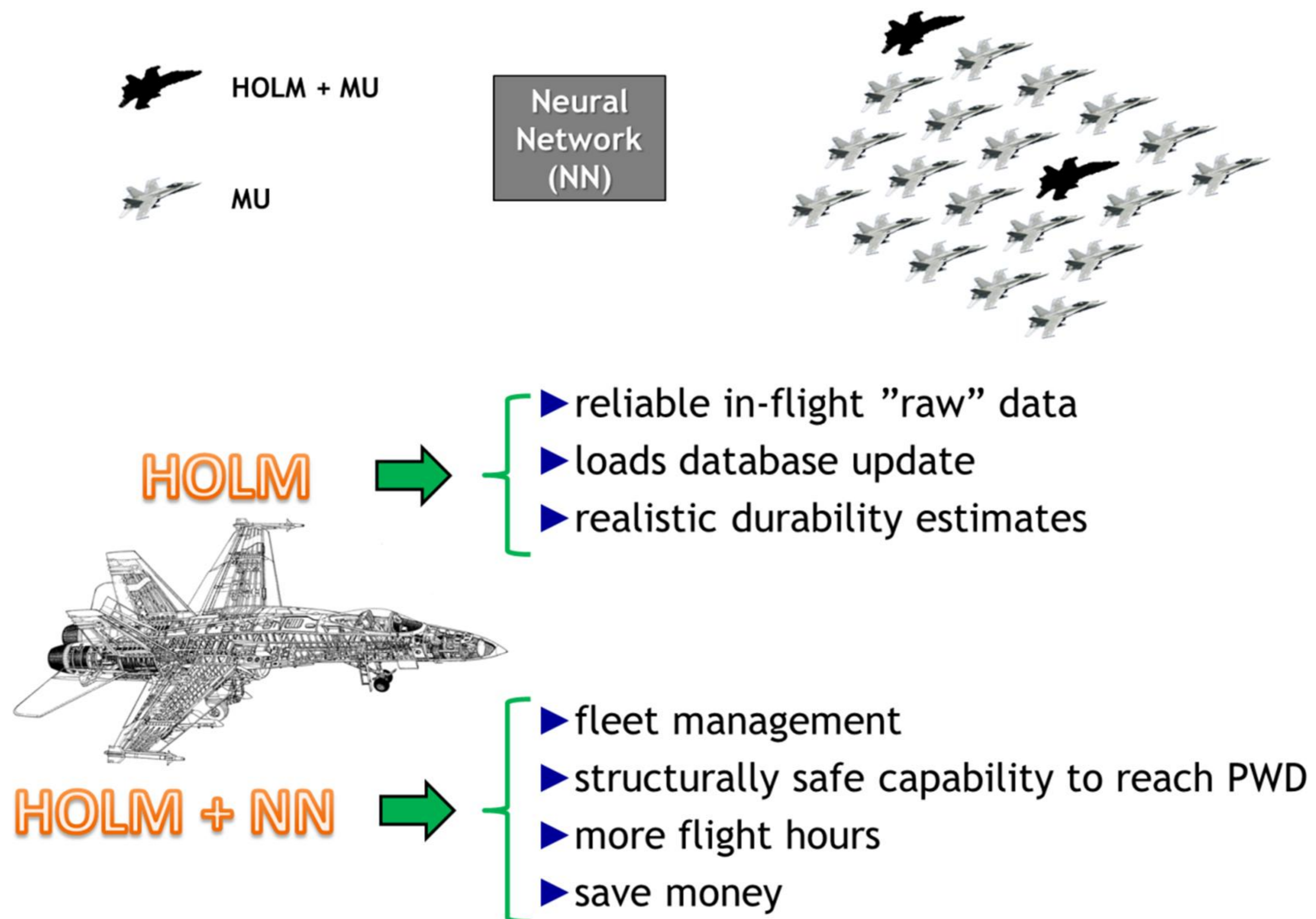


Figure 12: An overview of the Finnish “domestic fleet management system”, with which the risk associated with structural integrity can be minimized by managing the activities needed to reach the planned withdrawal date [36, 37]. Picture by courtesy of VTT and Patria Aviation Oy.

To account for the increased buffet-induced dynamic stressing of the FY508 and the vertical tail regions of the FINAF F/A-18 Hornets, a decision was made during 2011 to begin a project to modify the existing on-board HOLM system. In the project design phase e.g. [38 – 42, 57] it was agreed to add 12 new channels (8 strains + 4 accelerations) in the HOLM system. The existing data acquisition system was upgraded. The project contained design, implementation and testing activities for the upgraded measuring system. During the writing of this review, Patria and VTT are performing "ready to fly" installation for HN-416 aircraft, where needed new sensors, LRU, system cable harnesses and other needed accessories will be installed, tested and calibrated.

13.2.2.2 Flight maneuver identification (FMI) – update

Previous FMI activities have been reported in e.g. [4 Chapter 13.2.2.2].

Aircraft load history and usage monitoring plays an important role in the case of the FINAF F-18 fleet. The usage of the fleet is quite severe leading to unfavorable FLE trends of several structural areas. In order to ensure the designed lifetime for the aircraft, preventive actions are derived and conducted. One principle for deriving preventive actions is to remove such usage of aircraft that is not justified by operational or training objectives. This calls for detailed knowledge of the usage of the aircraft in different missions and flight conditions. Concerning the FINAF F-18 fleet, the usage data is provided by the HOLM system [2 Chapter 13.2.2.1; 26 Chapter 13.5.1.3] equipped in two dedicated aircraft. The HOLM system records all the necessary flight parameters as well as high-quality strain gauge data of the fatigue critical structural details. It enables reliable estimation of fatigue damage accumulation for each fatigue critical structural detail even for in-flight events and/or maneuvers having duration of seconds.

Patria Aviation, TUT/DSP and VTT, under the FINAF funding, started the research concerning flight maneuver identification and automated flight-maneuver-specific fatigue damage analysis of F-18 in 2007 [2 Chapter 13.2.2.2]. **Fig. 13** illustrates the data mining environment that has been

developed during the research. A template-based procedure for identifying actual in-flight events from flight parameter data [43] and corresponding software, AMANA Detector [44], were proposed in 2009. In 2011, a flight maneuver template library aiming to cover all maneuver types that cause the major FLE to the fatigue-critical structural details of F-18 was considered [45]. In addition, flight-maneuver-specific fatigue estimation methods were discussed in more detail in [45]. The automatic extraction of flight maneuvers from the HOLM data allows performing flight maneuver-specific fatigue assessment and achieving knowledge concerning the fatigue-criticality of various flight maneuver types to each structural detail. The newest block in *Fig. 13* is AMANA Reasoner, software for the reasoning flight parameter based rules for explaining the degree of damage of nominally similar flight maneuvers [46].

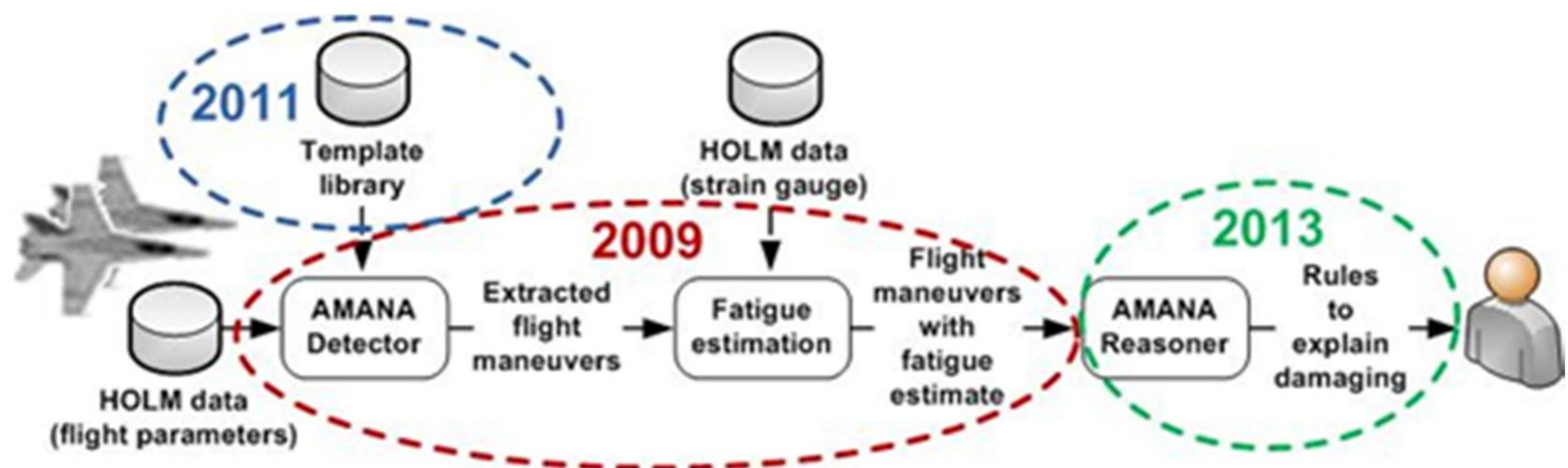


Figure 13: The block diagram of the procedure for flight-maneuver-specific fatigue estimation and rule reasoning. The creation of the template library requires manual work of an analyst, but extraction of flight maneuvers as well as reasoning of the rules, which explain the degree of damage, is performed automatically using the AMANA software. Years in the figure illustrate chronological progress of the procedure development. Picture by courtesy of TUT/DSP.

13.2.2.2.1 Fatigue damage of nominally similar flight maneuvers

The analysis procedure, presented in *Fig. 13*, concentrates on the flight maneuver types that have been found to be the most severe for each critical structural detail in fatigue damage sense. For these maneuver types, the degree of fatigue damage caused by nominally similar maneuver instances can vary considerably. Consequently, reasoning the flight parameter based rules for explaining the degree of fatigue damage can produce valuable information for reducing the fatigue accumulation rate of the structural detail in question. Using the acquired knowledge, pilots could be taught to fly in such a way that minimizes highly damaging actions within maneuvers, i.e. so that flight conditions causing major damage are only rarely or never met. Flight safety, training and operational objectives set their own restrictions that must be taken into account when planning for changes into the syllabus.

Split-s, which can be described as a vertical U-turn, has been found to be a severe flight maneuver type for the vertical tail root. When studying a set of 90 split-s maneuvers extracted from hundreds of HOLM flights, they represent 32% of the total FLE accumulation caused to vertical tail root during the studied HOLM flights [46]. *Fig. 14* shows the FLE histogram and the cumulative FLE curve of vertical tail root for these split-s maneuvers. X-axis of the figure represents fatigue damage. The height of a bar represents the relative proportion of split-s maneuvers whose FLE falls into the histogram bin in question. The cumulative FLE curve visualizes FLE accumulation which is normalized with the total FLE of all the split-s maneuvers. Vertical lines represent median (left) and 90th percentile (right) of the maneuver-specific FLE values. The intersection of the cumulative FLE curve and the 90th percentile line indicates that the most damaging 10% of the split-s maneuvers explain 42% of the total accumulated damage of the extracted split-s maneuvers. Correspondingly, the most damaging 50% of the maneuvers explain 95% of the total FLE.

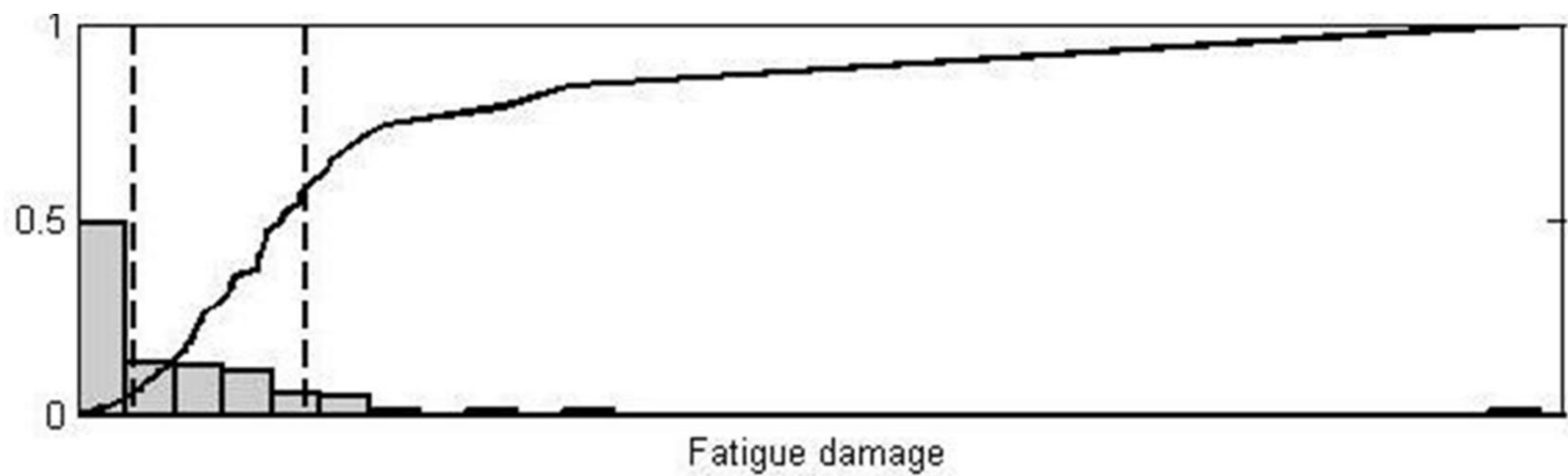


Figure 14: *FLE histogram and cumulative FLE curve for split-s maneuver in the case of vertical tail root [46]. Picture by courtesy of TUT/DSP.*

The FLE distribution of split-s, when plotted in a linear scale, is not narrow but it has a long tail towards high values of fatigue damage. The shape of the FLE histograms concerning many other critical ‘flight maneuver & structural detail’ pairs is similar [46]. This raises questions: what are the crucial actions within the maneuvers that explain the tail of the distribution, and how these actions could be avoided without downgrading the operational capability of the fleet?

13.2.2.2 Reasoning flight parameter based rules that explain the degree of damage

The reasoning of parameter-based rules calls for the analysis of the HOLM data, i.e. the comparison of several flight parameters during each maneuver. When analyzing hundreds of flights, the number of performed nominally similar flight maneuvers varies from tens to thousands depending on the maneuver type. It is evident that when having several interesting flight maneuvers and several critical structural details, the total amount of flight maneuvers to be analyzed and compared is so high that the task is exhaustive to be performed manually. For that reason, the AMANA Reasoner software was developed to automatically compare a set of flight maneuvers of a certain type. The software finds what kind of behavior of flight parameters is common to the most damaging flight maneuver instances, and at the same time, uncommon to the flight maneuver instances that cause minor damage. The reasoning of the optimal rules is implemented using genetic programming and fuzzy logic. The resulting rules categorize flight maneuver instances as causing either major or minor damage.

The case of split-s and vertical tail root has served as validation for the AMANA Reasoner software, because the case had earlier been studied by an experienced analyst with a pilot’s background. The conclusions drawn from manual analysis were similar thus proving the applicability of automated rule reasoning. The major advantage of the proposed data mining procedure, compared with manual perusal, is the ability of a computer to process huge amount of digital data. In other words, the idea of the procedure is to reason the rules from the statistically significant number of extracted maneuvers. Consequently, the influence of outliers on the rules is negligible. Instead, the rules characterize common actions or conditions within maneuvers that have a role in damaging of the fatigue-critical structures.

Based on the first experiences of the presented analysis procedure, it may provide important knowledge of aircraft usage and support the fatigue management process. The major challenge in the procedure is diversity of fighter aircraft maneuvering, which complicates the creation of a comprehensive maneuver template library. Due to miscellaneous flying that is not included in the templates, a significant part of the FLE is still unexplained. The analysis of nominally similar maneuvers produces numerical results for damaging and the interpretation of the results plays an important role in the procedure. The next task is to interpret all the reasoning results and to find out what kind of adjustments the acquired knowledge implicates in the pilot training syllabus. The overall goal is to learn to fly certain maneuvers in less damaging way to ensure the designed lifetime of the FINAF F-18 fleet and to reduce its operating costs. More details about the analysis of nominally similar flight maneuvers are provided in [46].

13.2.2.3 Parameter based fatigue life analysis - update

Previous development phases of the parameter based fatigue life analysis system have been presented in [4 Chapters 13.2.2.3-13.2.2.4; 2 Chapters 13.2.2.3-13.2.2.5; 26 Chapter 13.6.3; 47 Chapter 5.3]. The parameter based fatigue life analysis is an individual aircraft fatigue life monitoring system developed for the FINAF F-18 Hornet fleet. It utilizes flight parameter data, stored by standard aircraft systems, and artificial neural networks (ANN) to produce flight-specific fatigue damage. The fatigue damage (Safe-life) estimates are calculated for 15 structural locations; each consisting of 1-3 features (e.g. 3 fastener holes in the same structure).

The Parameter based fatigue life analysis is now a qualified system and its results are part of the decision making process in the fatigue life management of the FINAF F-18 fleet. The findings help get a general view of Fatigue Life Expenditure (FLE) in the fuselage, wing and tail areas and also provide FLEs of the structural details for each aircraft. Also, it enables arranging tail numbers into FLE order (ascending/descending) for any structural location. Repairs, inspections and structural part replacements can be scheduled based on the results. The FLE results for some critical locations are still unreliable by absolute values due to problems in the transfer function values produced by FEM, but as performance of the ANNs for all locations have been verified to be of good quality, the FLE results for all locations are usable for relative comparisons between individual aircrafts or for examining FLE trends in function of time. Additional information of the system is available in [48, 49].

13.2.2.3.1 Updated results (CFD – FEA – transfer functions)

Recently CFD and FE analysis results of the F-18 were improved causing changes in the transfer functions. Therefore the fatigue life estimations changed and the annual report delivered to the FINAF was updated. About half of the flights flown by the FINAF have been analyzed by now and the rest of the flights are in the process. An example of the results in *Fig. 15* shows FLE distribution of a structure in tail area for FINAF F-18 fleet. *Fig. 16* shows FLE accumulation rate of a fuselage longeron over period of 4 months and 12 months. It indicates how the usage of the aircrafts has been changed over the period 2000-2007.

Parallel to Patria's transfer function activities described above, the updated transfer functions have been transferred to VTT's HOLM ground station for the damage analyses therein [50]. To support the update activities of the transfer functions, the old representative FINAF spectrum [26 Chapter 13.5.1.3.1] was replaced with an updated spectrum, which is based on the in-flight measurement results of the two HOLM jets [50].

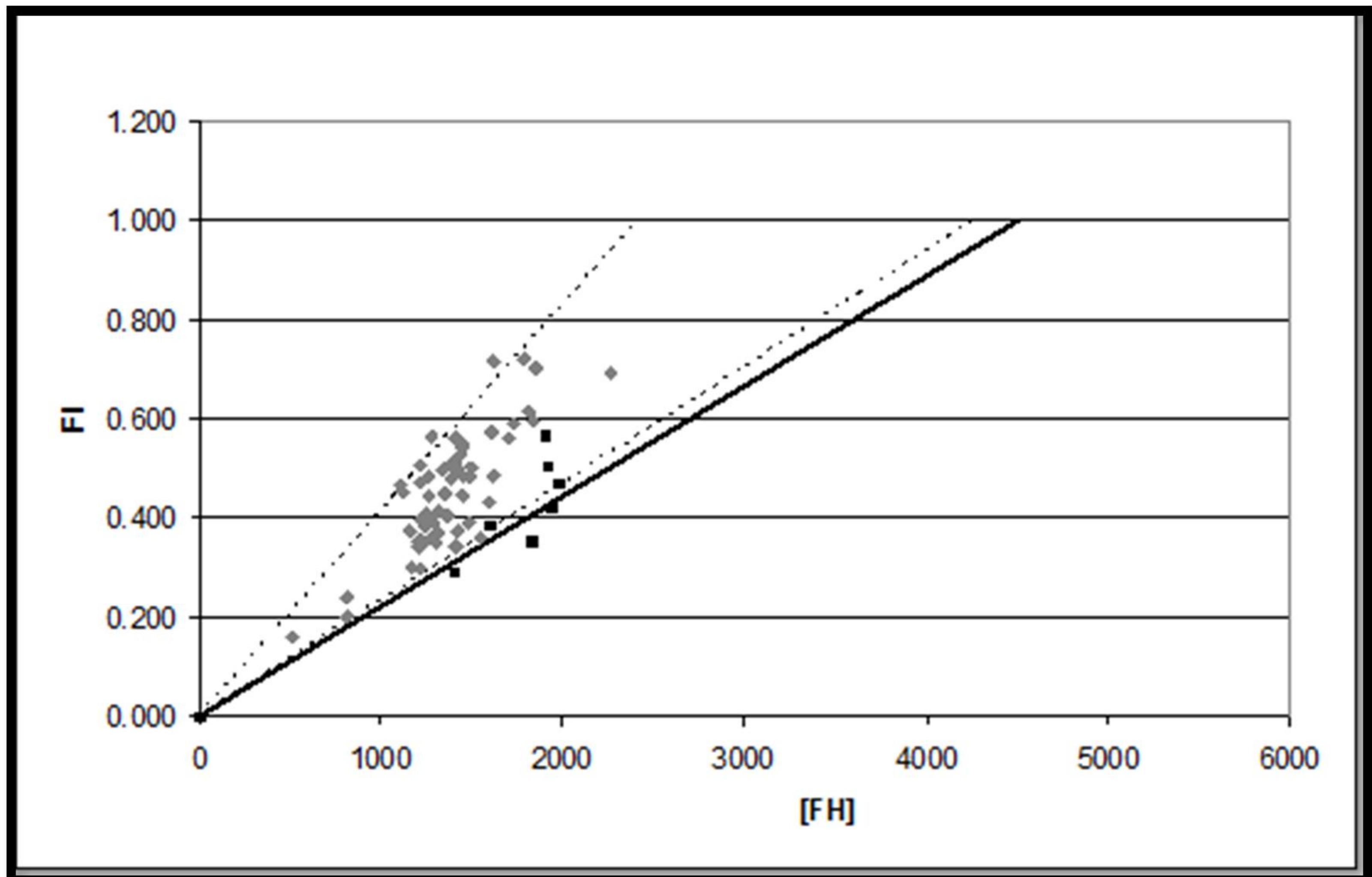


Figure 15: A scatter plot of the FLE calculated by the parameter based fatigue life analysis for a structural location in the tail area. Picture by courtesy of Patria Aviation.

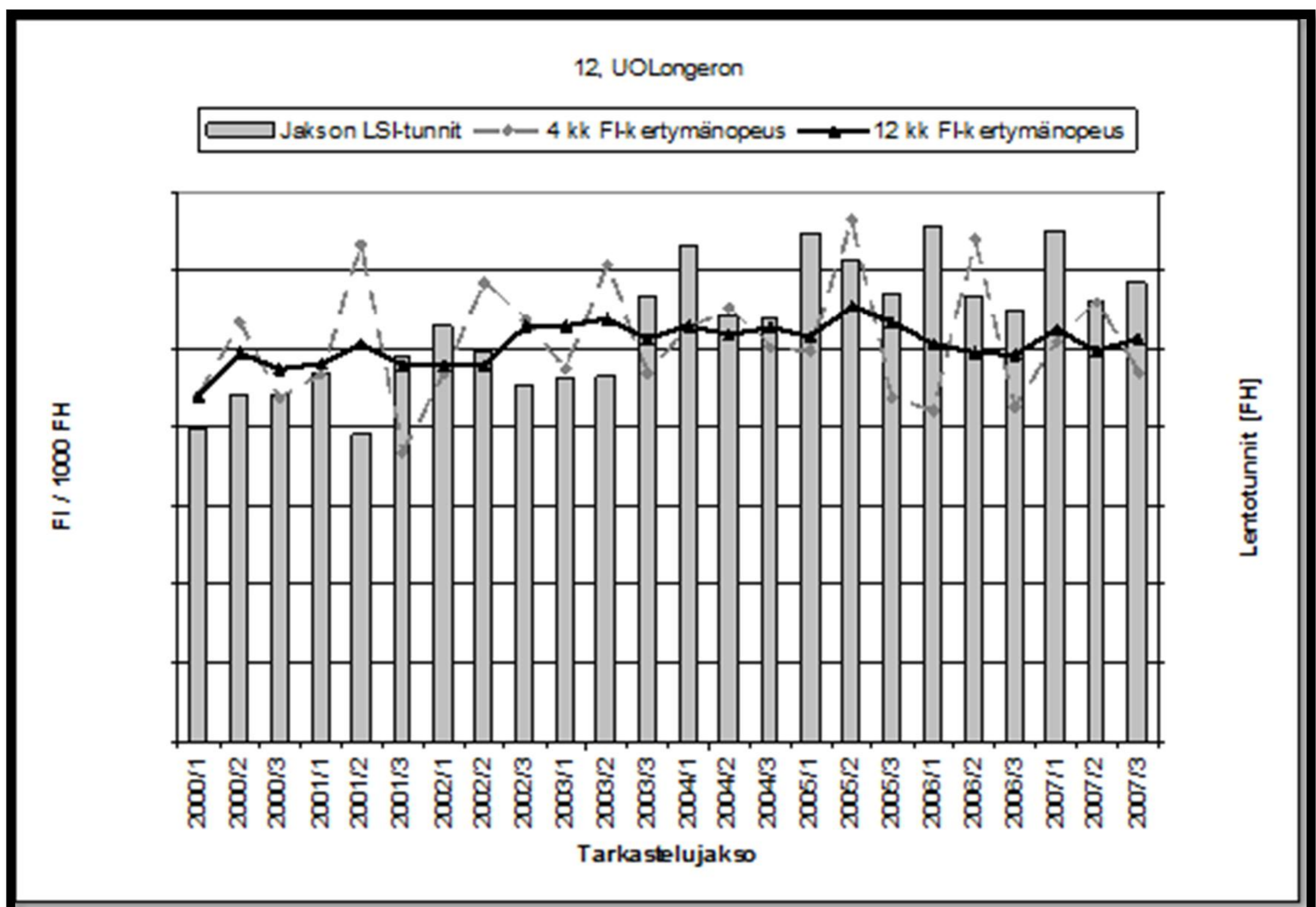


Figure 16: The whole fleet FLE accumulation rate of a fuselage longeron over period of 4 months and 12 months. The bars denote flight hours, the black line denotes 12 months accumulation rate and grey line denotes 4 months accumulation rate. Picture by courtesy of Patria Aviation.

13.2.2.3.2 In-service maintenance

In-service performance assessment of the parameter based analysis has been carried out during 2011 and 2012. It is a re-verification of the analysis where the data are compared to unseen flight parameters and strain gauge measurements. Both input data and analysis performance assessment are determined. A continued monitoring plan is required in order to ensure reliable functioning of the analysis. The assessments have proven that the analysis produces good or adequate results.

Fig. 17 and **Fig. 18** show flight specific damage scatter and accumulation plots from the in-service performance assessment.

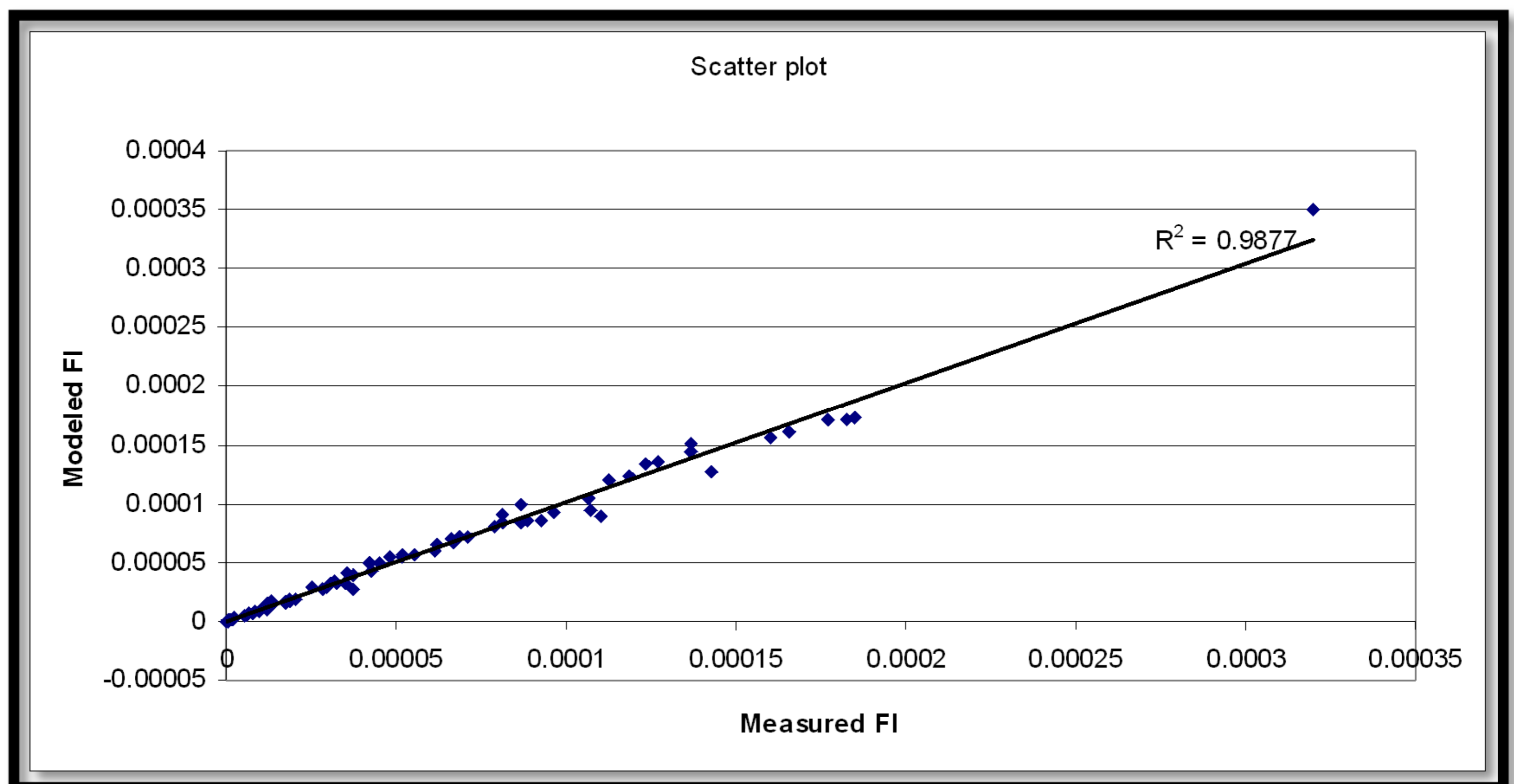


Figure 17: A proof of in-service performance of the parameter based fatigue life analysis. A scatter plot of flight specific damage from a fuselage bulkhead. Picture by courtesy of Patria Aviation.

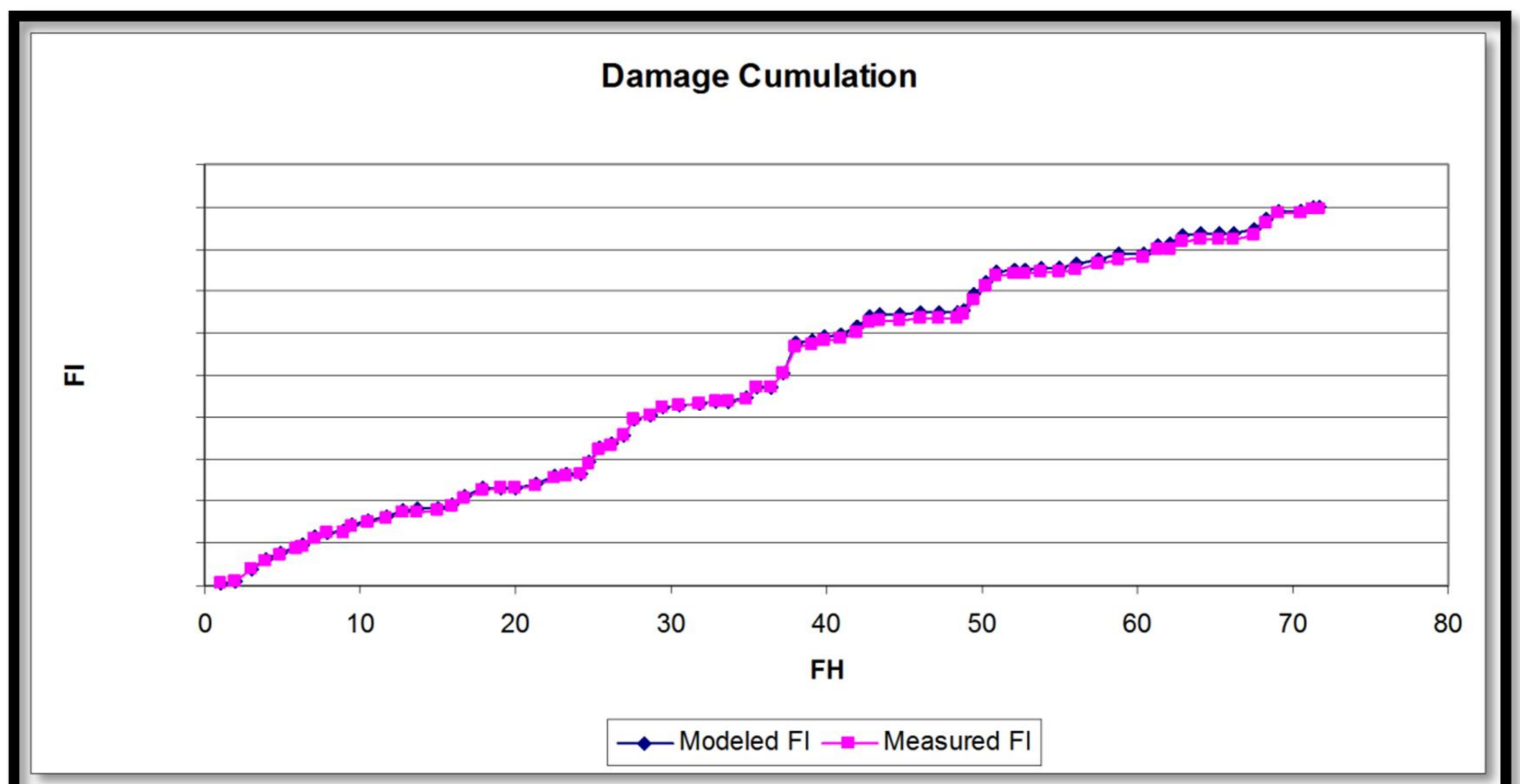


Figure 18: A proof of in-service performance of the parameter based fatigue life analysis. Modeled and measured damage accumulation over period of 70 FH. Picture by courtesy of Patria Aviation.

13.2.2.3.3 Add in new structural locations and future plans

During the last years the analysis has been extended by several structural details and adding new structures is straightforward. The FLE results for new details can be calculated back from the start of the aircraft's service life because flight parameter data of FINAF F-18's is available from the first flight.

A feasibility study to apply the parameter based fatigue life analysis for Hawk Mk.66 fleet will be started. The routine analysis of the F-18 data continues and new structural details will be added into the analysis.

13.2.2.4 Research efforts towards an OLM replacement system (Hawk Upgrade 2)

13.2.2.4.1 Structural health monitoring (SHM)

Previous activities related to the fatigue tracking activities of the FINAF Hawks are highlighted in previous ICAF reviews e.g. [4 Chapter 13.2.2.6]. The Hawk Mk.66s that the FINAF purchased from Switzerland were equipped with the electronic structural data acquisition system (ESDA). The original ESDA was developed by Spectralab and supported and operated by RUAG; former not existing and latter without activities in the field of Hawk any more. As the FINAF would like to follow the fatigue wear of the Mk.66s, a domestic project was started to study if Emmecon's strain measuring and analysis techniques could be utilized for this purpose. More background can be found in [4 Chapter 13.2.2.6].

During spring 2012 one FINAF Hawk Mk.66 aircraft was equipped with Emmecon's Mk.66 SHM system. This prototype monitors only two strain gauge channels, one from tailplane and one from vertical fin, which originally had been installed for ESDA. A short flight test period, consisting of about ten flights, was performed. The time histories and Rainflow counts from the two strain gauges were compared to FINAF Hawk Mk.51 OLM results obtained from the strain gauges, which had been located in the same position as the gauges in Mk.66. The correlation between Mk.66 SHM and Mk.51 OLM results was good. After the flight test period, the aircraft with the Mk.66 SHM system was put to normal flight service to collect more data to validate its performance.

13.2.2.4.2 Integrated eddy current inspection system for FINAF Hawks

Emmecon has also developed an eddy current inspection system (EDDY) which is integrated onto the structure and executes automated inspection sequence upon request or automatically. The system was tested with simplified test specimen simulating a butt strap joint in Hawk's tailplane, *Fig. 19*.

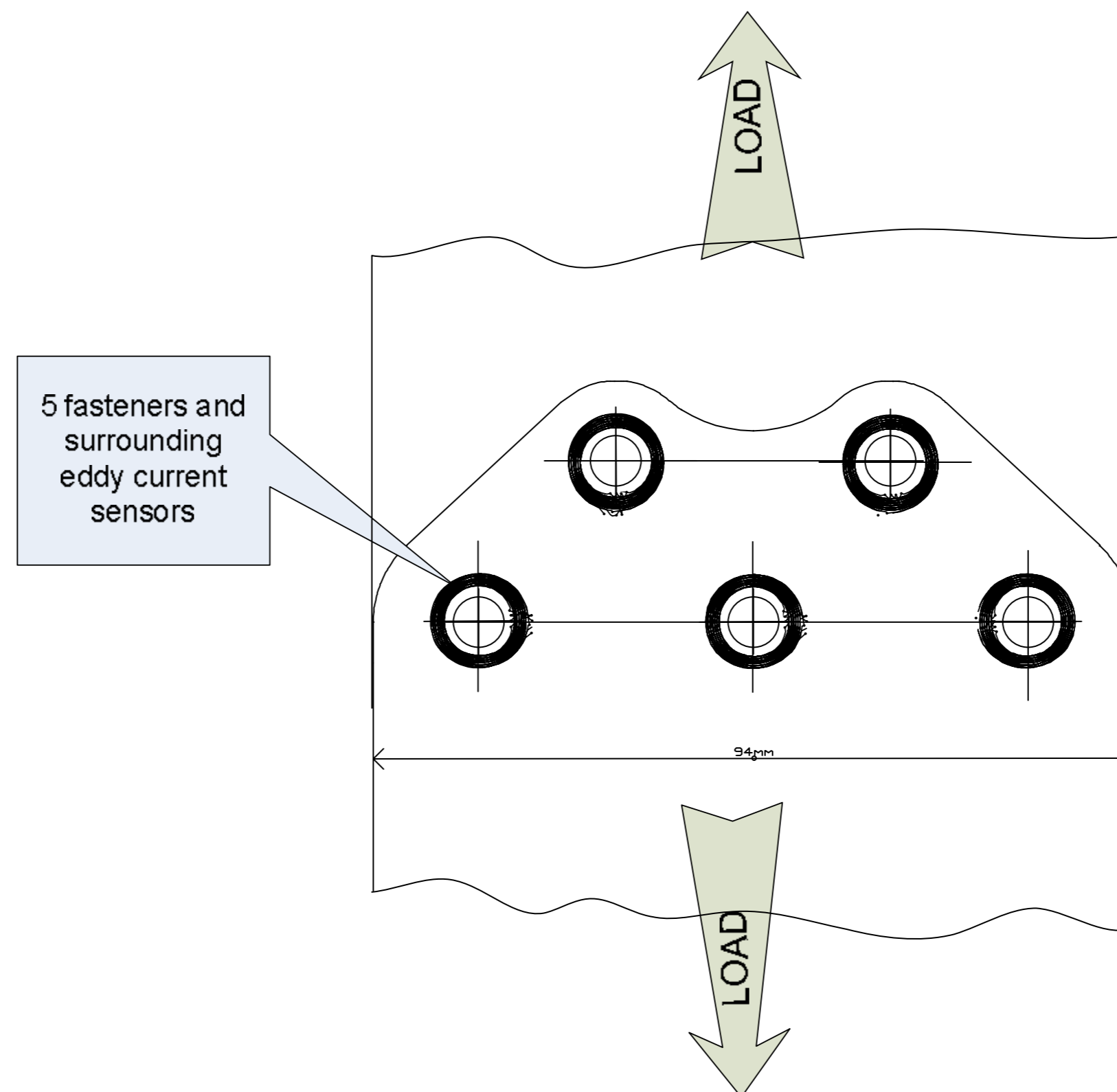


Figure 19: A specimen with five fasteners with an eddy current sensor (printed circuit board, PCB) around each fastener. Picture by courtesy of Emmecon Ltd.

Twelve (12) specimens as sketched in **Fig. 19** were tested. In four cases the EDDY alerted from a crack, one of them was a false alarm. In three cases the specimen broke without alarm. In none of the twelve specimen crack originated from a fastener hole but a couple of millimeters outside. The reason for this is the Hi-Tigue fasteners used, which create a cold-worked area around the fastener hole. If the crack does not originate from the fastener hole it is very challenging to catch for EDDY.

The remaining five specimens broke during the stage when the EDDY was not monitoring. The EDDY could not be monitoring the whole test period because of heating problems and the crack propagation was very fast after its formation.

To develop EDDY system, a narrower monitoring interval should be made possible and more tests should be done. At the moment these issues are not active.

13.2.3 Structural integrity of composite materials

13.2.3.1 Thermographic studies – update

Penetrated water in the composite sandwich structures is becoming a significant failure risk in aircraft structures. Flight surfaces have been lost during the flights, because moisture corrodes the honeycomb and further reduces the strength of the adhesive. By finding the moisture in early stage, structures can be repaired, which further leads to better safety and huge savings during aircraft lifetime.

The target of the work was to find a suitable procedure to detect penetrated water from the composite aircraft structures by using thermographic investigation method exploiting the phase transition of water. Previous thermographic activities were highlighted in [4 Chapter 13.2.3.1]. Since then, it was verified that 6 different flight surfaces (10 positions), **Fig. 20**, can be inspected during one inspection route at optimal temperature range with the developed thermographic method. One inspection route consists of rudder, trailing edge flap (around the middle and the main hinges) and horizontal stabilizer (pinion and main hinge) from both sides of the aircraft.



Figure 20: *The optimal thermographic inspection exploiting phase transition of water. **Left:** To succeed in the thermographic inspections, it is of paramount importance to ensure adequate cooling (freezing) of the aircraft before starting of the measurements. **Right:** The inspection consisted of six different flight surfaces (10 locations) in one sequence of inspection checks. Picture by courtesy of the FINAF.*

A reliable method to detect moisture was developed, thus the project target was achieved: With this thermographic method, even small amounts of penetrated water (moisture) can be reliably detected. Also, on the basis of the measurements completed, all 10 positions can be quantified with one inspection cycle, without removing the flight surfaces from the aircraft. This thermographic inspection method has shown to be the only method that detects small amounts of penetrated water from large areas without removing aircraft composite parts from the aircraft – and the only method within the FINAF which can detect small amounts of water, **Fig. 21**.

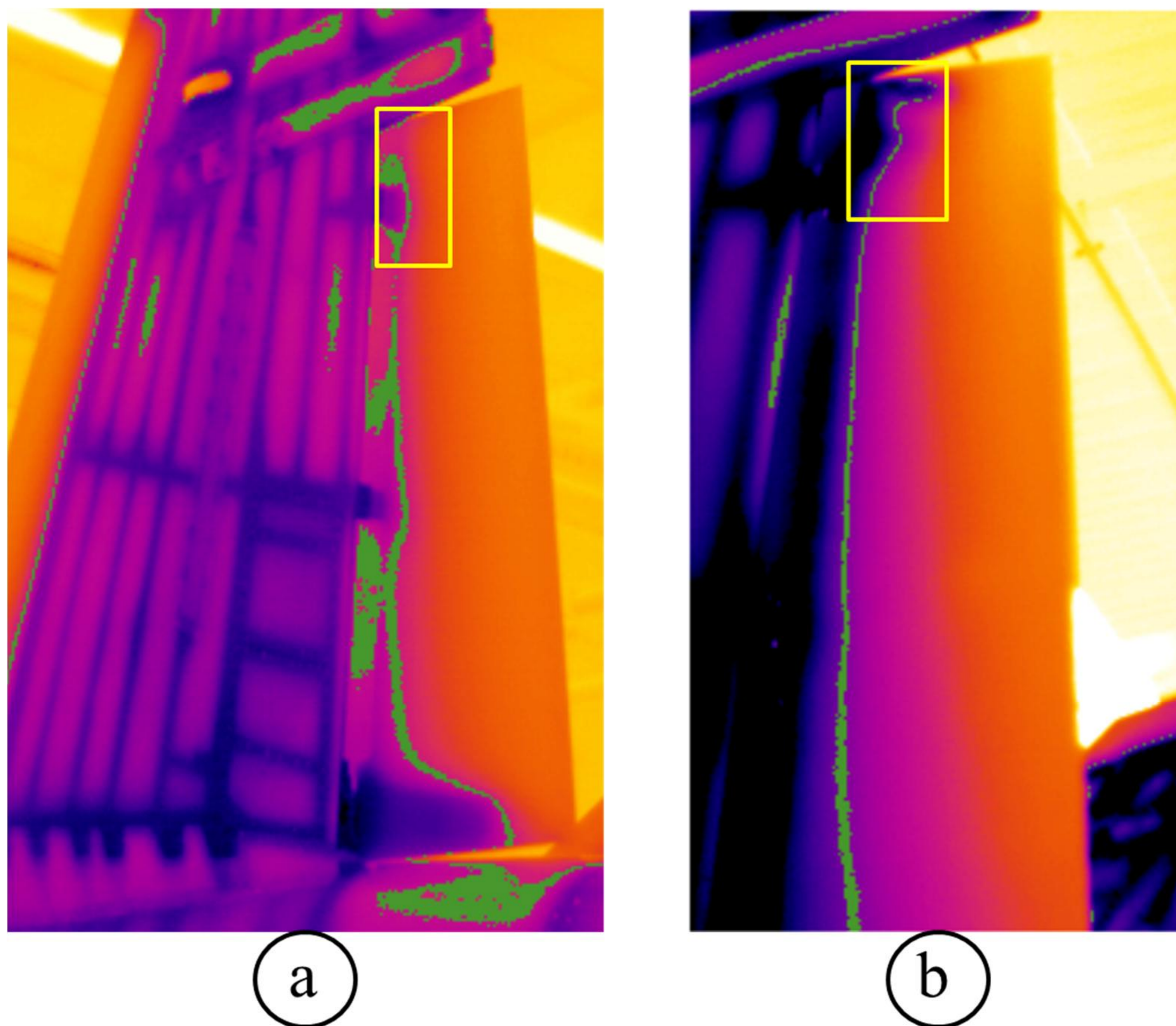


Figure 21: Rudders from the real inspections: **a)** Non-defected structure; **b)** Moisture detected beside and above the upper hinge. Picture by courtesy of VTT.

The presence of water (moisture) in the structure can be seen in **Fig. 21 b)** where the evolution of the abnormal temperature pattern can be seen beside and above the upper hinge.

The method (thermographic inspection routine exploiting phase transition of water for moisture detection in aircraft structures) was mainly developed in the FINAF's Satakunta Air Command and the most recent research period concentrated on preparing the specifications and individual working routines for the entire FINAF F-18 fleet. The developed thermographic method was successfully adapted to all Finnish F-18 Hornets.

13.2.3.2 Fracture mechanics based analysis and tests of delaminations

Previous fracture mechanics-based studies on composite structures were highlighted in [4 Chapter 13.2.3.3]. The work on numerical fracture mechanics using virtual crack closure technique (VCCT) has been continued. The follow-on work concentrated on 3D distributions of fracture properties and the effect of plasticity in adhesive joints. The software tool used in the work was ABAQUS. Experimental test setup was modified to improve the accuracy of measurements.

The effect of analysis parameters i.e. element type, mesh density, material properties and other analysis method dependent parameters were studied using both methods separately. The test cases used in the study were double cantilever beam (DCB) specimens corresponding to mode I. The uniformity of the GI distributions through the width of the specimen was studied with respect to the change of different analysis parameters. All analyses were performed using 3D elements [52, 53]. The main results were published in a conference paper [54].

The work on analysis and experiments was continued on adhesive joints in mode I where plasticity exists. The DCB specimen was used as a reference. The reference specimen was constructed using aluminum adherends and FM300-2 epoxy adhesive. The test arrangements were improved by measuring the crack length directly from the movement (i.e. *in-situ*) of the microscope used in observation. With the new test arrangements the quality of the test results were improved significantly and the scatter was reduced. With more accurate test results the correspondence between numerical simulation and test results became very good. With linear-elastic FE model and VCCT both insert and pre-crack cycles of the DCB test can be simulated realistically [55]. The simulation of pre-crack cycle is presented in *Fig. 22*.

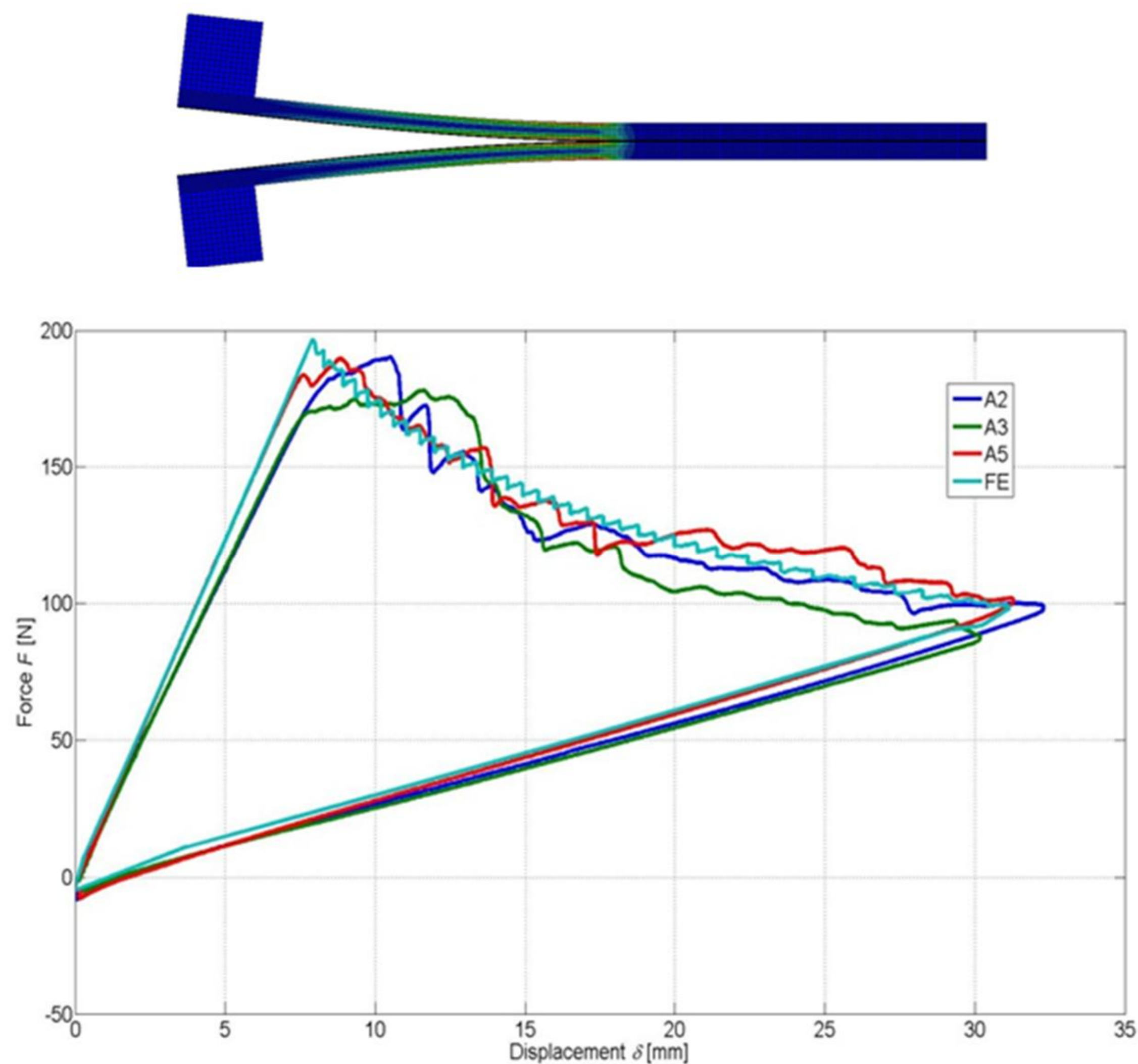


Figure 22: *FE model of a DCB specimen (top) and test results vs. FE analysis on DCB pre-crack cycle (bottom). Picture by courtesy of Aalto University.*

The VCCT analysis method was applied on actual delaminations on the F-18 trailing edge flap (TEF). The delaminations exist in the TEF spar around the hinge lug fastener holes. The purpose of the analysis was to estimate the criticality the growth of the delamination. The analysis was static and the load case selected for the study was defined as worst case. Several different damage scenarios were analyzed. Based on the analysis it was concluded that the small damages are not likely to grow with specified load case but in case of larger delaminations the risk for damage growth is significantly higher [56]. An example of the element mesh with multiple delaminations used in the analysis is presented in *Fig. 23*.

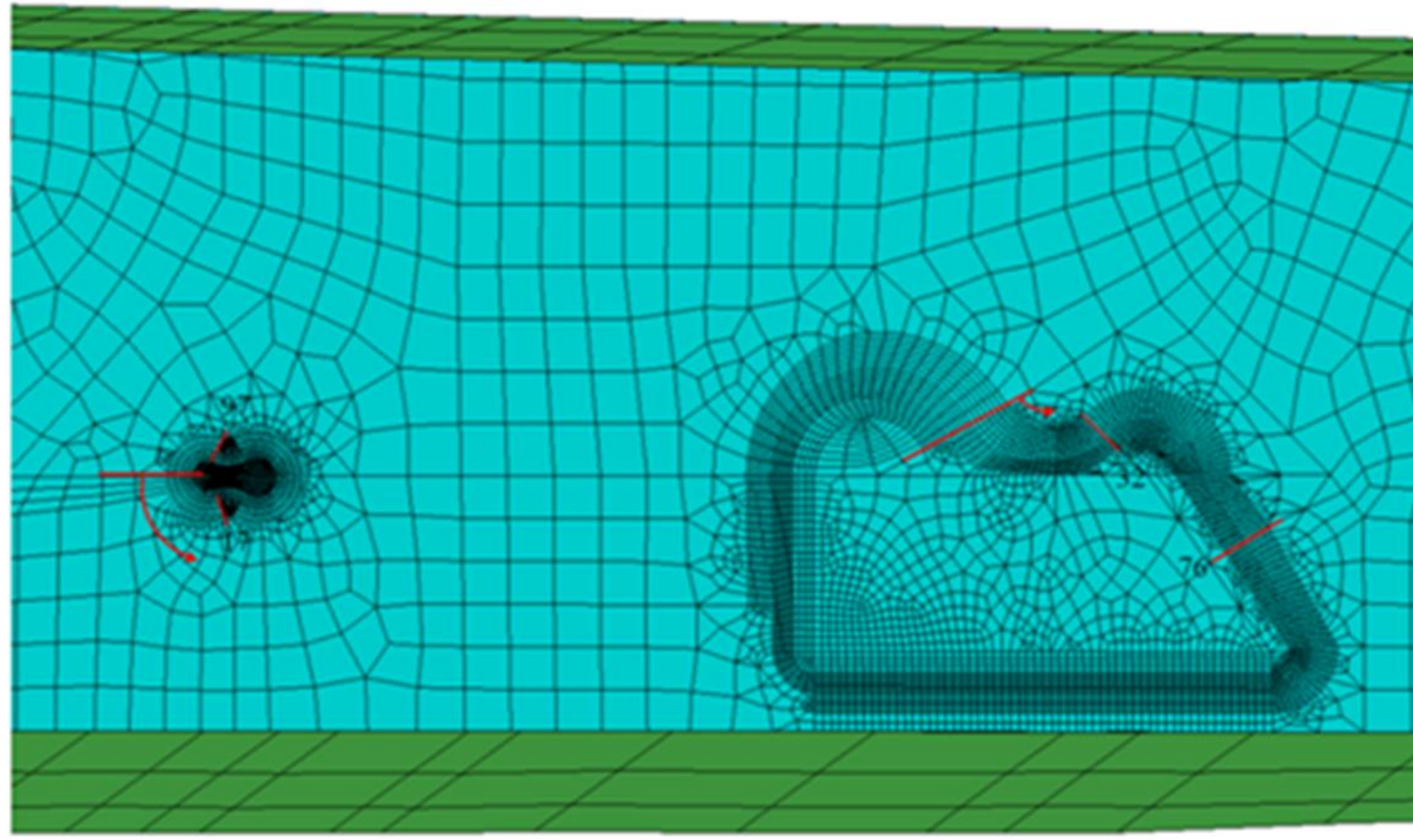


Figure 23: *An example of the element mesh used in analysis with multiple delaminations. Picture by courtesy of Aalto University.*

13.2.4 Structural integrity of metallic materials

Previous surface renewal activities have been reported in [4 Chapter 13.2.4]. The following summarizes the research efforts since the previous review.

13.2.4.1 FISIF Hole Salvage project

Under the auspices of the FISIF, a collaborative coupon testing program was conducted. As per the Canadian plan, the open-hole coupons were etched (by Australia), then pre-cycled (by Switzerland), after which the specimens were shipped to Patria, Finland, where the coupons' hole was first reamed (oversized), then cold worked (split sleeve) followed by interference fit or clearance fit fastener installation in order to have the coupons represent in-service usage. Patria then provided the coupons to VTT who conducted spectrum fatigue tests on the coupons and investigated the fracture surface characteristics using quantitative fractography on coupons with a hole with either clearance fit or interference fit, **Fig 24** [58]. Detailed analysis of the results is being done within the FISIF community.

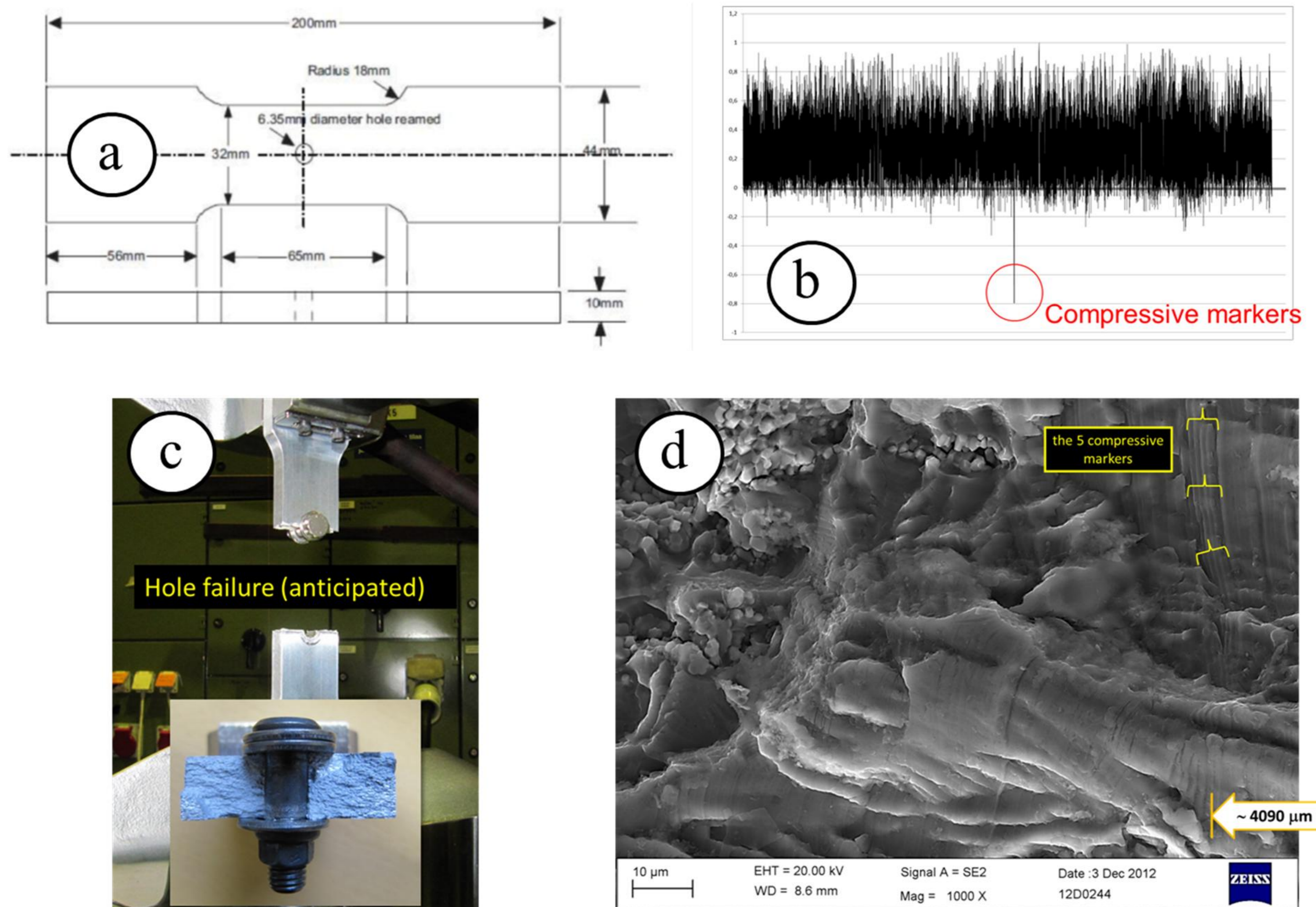


Figure 24: An overview of the project: **a)** specimen geometry; **b)** loading spectrum; **c)** failure from anticipated location (from fastener hole); **d)** scanning electron microscope picture from one of the fracture surfaces displaying the compressive markers. Picture by courtesy of VTT.

13.2.4.2 Non-destructive inspection (NDI) activities (metallic materials)

Previous non-destructive inspection (NDI) research activities to support the in-service inspections of the FINAF F-18 Hornets (metallic parts) have been reported in [4 Chapter 13.2.4.4]. Activities since then are reported below.

13.2.4.2.1 Experimental study of the sensitivity of the crack detection techniques applicable in the periodic in-service inspections using painted test specimen with real fatigue cracks.

Previous NDT activities at VTT, related to the F-18C/D Hornet fighters of the FINAF, have included the experimental studies of the sensitivity and application potential of the ultrasonic (UT exploiting Rayleigh waves) and eddy current (ET) techniques harnessed to the detection of artificial flaws (under 1 mm surface length) from reference specimens with artificial flaws. These results have been reported e.g. [4 Chapter 13.2.4.4].

In this experimental study, the NDT methods applicable for crack detection and sizing in the periodic aeronautical in-service inspections using unpainted and painted test specimens with real fatigue cracks were studied. The material of the test specimens were selected so that the results are applicable in the in-service inspection of the F-18 Hornet fighters. The studied mechanized NDT techniques included several eddy current techniques (ET) and immersion and contact ultrasonic techniques (UT) exploiting Rayleigh waves.

The material of laboratory test coupons and reference specimens was Al7050-T7451. The test coupons were fatigue loaded until failure (complete separation) in a previous project FISIF Surface Renewal Joint Coupon Program [2 Chapter 13.2.4.4]. The test coupons were inspected in various surface conditions: a) as-is (unpainted), b) repair painted as per Patria's production specifications). After the NDT the detected cracks were opened, photographed and the size of the cracks was

measured (depth, length). The true depth and length values of the detected cracks were compared to the results of the different NDT techniques.

The best UT results were achieved before painting with the 12 MHz material transducer. Altogether 16 fatigue cracks were detected. The size of the smallest detected crack was 0.63 mm x 0.26 mm. Defect depths were strongly undersized. The accuracy of the defect length sizing was quite good. After painting, only few defects were detected with this technique. With the lower frequency UT techniques more defects were detected after painting. However the defect depth sizing accuracy was poor. After painting the best results were achieved by ET. Differential and absolute probes were used. Sensitivity differences between the probes were surprisingly small. Altogether 16 cracks were detected. The accuracy of length sizing was good. The accuracy of defect depth sizing was reasonable if the defect length and thickness of painting are taken into account. The size of the smallest fatigue crack detected with ET after painting was 0.63 mm x 0.26 mm (length x depth). **Fig. 25** summarizes some of the ET results obtained. **Table 1** summarizes the recommendations concerning the high sensitivity ET and UT techniques applicable for sub-millimeter defect detection and sizing [59].

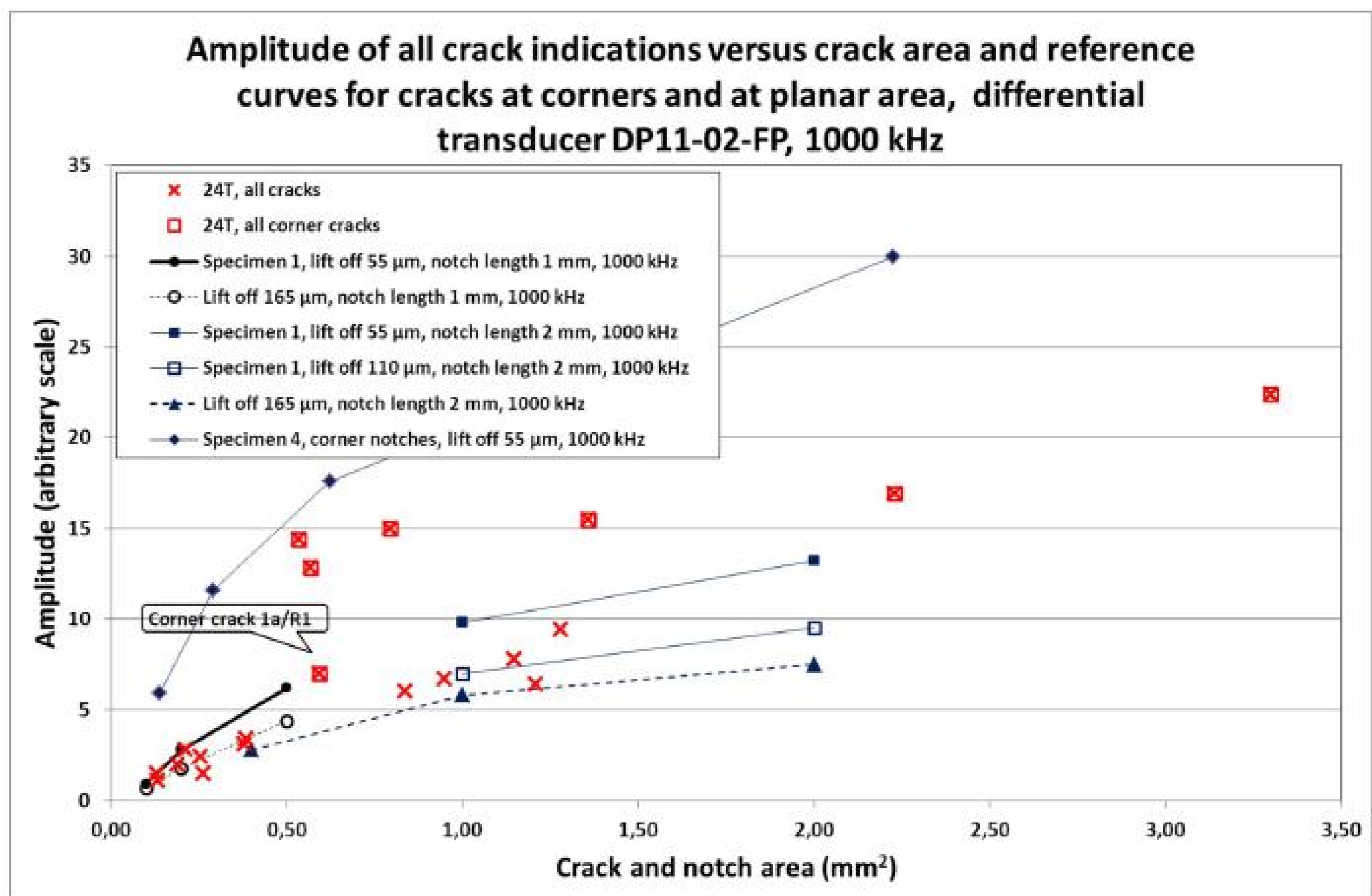


Figure 25: The specimen 24T, the amplitudes of all detected single fatigue crack indications black reference graphs for shorter and blue for longer indications. The small diameter transducer DP11-02-F4 was applied. The ET frequency was 1000 kHz. Picture by courtesy of VTT.

Table 1: Recommendations for ET and UT applicable for detection and sizing of sub-millimeter fatigue cracks on components fabricated of aluminum. Table by courtesy of VTT.

	Eddy current	Ultrasonic
Scanning	mechanised	mechanised
Paint	paint or protecting tape needed	removed
Scanning direction	diff probe: perpendicular or parallel to cracks ($\pm 45^\circ$)	n/a
	abs probe: any direction	any direction
Probe orientation	diff probe: perpendicular ($\pm 45^\circ$)	n/a
	abs probe: any direction	perpendicular to cracks ($\pm 20^\circ$)
Scanning pitch	e.g. 0.05 - 0.1 mm	e.g. 0.05 - 0.1 mm
Probe diameter	Diameter of probe tip 1 - 2 mm	size of the probe face 10 mm x 15 mm
Material of the probe surface	Hard: diamond, aluminium oxide	Plastic (e.g. acryl)
Quality of probe surface	Polished	Ra = 1.5 μ m
Orientation of "lift-off noise"	Horizontal	n/a
Applied for detection	Vertical amplitude of indication	Amplitude of indication
Applied for sizing	Vertical amplitude of indication (modelling recommended to increase accuracy)	Amplitude (under sizing in this study if not corrected)
Frequency	0.5-2 MHz	5-12 MHz
Acceptance testing of the probes	Sensitivity versus defect depth Sensitivity versus defect length Sensitivity versus lift-off	Sensitivity versus defect depth Sensitivity versus defect length
Reference flaws on planar area for characterizing the probes	Notches: lengths 1 mm, 2 mm, 5 mm, depths 0.1 mm, 0.2 mm, 0.5 mm, 1.0 and 2.0 mm, lift-off mm 0.1 mm and 0.15 mm and 0.2 mm	Notches: lengths 1 mm, 2 mm, 5 mm, depths 0.1 mm, 0.2 mm, 0.5 mm and 1.0 and 2.0 mm, Lift-off not accepted
Width of reference flaws on planar area	< 0.15 mm (spark erosion, thickness of electrode <0.1 mm)	< 0.15 mm (spark erosion, thickness of electrode <0.1 mm)
Reference flaws on corner for characterizing the probes and for sensitivity checks during in-service inspection	Notches, size 0.4 mm x 0.4 mm, 0.7 mm x 0.7 mm, 1 mm x 1 mm lift-off 0.1 mm and 0.15 mm and 0.2 mm	Notches, size 0.4 mm x 0.4 mm, 0.7 mm x 0.7 mm, 1 mm x 1 mm Lift-off not accepted
Width of reference flaws on corner	≤ 0.08 mm (wire machining, $\varnothing 0.05$ mm)	≤ 0.08 mm (wire machining, $\varnothing 0.05$ mm)
Surface quality of reference specimen	Ra 1.6 μ m	Ra 1.6 μ m
Reference flaws on planar area for checking the sensitivity during in-service inspection	Long notches: depths 0.1 mm, 0.2 mm, 0.5 mm, 1.0 and 2.0 mm, lift-off 0.05mm, 0.1 mm and 0.15 mm	Long notches: depths 0.1 mm, 0.2 mm, 0.5 mm, 1.0 and 2.0
Width of reference flaws on planar area for checking the sensitivity	< 0.15 mm (spark erosion, thickness of electrode < 0.1 mm)	≤ 0.15 mm (spark erosion, thickness of electrode 0.1 mm)

13.2.5 Repair technologies

13.2.5.1 Repair technologies for composite structures

13.2.5.1.1 Aircraft battle damage repair of composite structures

Damaged aircraft composite structures can be repaired with several different repair methods. Repairs are usually performed at a warm and dry depot where skilled personnel and facilities are available. The mechanical properties of the repaired structures must match the original performance. Aircraft battle damage repair (ABDR) of composite structures must be executed in the field with minimum equipment. ABDR is very important to keep the aircraft operational with a useful level of mission capability or to return them safely to the depot for major maintenance.

The objective of the Master's thesis [60] was to find applicable battle damage repair methods for monolithic and sandwich composite structures by means of literature survey and experimental study. In the theoretical part, typical battle damages and different repair methods were reviewed. The influence of ABDR was also evaluated.

In the experimental part, sandwich panels were made of carbon laminate face sheets and Nomex-honeycomb. A 25 mm hole was made to sandwich specimens representing battle damage. The damages were repaired by attaching pre-cured carbon fiber patches with four different rapid repair methods. The repairs were carried out under laboratory conditions. Repair times and tensile strength of each repaired sandwich specimen was measured.

The test results showed that riveted and adhesively bonded and only adhesively bonded procured composite patch repair methods could be applied within two hours. They restored 90 % and 75% of the static strength respectively. The riveted repair restored only 29 % of the strength. According to test results, first two repair methods restore moderately mechanical properties and have ability to be processed rapidly in the field using minimum equipment, *Fig. 26* and *Fig. 27* [60].

Repair method	Strength [kN]	Minimum repair time [min]	Strength of repaired vs. undamaged [%]
Reference (undamaged)	19,11		
Riveted composite patch (Cherry-rivets)	5,54	25	28,99
Riveted composite patch (steel rivets)	4,05	25	21,19
Bonded (EA9493) and riveted composite patch (Cherry-rivets)	17,33	124	90,69
Bonded (EA9396) and riveted composite patch (steel rivets)	16,32	111	85,41
Bonded composite patch with Superquick-epoxy	3,34	42	17,50
Bonded composite patch with Rapid-epoxy	14,43	58	75,52
Bonded composite patch with double-sided VHB-tape	1,34	35	7,01

Figure 26: An overview of the experimental results. Picture by courtesy of Aalto University.

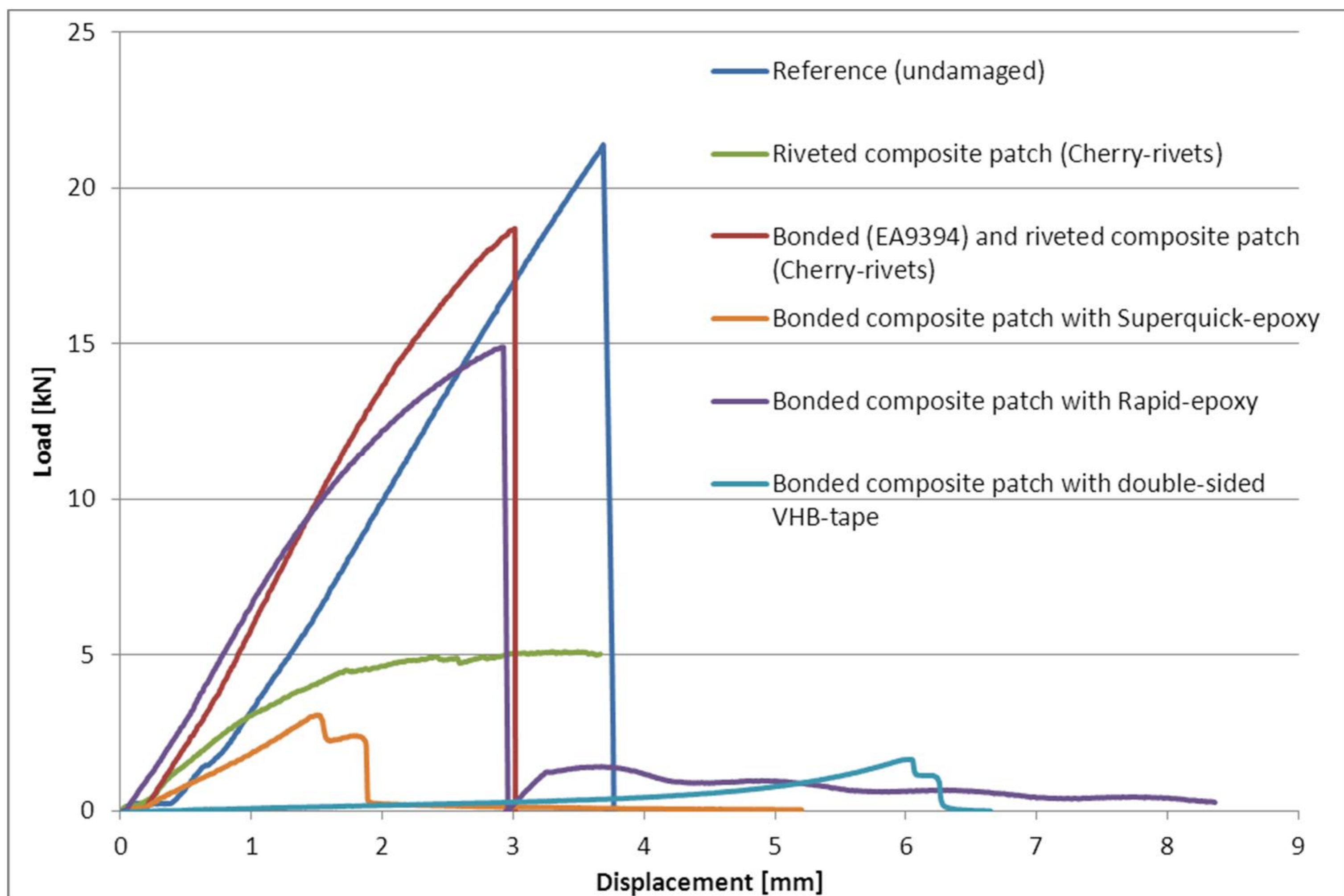


Figure 27: Graphical representation of the experimental results obtained. Picture by courtesy of Aalto University.

13.2.5.2 Repair technologies for the FINAF F-18 metallic primary structures

13.2.5.2.1 DIARC plasma coating for reliable and durable structural bonding of metals

Previous metal bonding activities, specifically those related to DIARC plasma coatings, have been reported earlier in [2 Chapter 13.2.3.3]. The lack of robust and highly reliable surface preparation techniques has limited the use of bonded joints in highly loaded metal to metal and metal to composite structural joints in aircraft applications. With aluminum and titanium the grit blast AC-130 Sol-Gel process can provide acceptable results, but the technique requires a competent mechanic following strict process instructions without any deviations. Also, in aircraft applications the process usually requires chromate primers, which induces a healthy risk. For steel there has not been an acceptable method available that would satisfy aircraft quality criteria for structural bonding.

The objective of this study [61] was to investigate the performance of new DIARC coating method for metal bonding. The results were compared to grit blast silane (GBS) and grit blast AC-130 Sol-Gel (SG) testing. **Fig. 28** summarizes the surface treatment comparisons.

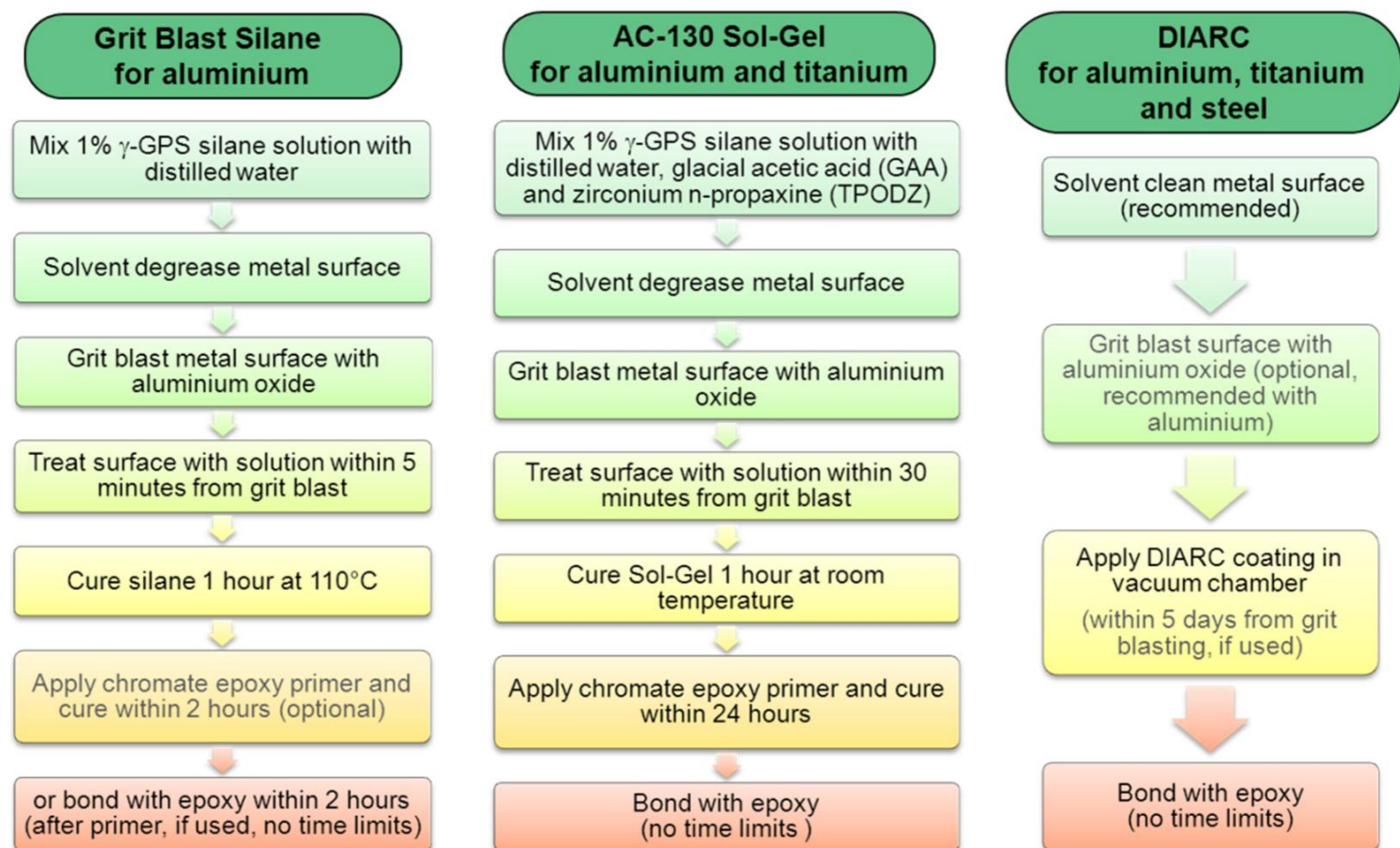


Figure 28: Surface treatment comparisons. Picture by courtesy of Aalto University.

Typical aircraft grade aluminum and titanium along with stainless and high strength steels were selected for testing: Aircraft grade 7075-T6 bare and clad aluminums were used in static single lap and double lap shear testing and in wedge testing. Clad was not removed from the specimens prior to surface treatment and bonding. Titanium 6Al-4V and AISI 304 stainless steel were used in static single lap and double lap shear testing and in wedge testing, high strength AISI 4130N steel specimens were also tested with wedge testing.

Static single lap shear and static double lap shear specimens were tested at room temperature as dry and wet. Wedge tests were also performed in different environments: Hot/wet humidity cabinet (60 °C / 98 % relative humidity); neutral salt fog cabinet (ASTM B 117) at 35 °C; hot fresh water immersion: tap water at 60 °C; hot salt water immersion: Baltic Sea water (0.5 % salt content) at 60 °C .

DIARC coating provided good results with all metals in all testing. In a case study the coating applied to sandwich honeycomb steel inserts improved their torque strength over 100 %, **Fig. 29**.

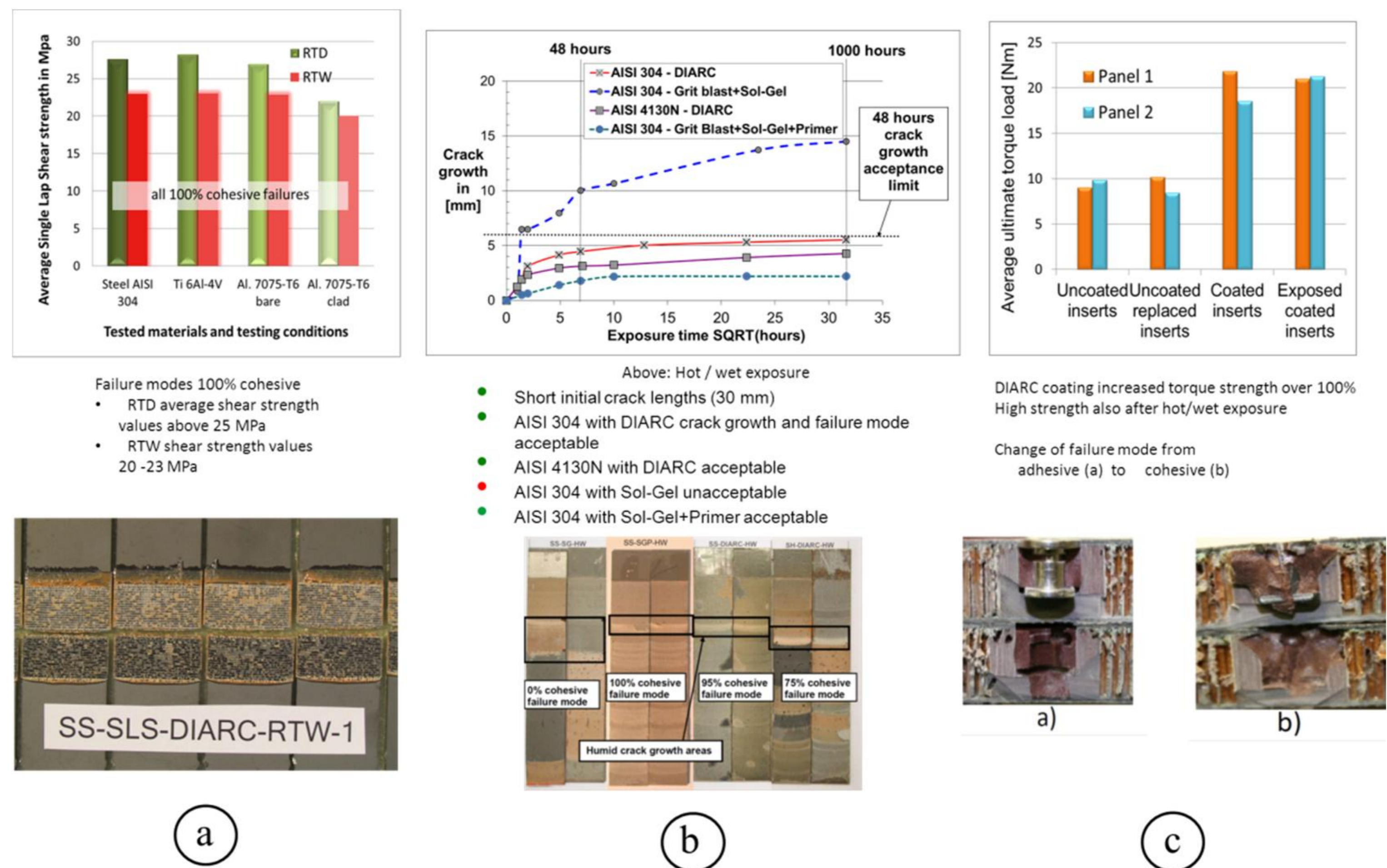


Figure 29: DIARC® (www.diacr.fi) vacuum plasma surface treatment was tested for comparing its performance in aluminium, titanium and steel structural epoxy bonding with existing methods. Static single lap shear and static double lap shear specimens were tested at room temperature as dry and wet. Wedge tests were also performed in different environments. DIARC coating provided good results with all metals in all testing. In a case study the coating applied to sandwich honeycomb steel inserts improved their torque strength over 100 %. Results: a) Single Lap Shear, DIARC Coating; b) Wedge Tests, AISI Specimens; c) Case study: Potted Steel Inserts. Picture by courtesy of Aalto University.

13.2.5.2.2 Computational fatigue life assessment of a metallic structure with a bonded composite repair

The purpose of the Master's thesis was to study the analytical and numerical methods available for analyzing the fatigue life of metallic structures with bonded composite repairs. The focus was on thin cracked aluminum plates and single-sided composite repairs. The cracks were through-cracks located in the center of the aluminum plates. The metallic structures were supported or unsupported structures under tension loading. Thermal residual stresses and secondary bending effects were taken into account in the studies. Stop-drilling holes at the ends of the crack were not considered.

The thesis covers a literature survey, which will comprise past studies on the subject, instructions on modeling the bonded structure, and computational methods to assess the stress distribution, static strength and fatigue life of a cracked aluminum plate with a bonded composite repair.

The main objective of the thesis was to model a cracked aluminum plate with a bonded composite repair and evaluate its stress distribution and fatigue life by different methods. The stress distribution was determined by analytical and finite element (FE) method, whereas the fatigue life was determined with analytical methods and the AFGROW software. The modeling of the composite laminate will be made with ESAComp. FE modeling was carried out with Abaqus/CAE and Franc2D/L. To validate the results, the obtained fatigue lives were compared to the experimental results conducted in the Laboratory of Lightweight Structures of the Aalto University's Department of Applied Mechanics.

According to the results, Abaqus/CAE-model was able to predict an acceptable fatigue life for the examined structure compared to the experimental results. Abaqus/CAE proved also to be the most versatile software for analyzing the metallic structure with bonded composite repair. Other methods were not capable of modeling the examined structure correctly due to their features and

limitations, which is why the results varied considerably [62]. An overview of the work is provided in *Fig. 30* and *Fig. 31*.



Figure 30: The examined structure; a 2024-T3 aluminum plate and a carbon/epoxy prepreg patch bonded with FM73M epoxy adhesive. Picture by courtesy of Aalto University.

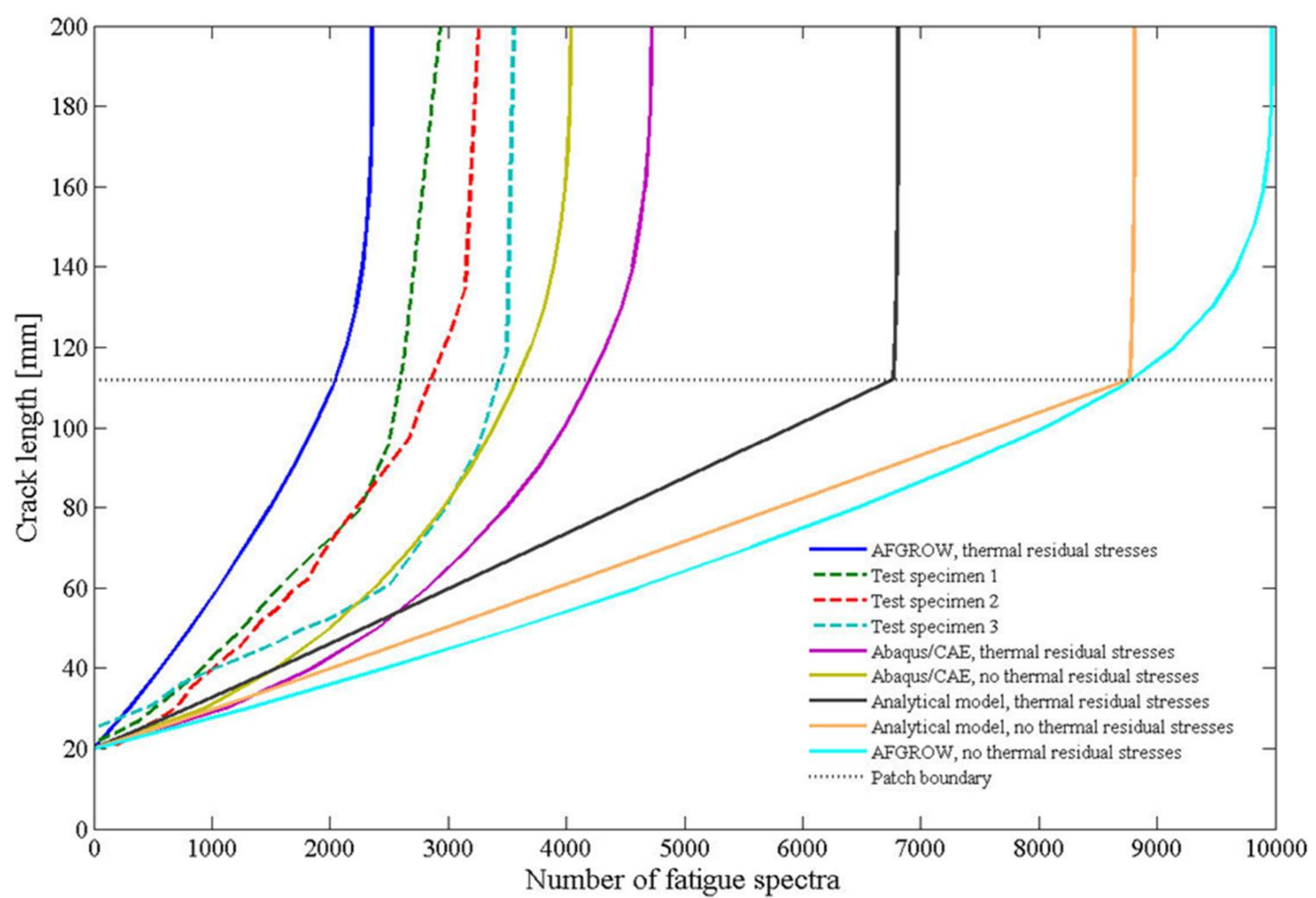


Figure 31: Fatigue life of the examined structure obtained by the various methods and compared with the experimental results. Picture by courtesy of Aalto University.

13.2.6 Mechanical systems integrity

Research on the field of mechanical systems integrity is divided in three main areas: Simulation and modeling, laboratory testing and condition control and monitoring. Besides of research towards larger scale scientific goals some efforts are also focused into problem oriented smaller scale research subjects. Previous mechanical systems integrity activities have been highlighted in [4 Chapter 13.2.6]. Below is an update of research areas, which is carried out in cooperation between the FINAF and TUT/IHA.

13.2.6.1 Simulation and modeling

Hydraulic system modelling is done in two different levels of detail to enable studying both complete system and individual component levels with appropriate accuracy. Detailed analytical component models are developed for single component or partial system simulation for situations where point of interest lies in single component and high level of accuracy and detail is needed [63, 64]. The complete system model, which is connected to the flight simulation model (HUTFLY2), utilizes simplified semi-empirical component models which enables model solving in real-time. This virtual ironbird can be used to study system hydraulic system behaviour in arbitrary flight and operating conditions. It also incorporates possibility to easily introduce simulated malfunctions and damages (wear, battle etc.) to the system and study their effect on the performance of the aircraft. Also studying effect of changing system components or their performance characteristics can be easily and effectively studied.

13.2.6.2 Laboratory testing

Hardware-in-the-loop (HIL) interface is used to include real components into the virtual ironbird discussed in the previous chapter. The HIL interface enables bidirectional communication in-between the simulator and the hardware components. In other words, it transforms simulated component command values into real-life command signals and simulated loads into real-life load forces. Exchange of hydraulic system variables (such as available flow rate, system pressure etc.) is also incorporated into the interface. Output parameters of the hardware component are measured and the HIL interface transmits them to the simulator. There are also simplified possibilities for pilot-in-the-loop (PIL) simulations. The HIL simulation environment and the virtual ironbird together give a possibility to study real hardware components in an arbitrary in-flight operation point relatively easily. HIL testing environment can also be used to perform life testing of hydraulic components. Using HIL testing environment offers possibilities to perform life testing in more realistic operating and load conditions without compromising test reliability.

As a pilot test, the life times of two different but interchangeable hydraulic pumps were compared using eight minute test cycle which was ran as a continuous loop. Test cycle was defined by studying real mission data with virtual ironbird and finding most loading sets of flight maneuvers from it. The pilot test showed that this testing procedure brings out key issues also found in the particular aircraft type in practice, which in the other hand may be issues that cannot be tested by any more common or standardized testing procedures or methods.

13.2.6.3 Condition control and monitoring

Condition control and monitoring research is targeted into developing an inline hydraulic system condition monitoring unit [65, 66]. The development is done in co-operation with Emmecon Ltd.

The inline condition monitoring unit is based on COTS condition monitoring sensor technology (chemical quality sensors and particle counters). The unit is installed in-between aircraft and portable test stand where it can monitor the quality of the fluid returning from the aircraft's system and also the fluid quality in the test stand itself. Thus the unit has two main applications: It can be used for determining the condition of the hydraulic system for predictive maintenance purposes and it acts as contamination migration safe guard in between individual air vehicles by indicating

contamination in the fluid of the test stand. Hydraulic system condition monitoring unit went successfully through field and laboratory tests. Its application for fault finding was also studied extensively. *Fig. 32* shows the hydraulic diagram and control/analysis unit of the system.

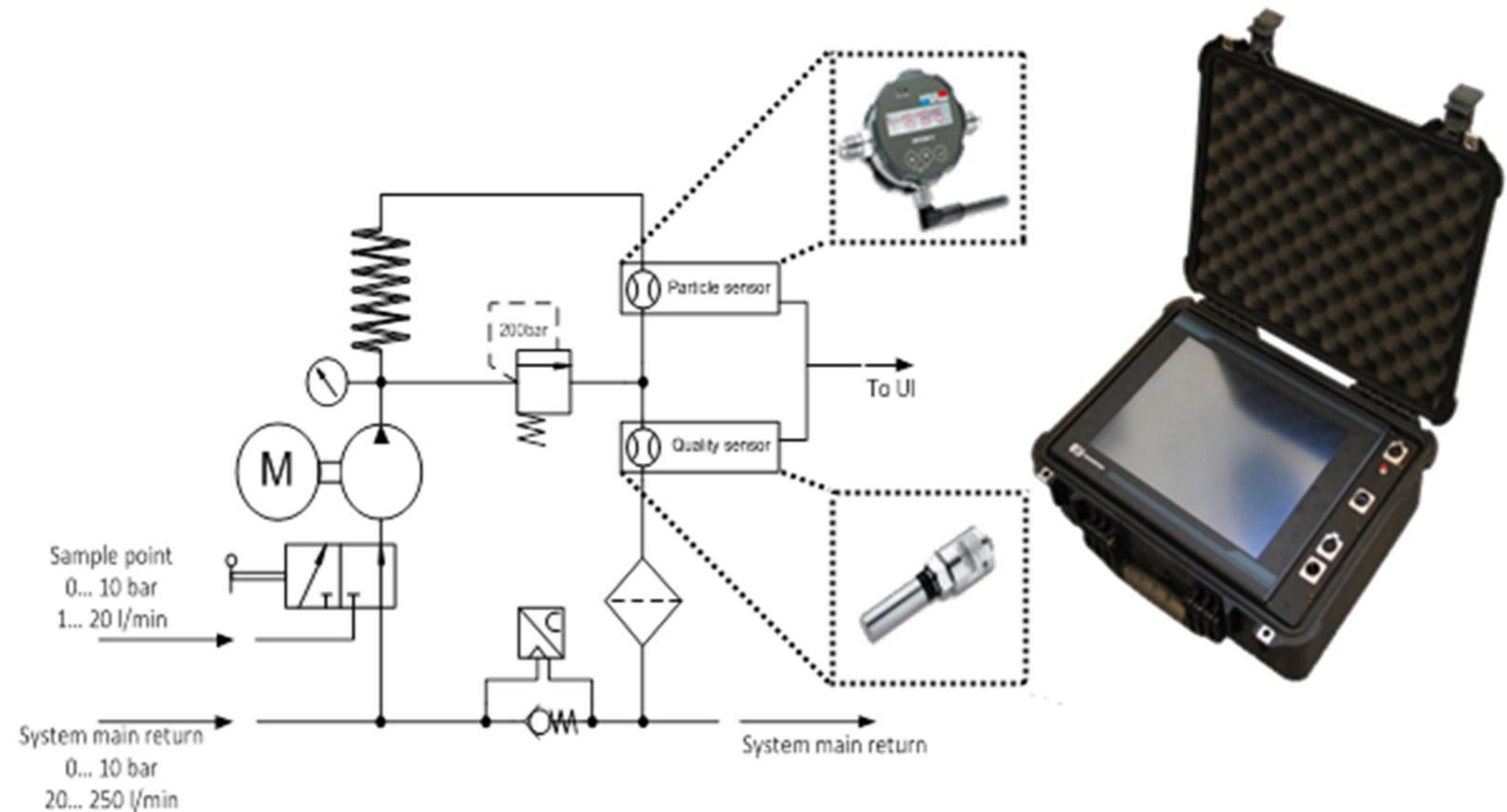


Figure 32: *The hydraulic diagram and control/analysis unit of the system. Picture by courtesy of TUT/IHA and Emmecon Ltd.*

13.2.7 Engine integrity

Previous engine integrity research activities have been reported in [4 Chapter 13.2.7]. The following provides an update.

13.2.7.1 Microstructural degradation of a single-crystal gas turbine blade

This work [67] was aimed to evaluate and classify the microstructural degradation of a diffusion coated single-crystal gas turbine blade, so that the characterized features of degradation could be used for assessing the effective in-service material temperatures at the corresponding blade locations. Four potentially useful indicative measures were evaluated for this purpose: **a)** gamma prime (γ') coarsening and degradation in the substrate microstructure to indicate the condition and temperature in the blade interior, **b)** combined thickness of the intermediate diffusion zone (IDZ) and topologically close-packed (TCP) precipitate layer to indicate the condition and temperature at the blade coating, **c)** combined thickness of the top oxide and gamma prime depleted layer of the blade material to indicate the condition and temperature (or age) of a crack, and **d)** depth of the oxidized diffusion zone below the coating, also to indicate the surface temperature. All of these measures appear to provide meaningful indications of the service temperature, although not with equal accuracy or applicability to different parts of the blade. For example, the thickness of IDZ+TPC layers can be used to assess the temperatures with relatively good accuracy but only for blade surface until these layers remain sufficiently intact for the assessment.

For verification and demonstration purposes, two case examples are presented on ex-service turbine blades, *Fig. 33* and *Fig. 34*.

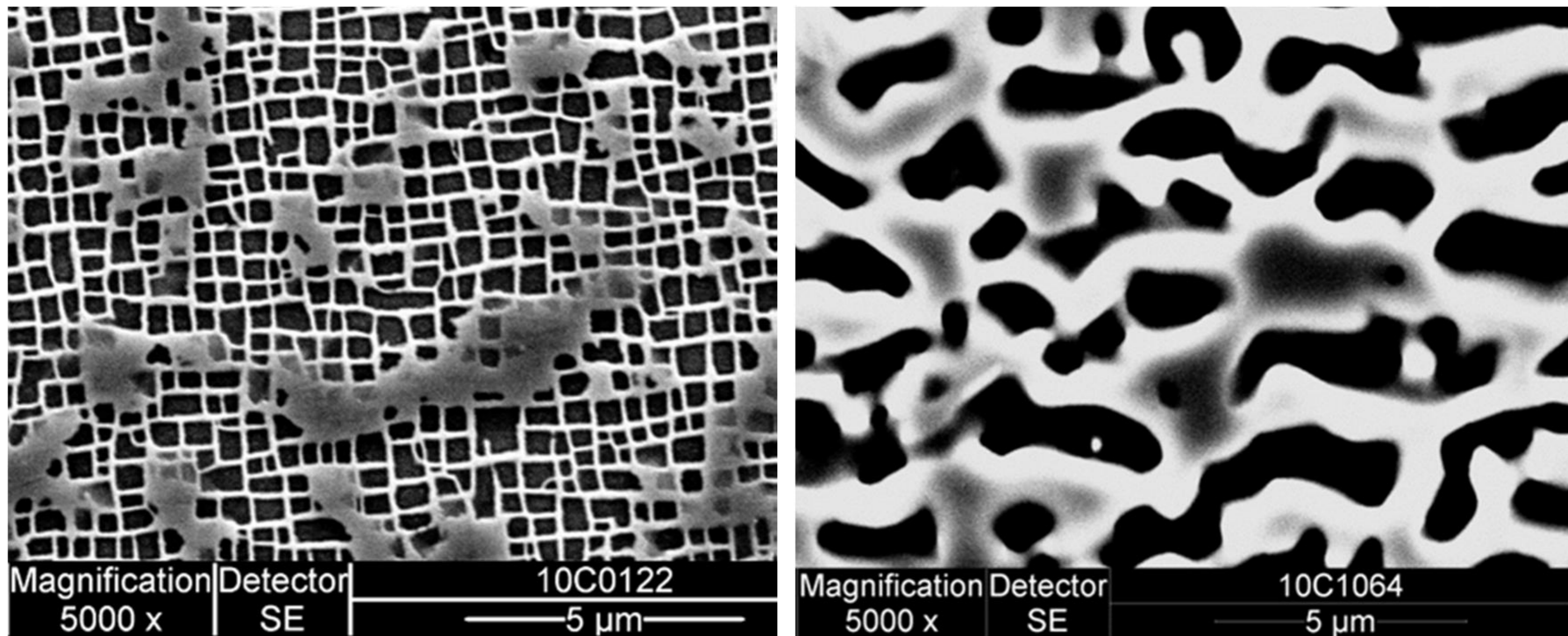


Figure 33: *Left: As-new microstructure with cubic gamma prime (γ') particles. Right: heavily degraded microstructure. Picture by courtesy of VTT.*

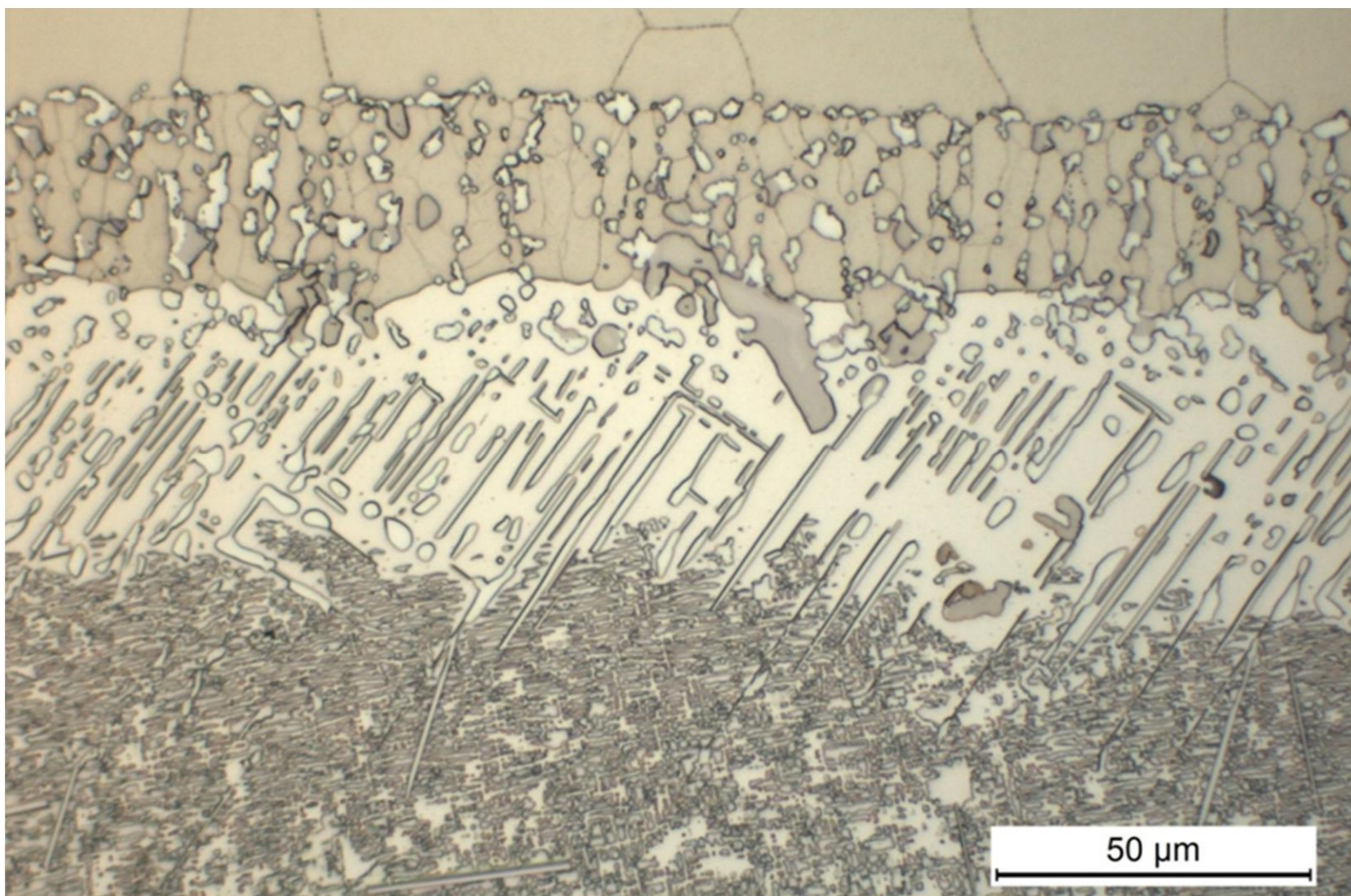


Figure 34: *IDZ and TCP layers after 700 h at 1050°C (LOM image). Picture by courtesy of VTT.*

13.2.7.2 Guideline - turbine blade failures

Various different turbine blade cracks were collected for this report with the aim to produce a guideline for turbine blade failure inspection. The purpose of this handbook is to ease the visual inspection when analysing the severity of turbine blade cracks [68]. Examples of the turbine blade failures are shown in *Fig. 35* and *Fig. 36*.

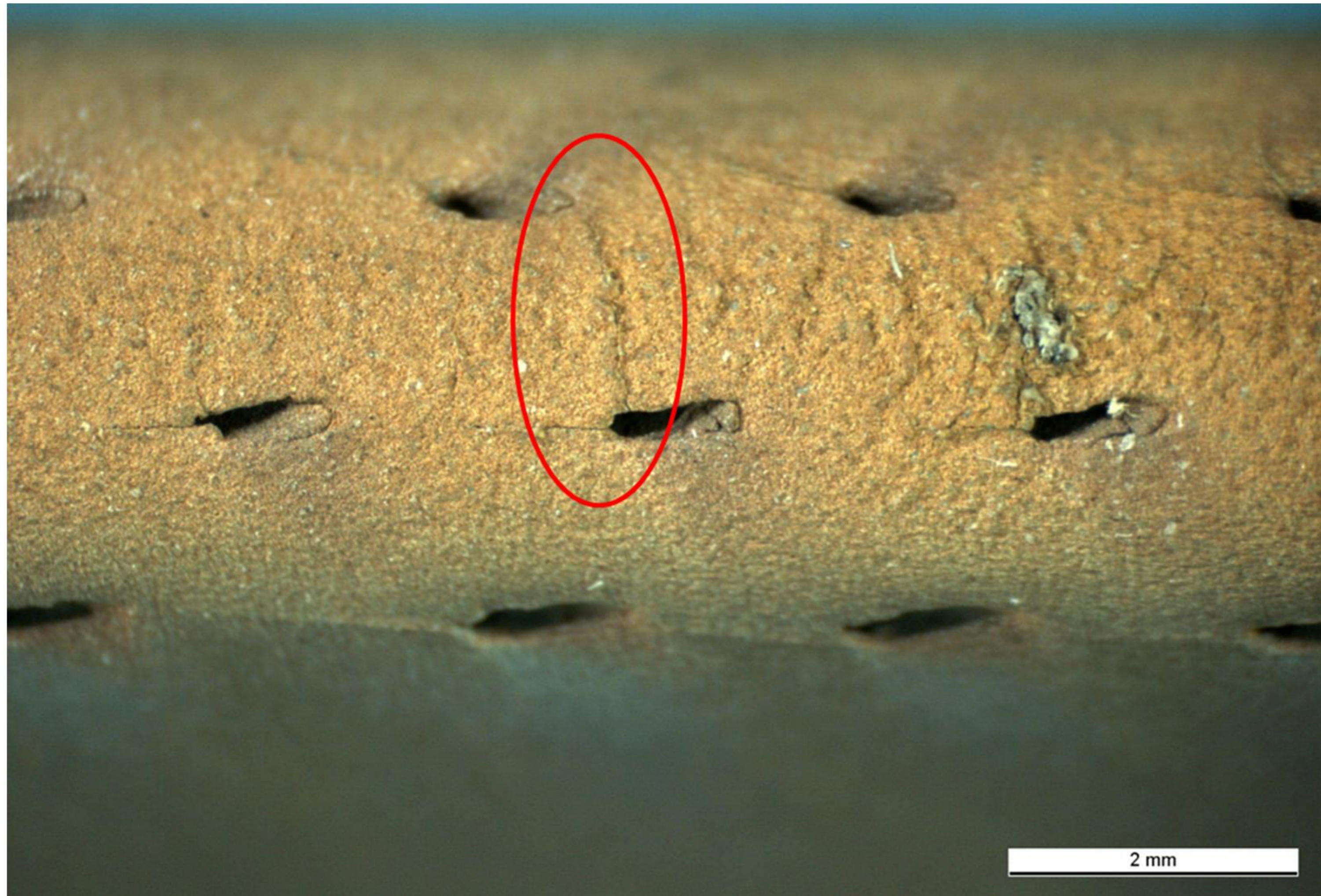


Figure 35: Cracks on the leading edge of blade 5569, opened crack circled. Picture by courtesy of VTT.

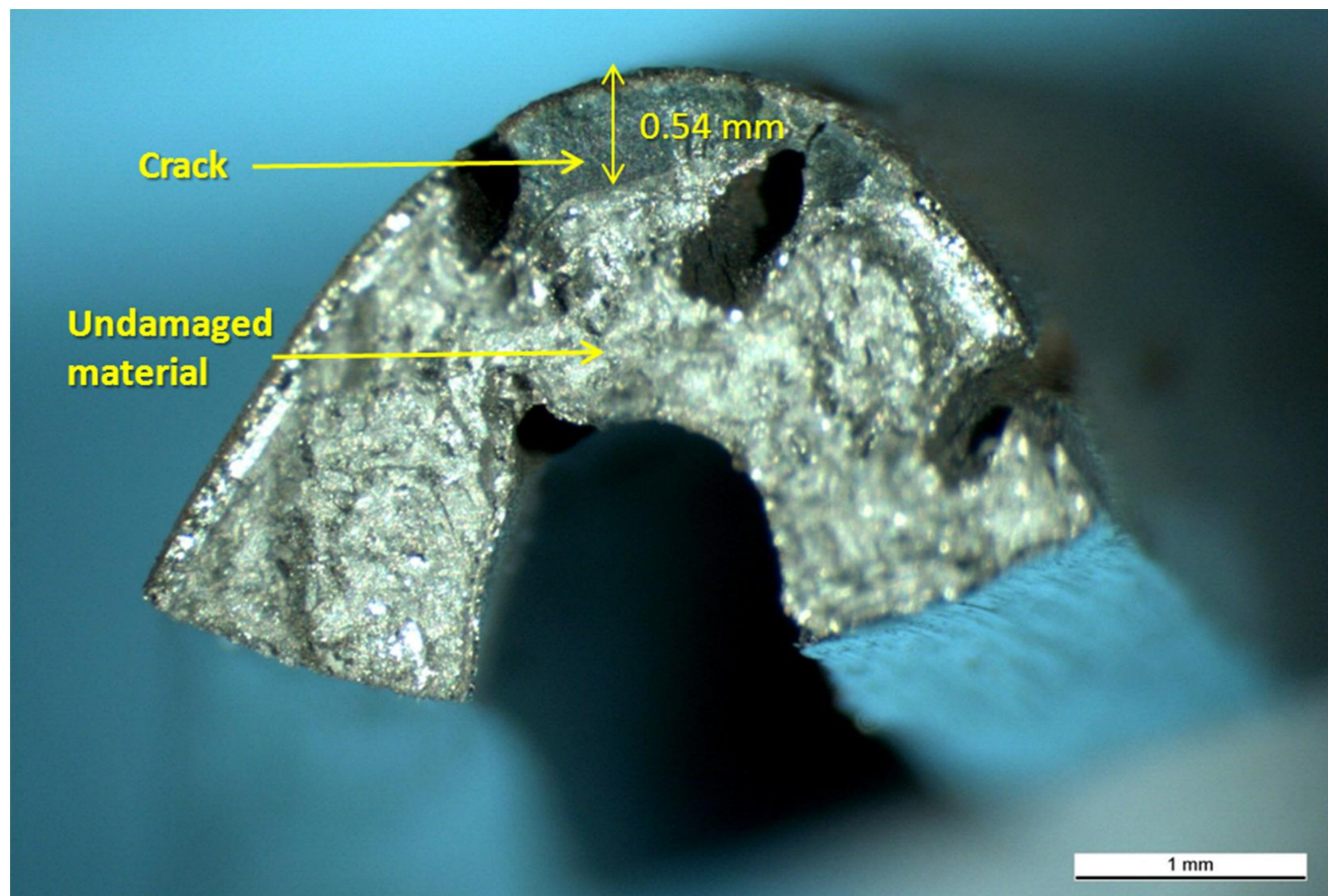


Figure 36: Opened crack from Fig. 35. Picture by courtesy of VTT.

13.2.7.3 The effect of volcanic ash on gas turbine blades and vanes

The goal of this investigation [69] was to examine whether exposure to volcanic ash could cause corrosion damage on HPT and LPT blades and HPT vanes if the molten ash remains on the metal surface and the engine remains in service.

There was hardly any ash particles observed on the HPT blades but some on the LPT blades. The ash had not caused any immediate damage to the blades. The ash spraying experiment and subsequent annealing did not reveal any corrosion processes neither on the coating nor on the base material of the HPT blade, *Fig. 37*.

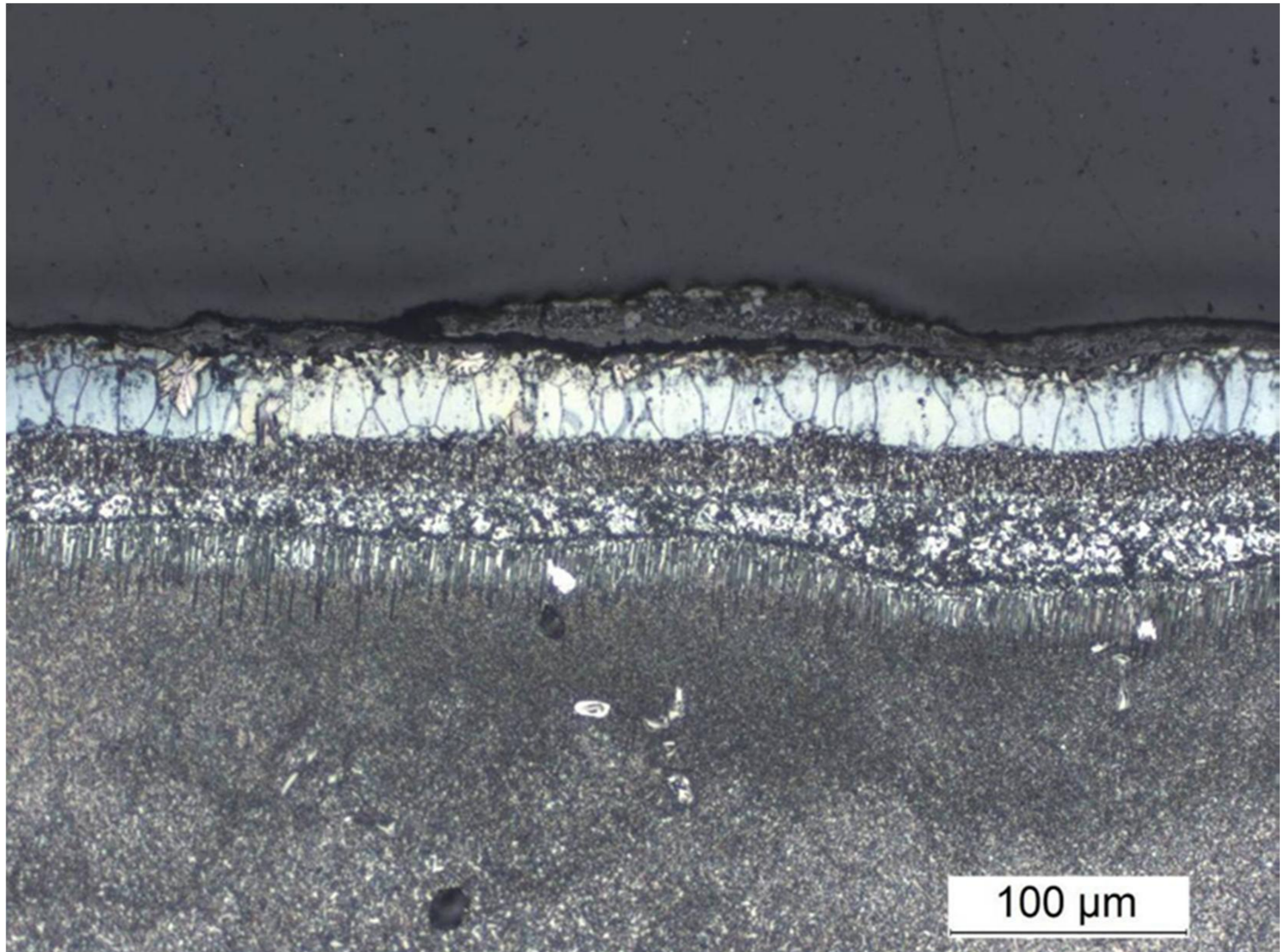


Figure 37: *HVOF sprayed volcanic ash on the coating of a HPT blade after annealing for 1000 h at 950°C, LOM. Picture by courtesy of VTT.*

On the basis of the inspection of the vanes exposed to ash and then kept in service for an additional 100 flight hours (results not included in this version of the report) indicate that molten ash will stay on the vane outer surface but will not have a long term corrosion effect. A more likely danger would be that the ash would block the cooling holes. The corrosion effect of ash on the HPT vane material after ash spraying and annealing were not tested in this project.

The coating on the cooled inner side of the HPT reference vane at least in some parts of the vane had been lost completely, including the diffusion zone, leaving the base metal without oxidation protection. This is rather surprising as the inner surface is cooled and not exposed to the flow of exhaust gases.

As a final conclusion it could be summarized that exposure to ash does not form any threat to the HPT and LPT blades. The HPT vanes are the critical component and they should be inspected after exposure to ash. The engine could be kept in service as long as the cooling channels of the vane are not blocked.

13.2.7.4 The effect of volcanic ash on gas turbine vanes

The purpose of this investigation was to see whether volcanic ash will cause any damage on the coating or the base material of the HPT vanes [70]. There were three different kinds of vanes delivered for the examination. The vane JMM192AA had been flown through the ash clouds and was removed from the engine soon after this flight. The vane JMM981AB had been flown through the ash clouds, inspected and put back to the engine, and has thereafter seen 117 h of service. The reference vane MDK08DYC had only seen normal flight, without exposure to ash clouds.

The coating on the outer surface of the vanes was in good condition almost everywhere in the inspected vanes. Only the vane which had flown 117 hours after the ash encounter showed some transverse cracks on the leading edge penetrating into the base metal. These cracks did not seem to put the integrity of the vanes in any immediate danger. There is no indication that the cracks could be a result of ash deposits. In this vane many cooling holes were partially blocked but the vane showed no clear signs of excessive overheating or surface attack. In the reference vane the coating of the internal surface was practically missing. The coating on the inner surface of all the vanes had suffered from at least some surface blistering, that was most pronounced in the vane JMM192AA. Some blistering was observed also on the inside of the vane cooling holes.

Annealing for 1000 hours at 1000°C of the vane sample coated with ash did not show any signs of additional oxidation or corrosion damage on the coating or on the base material. It is concluded that even a long-term ash exposure does not seem to pose a threat to the integrity of the vanes other than possible blocking of the cooling holes. Some examples of the results are shown in *Fig. 38* and *Fig. 39*.

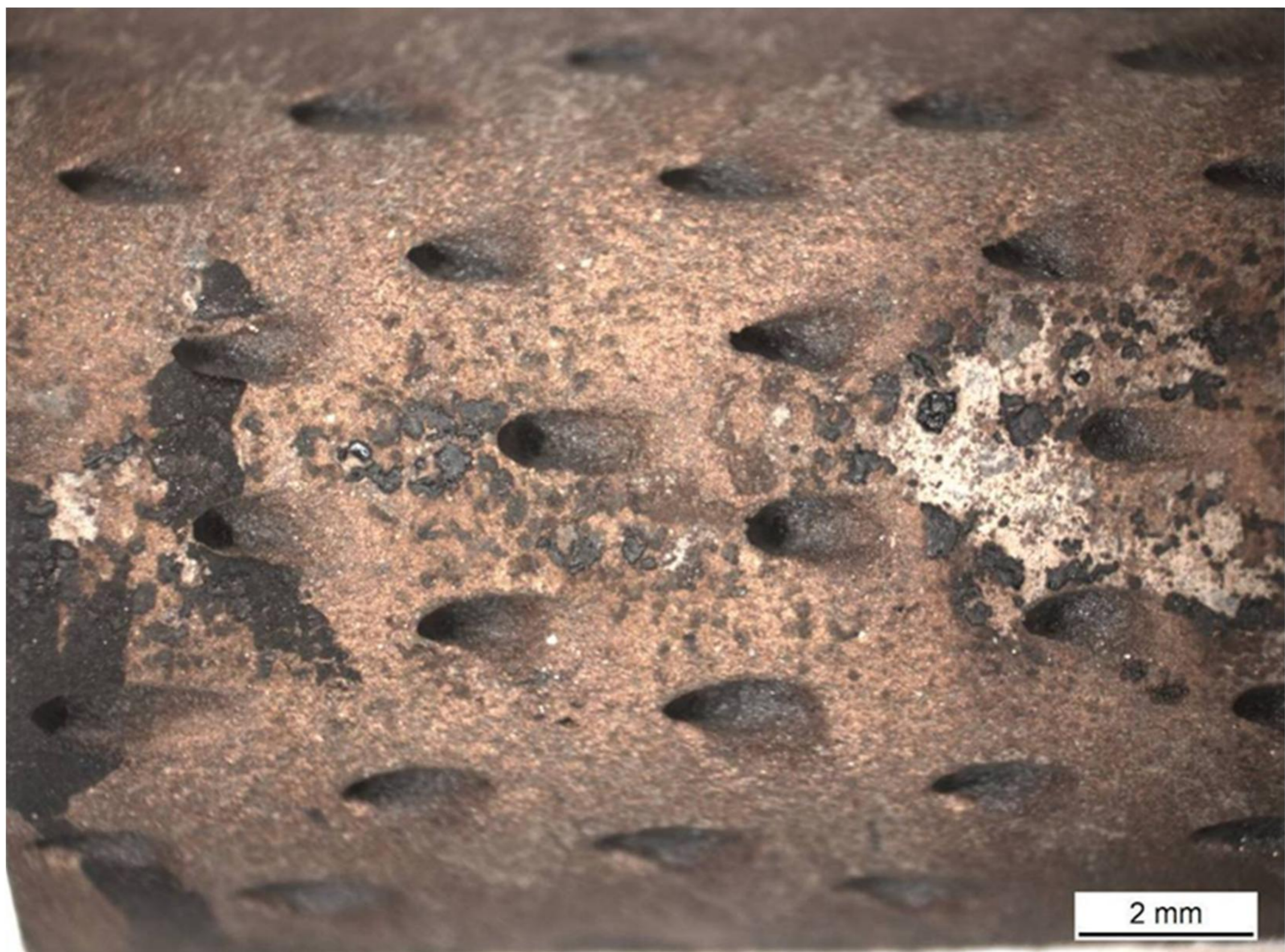


Figure 38: Volcanic ash on a HPT vane. Picture by courtesy of VTT.

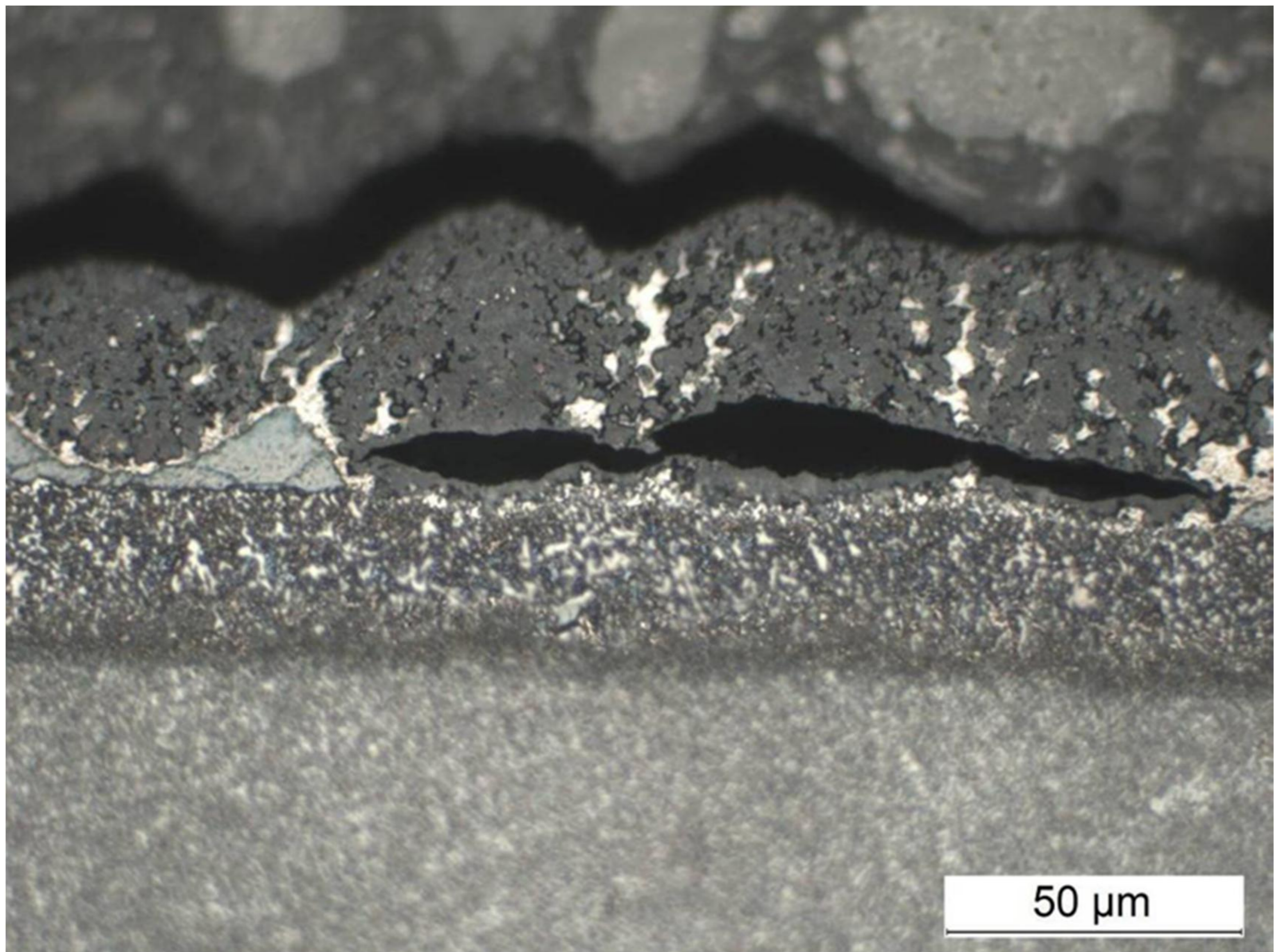


Figure 39: Oxidized coating on the inner surface of a HPT vane. Picture by courtesy of VTT.

13.3 Related activities

13.3.1 Environmentally friendly corrosion protection studies

Since the previous ICAF report [4 Chapter 13.3.2], the work related to the EDA ECOCOAT project (European Defence Agency, Environmentally Compliant Coatings in Aeronautic) have been successfully completed.

Currently much of corrosion protection for aluminium, magnesium and steel is based on hexavalent chromium passivation and cadmium substances. These substances are considered as very toxic (T+) substances by the REACH and the IPPC directive. Due to tightening legislation and directive requirements, alternative coating solutions, particularly for corrosion protection, have been investigated recently.

Furthermore, corrosion damage on aircraft on coated and non-coated components during service and maintenance has become significantly more frequent than before, especially in the North European countries. This is suggested to be due to the introduction of acetate- and formate-based de-icing chemicals on airfield runways. Earlier, urea was used for the chemical de-icing of the airfield runways, but today's environmental regulations prohibit its use in many countries. Thus, alternative chemicals that are mainly based on acetates and formates are used. As only very few studies report on the corrosion behaviour of aircraft materials in acetate- and formate-based de-icing chemicals, it is apparent that such studies are urgently needed to facilitate the proper selection of the de-icing chemicals and the materials in contact with them, for example by selecting new alternative coatings for corrosion protection. [71, 72].

In our recent study sol-gel based inorganic-organic hybrid coatings were developed and coated on aeronautical parts including cadmium plated steel. [73] The hybrid coatings were targeted to

provide two kinds of solutions. Firstly, the aim was to protect the cadmium-plating against the corrosion initiated especially by runway de-icing chemicals. Secondly, the hybrid coating approach was targeted to provide alternative coating solutions for cadmium plating as well as hexavalent chromium conversion coatings. In order to improve the corrosion resistance of the selected substances, the chemistry of the inorganic backbone of the hybrid coating was varied by using silane and aluminium alkoxides. Furthermore, the organic components of the hybrid coating were also varied. The corrosion performance of the coated specimens were investigated by using standardised runway de-icing corrosion test (AMS G-12) and salt spray test (ISO 9227). Based on the AMS G-12 test results, the use of the hybrid coatings improved the corrosion protection of cadmium plating against runway de-icing corrosion, *Fig. 40*. All the sol-gel coating systems coated specimens experienced much lower weight losses in the corrosion test AMS G-12 than the reference specimens without the sol-gel coating. Cadmium plated steel without additional sol-gel coating was tested as reference specimen (REF). The salt spray test showed that the corrosion protection performance of the hybrid coating on cadmium-plating was similar to uncoated cadmium plating.

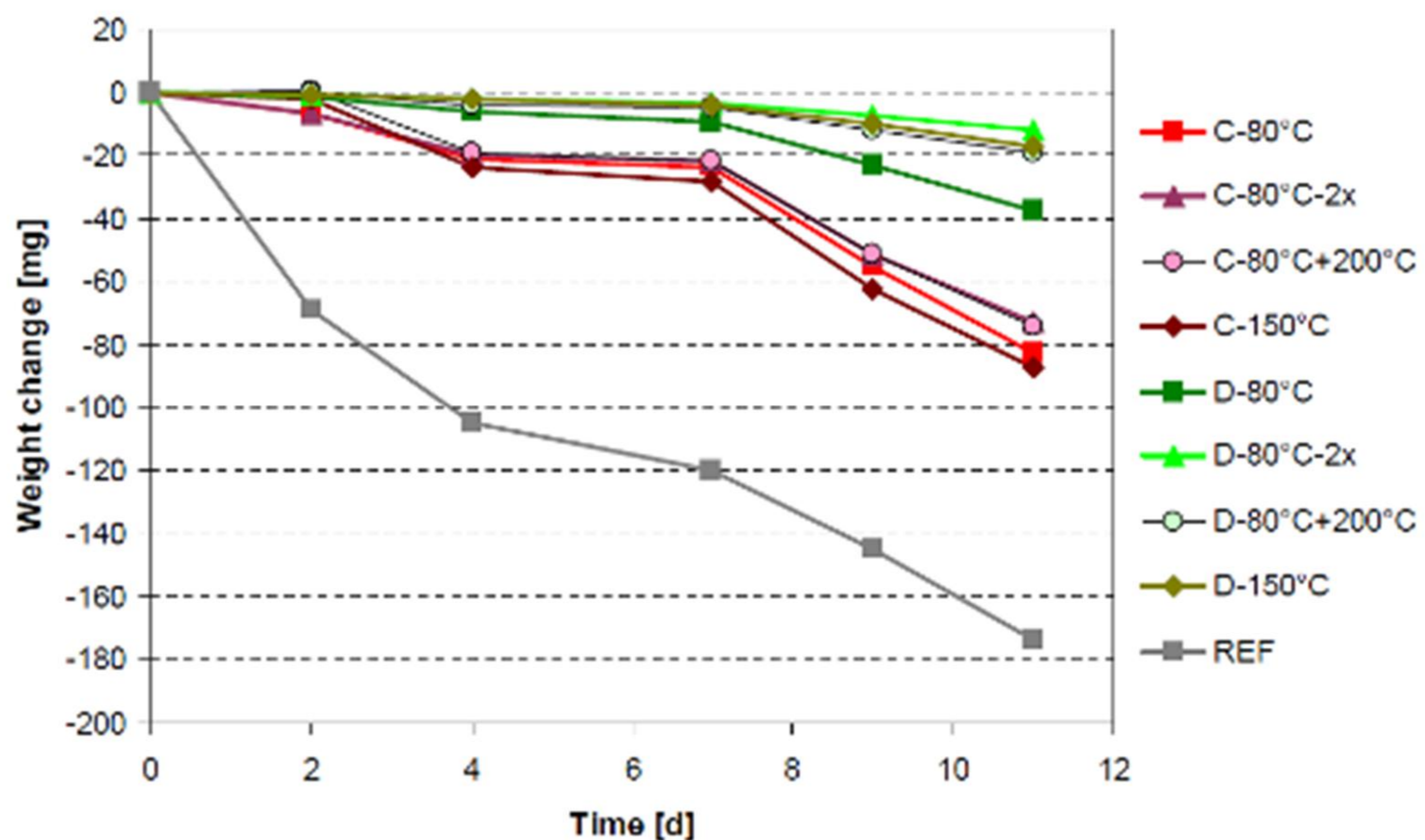


Figure 40: Weight change curves for sol-gel coated specimens EC136-C and EC134-D with different heat treatments and reference specimens during an AMS G-12 corrosion test, carried out using 50 wt.% potassium formate solution. Picture by courtesy of the FINAF.

13.4 References

1. FINAF 2013. History of the Finnish Air Force since 1918. Available via www.ilmavoimat.fi (reference: March 2013).
2. ICAF 2009. *A review of aeronautical fatigue investigations in Finland during the period May 2007 to April 2009*. (A. Siljander, Ed.). ICAF Document 2418 (VTT Research Report VTTR-02540-09). Espoo: VTT Industrial Systems. April 4, 2009. Available at: http://www.vtt.fi/inf/julkaisut/muut/2009/ICAF_Doc2418.pdf (reference: March 2013).
3. Patria 2011. Patria delivers first modernised Hawk Mk 66 aircraft to the Finnish Air Force. Patria press release 17.11.2011. Available at: www.patria.fi (reference: March 2013).
4. ICAF 2011. *A review of aeronautical fatigue investigations in Finland during the period May 2009 – March 2011*. (A. Siljander, Ed.). ICAF Document 2427 (VTT Research Report VTT-R-02827-11). Espoo: VTT 12 April 2011. Available at: http://www.vtt.fi/inf/julkaisut/muut/2011/ICAF_Doc2427_FinlandReview_2011.pdf (reference: March 2013).
5. Hoffren, J. 2011a. *CFD model of NH90 helicopter fuselage*. Report № NH-S-0015. Halli: Patria Aviation, Finland (in Finnish).
6. Hoffren, J. 2011b. *Modeling of an actuator disk for helicopter CFD analysis*. Report № NH-S-0016. Halli: Patria Aviation, Finland (in Finnish).
7. Hoffren, J. 2012. *Flow simulations for NH90 helicopter fuselage with an actuator disc*. Report № NH-S-0018. Halli: Patria Aviation, Finland (in Finnish).
8. Siikonen, T., Rautaheimo, P. and Salminen, E. 2000. *Numerical Techniques for Complex Aeronautical Flows*. European Congress on Computational Methods in Applied Sciences and Engineering, Barcelona, Spain, Sept. 11-14, 2000.
9. Guillaume, M., Gehri, A., Stefanie, P., Vos, J., Siikonen, T., Salminen E., and Mandanis, G. 2012. *Swiss/Finland Computational Fluid Dynamics Simulation on the F/A-18*. The 28th International Congress of the Aeronautical Sciences, Brisbane, Australia, Sept. 23-28, 2012.
10. Viitanen, T. 2012. *Initial values for Finflo's CFD analyses 2012*. Espoo: VTT Technical Research Centre of Finland, Aircraft Structures. Report № VTT-R-06605-12 (in Finnish, classified).
11. Öström, J. 2003. *HUTFLY2, Matlab / Simulink –based flight simulation software*. Espoo: Helsinki University of Technology, Laboratory of Aerodynamics (now Aalto University), , 2003. Report № T-186 (in Finnish).
12. Öström, J. 2004a. *F-18C Hornet aircraft model to the HUTFLY2 flight simulation software*. Espoo: Helsinki University of Technology, Laboratory of Aerodynamics (now Aalto University), 2004. Report № T-187 (in Finnish, classified).
13. Öström, J. & Hukkanen, T. 2006. *Improvements to the HUTFLY2 F-18C Hornet –aircraft model*. Espoo: Espoo: Helsinki University of Technology, Laboratory of Aerodynamics (now Aalto University), 2006. Report № T-221 (in Finnish, classified).
14. Hukkanen, T. 2007. *Modifications to the HUTFLY2 F-18C aircraft model*. Espoo: Helsinki University of Technology, Laboratory of Aerodynamics (now Aalto University), 2007. memorandum 7 May 2007 (in Finnish, classified).
15. Kaarlonen, K. & Öström, J. 2008. *Updated F-18C Hornet aerodynamic model to the HUTFLY2 flight simulation software*. Espoo: Helsinki University of Technology, Laboratory of Applied Mechanics (now Aalto University), 2008. Report № T-259 (in Finnish, classified).
16. Soimakallio, A. & Vesaoja, A. 2008. *The improvements in the HUTFLY2 F-18C Hornet engine model*. Espoo: Helsinki University of Technology, Laboratory of Applied Mechanics (now Aalto University), 2008. Report № T-260 (in Finnish, classified).
17. Viitanen, T. 2013. *Upgraded F-18C Hornet Flight Control System to the HUTFLY2 flight simulation software*. Espoo: VTT Technical Research Centre of Finland, Aircraft Structures, 2013. Report № VTT-R-04845-12 (in Finnish, classified).

18. Öström, J. 2004b. *Operational description of the F-18C Hornet flight control system*. Espoo: Helsinki University of Technology, Laboratory of Aerodynamics (now Aalto University), 2004. Report № T-196 (in Finnish, classified).
19. Liius, M. 2012a. *Former Y508 shear tie detailed FE model*. Report № HN-L-0204. Halli: Patria Aviation, Finland (in Finnish).
20. Liius, M. 2012b. *Inner Wing Aft Closure Rib detailed FE model*. Report № HN-L-0207. Halli: Patria Aviation, Finland (in Finnish).
21. Linna, J. 2010. *Missile Rib detailed FE model and necessary modifications*. Report № HN-L-0184. Halli: Patria Aviation, Finland (in Finnish).
22. Liius, M. 2012c. *HT Spindle detailed FE model, Rev A*. Report № HN-L-0169A. Halli: Patria Aviation, Finland (in Finnish).
23. Malmi, S. 2012a. *Update of transfer functions and life estimates of the critical structural locations of F-18 Hornet using FINFLO-3g - loads*. Report № HN-L-0200A. Halli: Patria Aviation, Finland (in Finnish, classified).
24. Malmi, S. 2012b. *Inner Wing Fold Rib detailed FE model*. Report № HN-L-0187A. Halli: Patria Aviation, Finland (in Finnish, classified).
25. Malmi, S. 2012c. *FINFLO-3g CFD-loads for the F-18 FE-model*, Report № HN-L-0199. Halli: Patria Aviation, Finland (in Finnish, classified).
26. ICAF 2007. *A review of aeronautical fatigue investigations in Finland during the period May 2005 to April 2007*. (A. Siljander, Ed.). ICAF Document 2410 (VTT Research Report VTTR- 03406-07). Espoo: VTT Industrial Systems. April 25, 2007. Available at: http://www.vtt.fi/inf/julkaisut/muut/2007/ICAF_FinlandReview_2007.pdf (reference: March 2013).
27. Laakso, R.; Viitanen, T.; Merinen, S.; Peltoniemi, E. 2011. *F-18 Hornet: Fatigue tracking results of the aircraft HN-416 and HN-432 using VTT's ground station – semi-annual report (V/2011)*. Report № VTT-R-01951-11 / 31.5.2009. Espoo: VTT Technical Research Centre of Finland (in Finnish, classified).
28. Laakso, R.; Viitanen, T.; Merinen, S.; Peltoniemi, E. 2012. *F-18 Hornet: Fatigue tracking results of the aircraft HN-416 and HN-432 using VTT's ground station – semi-annual report (VI/2011)*. Report № VTT-R-07507-11 / 15.3.2012. Espoo: VTT Technical Research Centre of Finland (in Finnish, classified).
29. Laakso, R.; Viitanen, T.; Merinen, S. 2013. *F-18 Hornet: Fatigue tracking results of the aircraft HN-416 and HN-432 using VTT's ground station – semi-annual report (VII/2012)*. Report № VTT-R-07233-12 / 28.1.2013. Espoo: VTT Technical Research Centre of Finland (in Finnish, classified).
30. Laakso, R. 2012. *F-18 Hornet: The compendium #1 of SAFE-NN-HOLM results*. Report № VTT-R-08696-11 / 31.1.2012. Espoo: VTT Technical Research Centre of Finland (in Finnish, classified).
31. Viitanen, T. 2011a. *HOLM: Electrical calibration of HN-432*. Report № VTT-R-04691-11 / 22.6.2011. Espoo: VTT Technical Research Centre of Finland, Aircraft Structures (in Finnish, classified).
32. Viitanen, T. 2011b. *HOLM: Electrical calibration of HN-416*. Report № VTT-R-06444-11 / 6.10.2011. Espoo: VTT Technical Research Centre of Finland, Aircraft Structures (in Finnish, classified).
33. Viitanen, T., Laakso, R., Janhunen, H., Merinen, S. 2012. *HOLM fatigue analysis database, HOLM_BASE v3.0.0*. Report № VTT-R-00922-12 / 28.5.2012. Espoo: VTT Technical Research Centre of Finland, Aircraft Structures (in Finnish, classified).
34. Viitanen, T.; Janhunen, H. 2013. *FINAF data package*. Memorandum № VTT-M-00192-13 / 11.1.2013. Espoo: VTT Technical Research Centre of Finland, Aircraft Structures (in Finnish, classified).
35. Viitanen, T.; Liukkonen, S. 2011. *Hornet's Vertical tail's buffeting: Analysis of the international flights*. Report № VTT-R-07709-11 / 22.11.2011. Espoo: VTT Technical Research Centre of Finland, Aircraft Structures (in Finnish, classified).
36. Siljander, A., Tikka, J. 2012a. *Domestic fleet management system*. Presentation given at the F/A-18A-D AV TCM (Air Vehicle Technical Coordination Meeting), St. Louis MO, USA, 15 – 18 March 2012.
37. Siljander, A., Tikka, J. 2012b. *Domestic fleet management system*. Presentation given at the HIC (Hornet International Conference), St. Augustine FL 18–21 June 2012.

38. Liukkonen, S.; Teittinen, T. 2011. *Preliminary design of the HOLM modification (onboard system)*. Report № VTT-R-07576-11 / 2.11.2011. Espoo: VTT Technical Research Centre of Finland (in Finnish, classified).
39. Vuori, M., Liukkonen, S. 2011. *FINAF F-18 HOLM Implementation Plan, alternative solutions, HOLM-lentokonejärjestelmän päivitys, Toteutusvaihtoehtosuunnitelma*. Report № 14522W71/ 2.9.2011. Halli: Patria Aviation, Finland (in Finnish, classified).
40. Vuori, M., Liukkonen, S. 2012. *FINAF F-18 HOLM System Requirement Specification, HOLM-lentokonejärjestelmän päivitys, Vaatimusmäärittely*. Report № 14522W70 / 16.5.2012. Halli: Patria Aviation, Finland (in Finnish, classified).
41. Vuori, M., Mäntylä, M. 2012. *FINAF F-18 HOLM System Design Document, F-18 HOLM-järjestelmän päivityksen toteutussuunnittelu, Laitteiston suunnitteludokumentti*, Report № 14003W71 / 23.8.2012. Halli: Patria Aviation, Finland (in Finnish, classified).
42. Mäntylä, M., Vuori, M. 2012. *FINAF F-18 HOLM System Test Plan, F-18 HOLM-järjestelmän päivityksen toteutussuunnittelu, Testaus*, Report № 14003W72.010 / 30.7.2012. Halli: Patria Aviation, Finland (in Finnish, classified).
43. Jylhä, J.; Ruotsalainen, M.; Salonen, T.; Janhunen, H.; Viitanen, T.; Vihonen, J. and Visa, A. 2009. *Towards automated flight-maneuver-specific fatigue analysis*. In: Bridging the Gap between Theory and Operational Practice, Proceedings of the 25th ICAF Symposium, pp. 1121-1134. Bos, M. J. (Ed.), Rotterdam, the Netherlands.
44. Ruotsalainen, M.; Jylhä, J.; Vihonen, J. and Visa, A. 2009. *A novel algorithm for identifying patterns from multisensor time series*. In: Proceedings of the 2009 WRI World Congress on Computer Science and Information Engineering (CSIE 2009), vol. 5, pp. 100-105. IEEE, Los Angeles, the USA.
45. Jylhä, J.; Ruotsalainen, M.; Salonen, T.; Janhunen, H.; Venäläinen, I.; Siljander, A. and Visa, A. 2011. *Link between flight maneuvers and fatigue*. In: Influence of Efficiency and Green Imperatives, Proceedings of the 26th ICAF Symposium, pp. 453-463. Komorowski, J. (Ed.), Montreal, Canada.
46. Ruotsalainen, M.; Jylhä, J.; Salonen, T.; Janhunen, H. and Visa, A. 2013. *Reasoning flight parameter based rules: Why do nominally similar flight maneuvers cause diverse fatigue damage?* To be published in: Maintaining Structural Integrity of Unmanned Aerial Vehicles, Proceedings of the 27th ICAF Symposium (Jerusalem, Israel).
47. ICAF 2005. *A review of aeronautical fatigue investigations in Finland during the period April 2003 to April 2005*. Research Report BTUO33-051366 (A. Siljander, Ed.). Espoo: VTT Industrial Systems. June 2, 2005. Available at: http://www.vtt.fi/inf/julkaisut/muut/2005/icaf_2005_finland_review_issue1.pdf (reference: March 2013).
48. Tikka, J., Salonen, T. 2007. *Parameter Based Fatigue Life Analysis of F18 Aircraft*. Durability and Damage Tolerance of Aircraft Structures: Metals vs. Composites. Proceedings of the 24th Symposium of the International Committee on Aeronautical Fatigue (ICAF), Naples, Italy, 16-18 May 2007. Volume I (lecture papers; L. Lazzeri & A. Salvetti, Eds.) pp 412-426.
49. Jylhä, J., Vihonen, J., Ala-Kleemola, T., Kerminen, R., Tikka, J., Visa, A. 2007. *Modelling structural vibrations for automated aircraft fatigue monitoring*. In: Durability and Damage Tolerance of Aircraft Structures: Metals vs. Composites, Proceedings of the 24th ICAF Symposium, pp. 1031-1042. Lazzeri, L.; Salvetti, A (Eds.), Naples, Italy.
50. Laakso, R.; Koski, K. 2012. *The damage analysis locations 4 within VTT's HOLM ground station*. Report № VTT-R-00740-12 / 30.11.2012. Espoo: VTT Technical Research Centre of Finland (in Finnish, classified).
51. Koski, K. 2012. *The Hornet loading spectrum corresponding to the FINAF's average usage*. Report № VTT-R-08385-11 / 23.1.2012. Espoo: VTT Technical Research Centre of Finland (in Finnish, classified).
52. Jokinen J. 2010. *Effect of interfaces and analysis parameters on 1D damage modeling*. Aalto University, School of Engineering, Department of Applied Mechanics, Aeronautical engineering, report № KRT-T364, 2010 (in Finnish).
53. Jokinen J. 2011. *Analysis of a symmetric 1D damage*. Aalto University, School of Engineering, Department of Applied Mechanics, Aeronautical engineering, report № KRT-T363, 2011 (in Finnish).

54. Jokinen J., Wallin, M., Saarela, O. 2011. *Three-Dimensional Analysis of DCB Specimen Energy Release Rate Distributions*, Composites 2011, Hannover 21.9.-23.9.2011.
55. Jokinen J., Wallin, M. 2012. *Fracture of adhesive joint in mode I loading*, Aalto University, School of Engineering, Department of Applied Mechanics, Aeronautical engineering. Presentation 13.-14.9.2012 (in Finnish).
56. Jokinen J. 2012. *Modelling of trailing edge flap delaminations*, Aalto University, School of Engineering, Department of Applied Mechanics, Aeronautical Engineering, report № KRT-T366, 2012 (in Finnish).
57. Hukkanen, T., Keinonen, M. 2012. *FINAF F-18 HOLM System Design Report, HOLM-asennuksen päivitys uusilla venymäliuskoilla ja kiihtyvyyssantureilla, Suunnitteluraportti*. Report № HN-L-0203 / 29.8.2012. Halli: Patria Aviation, Finland (in Finnish, classified).
58. Koski, K., Laakso, R., Siljander, A. 2013. *Fatigue tests and fractographic analyses of the FISIF coupons*. Report № VTT-R-00314-13/ 28.2.2013. Espoo: VTT Technical Research Centre of Finland (in Finnish, classified).
59. Lahdenperä, K., Leskelä, E., Veivo, J., Siljander, A. 2012. *Experimental study of the sensitivity of the crack detection techniques applicable in the periodic inservice inspections using unpainted and painted test specimen with real fatigue cracks*. Report № VTT-R-10255-10 / 21.2.2012. Espoo: VTT Technical Research Centre of Finland.
60. Korhikoski, S. 2011. *Aircraft battle damage repair*. Master's Thesis (in Finnish). Aalto University, School of Science and Technology, PO Box 11000, FI-00076 AALTO, <http://www.aalto.fi>.
61. Aakkula, J., Saarela, O., Haikola, T., Tervakangas, S. 2012. *DIARC plasma coating for reliable and durable structural bonding of metals*. ICAS 2012, the 28th International Congress of the Aeronautical Sciences. Paper available at: http://www.icas.org/ICAS_ARCHIVE/ICAS2012/PAPERS/148.PDF (reference: March 2013).
62. Varis, P. 2012. *Computational fatigue life assessment of a metallic structure with a bonded composite repair*. Master's Thesis (in Finnish). Aalto University, Schools of Technology, PO Box 12100, FI-00076 AALTO, <http://www.aalto.fi>.
63. Hietala, J.-P.; Aaltonen, J.; Koskinen, K. T.; Vilenius, M. 2011a. *Comparison between an aircraft speed brake actuator high order linear model and a semi-empirical non-linear model in real time simulation*. AST 2011, the 3rd International Workshop on Aircraft System Technologies, March 31 - April 1, 2011, Hamburg, Germany . International Workshop on Aircraft System Technologies AST vol. 3, Hamburg, Hamburg University of Technology, pp. 65-71.
64. Hietala, J.-P.; Aaltonen, J.; Koskinen, K. T.; Vilenius, M. 2011b. *Aircraft hydraulic system model integration to flight simulation model* . The 12th Scandinavian International Conference on Fluid Power, SICFP'11, May 18-20, 2011, Tampere, Finland . Scandinavian International Conference on Fluid Power SICFP vol. 12, num. 1, Tampere, Scandinavian International Conference on Fluid Power, pp. 271-280.
65. Aaltonen, J.; Alarotu, V.; Koskinen, K. T. 2011. *Aircraft Hydraulic System Fault Finding and Troubleshooting Using On-Line Particle Counters*. The 8th International Conference on Condition Monitoring and Machinery Failure Prevention Technologies, 20-22 June 2011, Cardiff, Wales. International Conference on Condition Monitoring and Machinery Failure Prevention Technologies vol. 2, Northampton, British Institute of Non-Destructive Testing, pp. 1275-1282.
66. Aaltonen, J.; Koskinen, K. T. 2011. *Detecting and eliminating the measurement error caused by free air in aircraft hydraulic system on-line particle counting*. The 12th Scandinavian International Conference on Fluid Power, SICFP'11, May 18-20, 2011, Tampere, Finland . Scandinavian International Conference on Fluid Power SICFP vol. 12, num. 1, Tampere, Scandinavian International Conference on Fluid Power, pp. 229-240.
67. Jauhiainen, P.; Yli-Olli, S.; Salonen, J.; Auerkari, P.; Rantala, J. 2013. *Microstructural degradation of a single-crystal gas turbine blade*. Report № VTT-CR-01528-13. Espoo: VTT Technical Research Centre of Finland (in Finnish, classified).
68. Salonen, J.; Yli-Olli, S.; Rantala J. 2013. *Guideline - turbine blade failures*. Report № VTT-R-01519-13. Espoo: VTT Technical Research Centre of Finland (in Finnish, classified).

69. Jauhiainen, P.; Salonen, J.; Rantala, J. 2011a. *The effect of volcanic ash on gas turbine blades and vanes*. Report № VTT-CR-04755-11. Espoo: VTT Technical Research Centre of Finland (in Finnish, classified).
70. Jauhiainen, P.; Salonen, J.; Rantala, J. 2011b. *The effect of volcanic ash on gas turbine vanes*. Report № VTT-CR-05936-11. Espoo: VTT Technical Research Centre of Finland (in Finnish, classified).
71. Huttunen-Saarivirta, E., Kuokkala, V.-T., Kokkonen, J., and Paajanen, H. 2008. Corrosion Engineering, Science and Technology 2008, 43, No.1.
72. Huttunen-Saarivirta, E., Kuokkala, V.-T., Kokkonen, J., and Paajanen, H. 2009. Materials and Corrosion 2009, 60, No.3.
73. Nikkola, J., Huttunen-Saarivirta, E., Mannila, J., Sorsa, P., Siivinen, J., and Paajanen, H. 2012. The European Corrosion Congress 2012, EUROCORR2012. Istanbul, 9 - 13 Sept. 2012. European Federation of Corrosion (2012).

Report's title	
A REVIEW OF AERONAUTICAL FATIGUE INVESTIGATIONS IN FINLAND APRIL 2011 – FEBRUARY 2013	
Customer, contact person, address	
The Finnish Air Force Materiel Command Programmes Division Mr. Ari Välikangas P. O. Box 14; FI-41161 Tikkakoski; Finland	
Project name	
83300 – ICAF_2013	
Editors	Pages
Aslak Siljander	50/
Keywords	Report identification code
Aeronautical fatigue, military aircraft, fixed wing, research project, structural integrity, Finland	ICAF Doc № 2428 / 15.3.2013 (VTT- VTT-R-02105-13/ 21.3.2013)
Summary	
<p>This document was prepared for the delivery to the 33rd Conference of the International Committee on Aeronautical Fatigue and Structural Integrity scheduled to be held in Jerusalem, Israel on 3-4 June 2013.</p> <p>A review is given of the aircraft structural fatigue research and associated activities which form part of the programs within the Finnish Air Force Materiel Command (FINAFMC): Programmes Division, Plans Division and Aircraft Division; Patria Aviation Oy; VTT Technical Research Centre of Finland (VTT); Aalto University (Aalto); Tampere University of Technology, Institute of Signal Processing (TUT/ISP), Department of Materials Science (TUT/DMS); Finflo Ltd., Emmecon Ltd. and Millidyne Ltd.</p> <p>The review summarizes fatigue related research programs and investigations on specific military fixed wing aircraft since the previous Finnish National Review (tabled in the 32nd Conference, ICAF, Montréal, Canada) up to February 2013.</p>	
Confidentiality	Public
Espoo 3.4.2013 Approved by	
Aslak Siljander ICAF National Delegate / Finland (VTT)	
Editors' contact address	
VTT, P. O. Box 1000, FI-02044 VTT, Finland (Street: Vuorimiehentie 3, Espoo, Finland)	
Distribution	
Unclassified. Distribution unlimited. This document has been authorized by the FINAFMC for unlimited public release [Permission № CJ5157 / 3.4.2013].	